The Dissertation Committee for Chien-Hung Liu Certifies that this is the approved version of the following dissertation:

Battle Between Influenza A Virus And A Newly Identified ZAPL Antiviral Activity

Committee:

Robert M. Krug, Supervisor

Jon M Huibregtse

Rick Russell

Christopher S. Sullivan

Jason Upton

Battle Between Influenza A Virus And A Newly Identified ZAPL Antiviral Activity

by

Chien-Hung Liu, B.S.; M.S.

Dissertation

Presented to the Faculty of the Graduate School of

The University of Texas at Austin

in Partial Fulfillment

of the Requirements

for the Degree of

Doctor of Philosophy

The University of Texas at Austin

May, 2015

Dedication

To:

My family for their love and support.

Acknowledgements

First I would like to express my gratefulness to my supervisor, Dr. Robert M. Krug for his kind support and guidance throughout my graduate study. Without his assistance and supervision, this research work could not have been done.

I would like to thank my committee members, Dr. Jon M Huibregtse, Dr. Rick Russell, Dr. Christopher S. Sullivan, Dr. Jason Upton, and previous committee member Dr. Sara Sawyer, for their precious suggestions for my research work.

For all the valuable feedback to my research work, I would like to thank the previous and current members of Krug laboratory, including Drs. Chen Zhao, Rei-Lin Kuo, Tien-Ying Hsiang, Guifang Chen, Ligang Zhou, Mark Collins, Shanshan Wang, and graduate student Bart Smith. I would like to extend my thanks to Dr. Rei-Lin Kuo for his guidance and help when I began my research in the Krug laboratory, and Dr. Chen Zhao for his vital insights and suggestions throughout my graduate work.

I would like to thank my family for their thoughtfulness and support for my graduate study. I especially would like to thank my wife, Chu-Chiao Wu, who is also a graduate student in UT, for her love, support, thoughtfulness and encouragement to each other throughout my graduate work and life, particularly when we need to give consideration to raising our lovely baby son, maintaining family life and doing graduate work for both at the same time.

Battle Between Influenza A Virus And A Newly Identified ZAPL Antiviral Activity

Chien-Hung Liu, Ph.D.

The University of Texas at Austin, 2015

Supervisor: Robert M. Krug

Influenza A virus infection causes a highly contagious annual respiratory disease in humans as well as periodic pandemics with higher mortality rates. The Krug laboratory has shown that one of the major ways that the influenza virus NS1 protein counteracts host antiviral responses is to bind the 30 kDa subunit of the cleavage and polyadenylation specificity factor (CPSF30). As a consequence, 3' end processing of cellular pre-mRNAis is inhibited, leading to reduced production of cellular mRNAs, including interferon mRNAs. I showed that NS1-CPSF30 complexes contain an array of cellular proteins. I purified the NS1-CPSF30 complexes from virus infected cells by affinity selection of CPSF30 and the NS1 protein. I identified the associated cellular proteins by mass spectrometry. Two cellular RNA helicases, DDX21 and DHX30, were identified. SiRNA knockdown of either RNA helicase enhanced virus replication, indicating that DDX21 and DHX30 inhibit influenza A virus replication. Further study

demonstrated that DDX21 RNA helicase inhibits viral RNA synthesis, and is countered by the NS1 protein. The cellular ZAPL antiviral protein was also identified in the NS1-CPSF30 complexes. Previous studies have shown that ZAPL antiviral activity is mediated by its N-terminal zinc-fingers, which targets viral mRNA of several viruses for degradation. Little is known about the antiviral role of the ZAPL C-terminal PARP domain. Here I discovered the antiviral role of ZAPL C-terminal PARP domain against influenza A virus. I showed that the ZAPL PARP domain targets the viral polymerase PA and PB2 proteins. These two viral polymerases are poly(ADP-ribosylated), presumably by other PARP protein(s). The ZAPL-associated, poly(ADP-ribosylated) PA and PB2 are then ubiquitinated and proteasomally degraded. This ZAPL antiviral activity is counteracted by the binding of polymerase PB1 protein to the WWE region adjacent to the PARP domain, and causes PA and PB2 to dissociate from ZAPL and thus escape degradation. Because PB1 displaces PA and PB2 and protects them from ZAPL-mediated degradation, endogenous ZAPL only moderately inhibits influenza A virus replication (20-30-fold), as determined by siRNA knockdown experiment. These results suggest that influenza A virus has partially won the battle against the newly identified ZAPL antiviral activity.

Table of Contents

List of Tables

List of Figures

Chapter 1: Introduction of influenza virus

1.1 Influenza virus

1.1.1 Overview

Influenza, commonly known as “the Flu”, is a highly contagious respiratory disease in human, which is caused by influenza virus. Annual influenza epidemics cause 3 to 5 million cases of severe illness and about 250000 to 500000 death each year (World Health Organization, 2014). Larger influenza outbreaks in a worldwide range, or pandemics, are less frequent throughout human history. There were three major human pandemics occurred last century. Among them, the “Spanish flu” in 1918 was the most devastating one which killed more than 30 million people. The other two were “Asian flu” in 1957 and “Hong Kong flu” in 1968, which also resulted in high mortality rates. Influenza virus can cause pandemics due to its capability of gene reassortments between different strains, a process known as “antigenic shift”. The gene reassortments generate new influenza virus strain which is different from previous circulating strains. The little immunological protection against these new strains contributes to high mortality rates in human. The recent outbreaks of highly virulent avian influenza H5N1 and H7N9 have alerted people of the potential new pandemic outbreak (Lamb, 2013; Li et al., 2004). Fortunately, these viruses have been mainly limited to avain-to-human transmission, and have not acquired the ability to cause efficient human-to-human transmission.

Influenza virus is a member of the *Orthomyxoviridae* family, which

contains 5 different virus genera: influenza A, influenza B, influenza C, Thogoto virus, and Isavirus. These five different virus genera were defined by antigenic differences of their nucleoprotein (NP) and the matrix protein (M1). The *Orthomyxoviridae* family is enveloped viruses with single-stranded, negative sense segmented RNA genomes. The viruses in this family are capable of gene reassortement in the same type of virus due to their segmented genome. However, gene reassortment between different virus types (for example, influenza A virus and Thogoto virus) has not been reported. Influenza A virus causes human pandemics and it can infect a broad range of host, including birds, humans, pigs, horses, seals and whales. Influenza B virus infects mainly human and causes seasonal outbreaks, but not pandemics. Influenza C virus infects human and pigs with rare frequency (Lamb and Krug, 2001).

Influenza A virus can be further divided into subtypes based on their antigenic difference of two surface proteins, hemagglutinin (HA) and neuraminidase (NA). There are at least 16 known subtypes of HA (H1-H16) and 9 known subtypes of NA (N1-N9), which is used in naming influenza A strains (e.g. H1N1, H3N2, H5N1). All influenza A virus subtypes can be found in wild aquatic birds, which are natural reservoir of influenza A virus, whereas only a small subset can be found in humans. Recent circulating influenza A viruses in human are H1N1 and H3N2 strains (Holmes et al., 2005; Zambon, 2001).

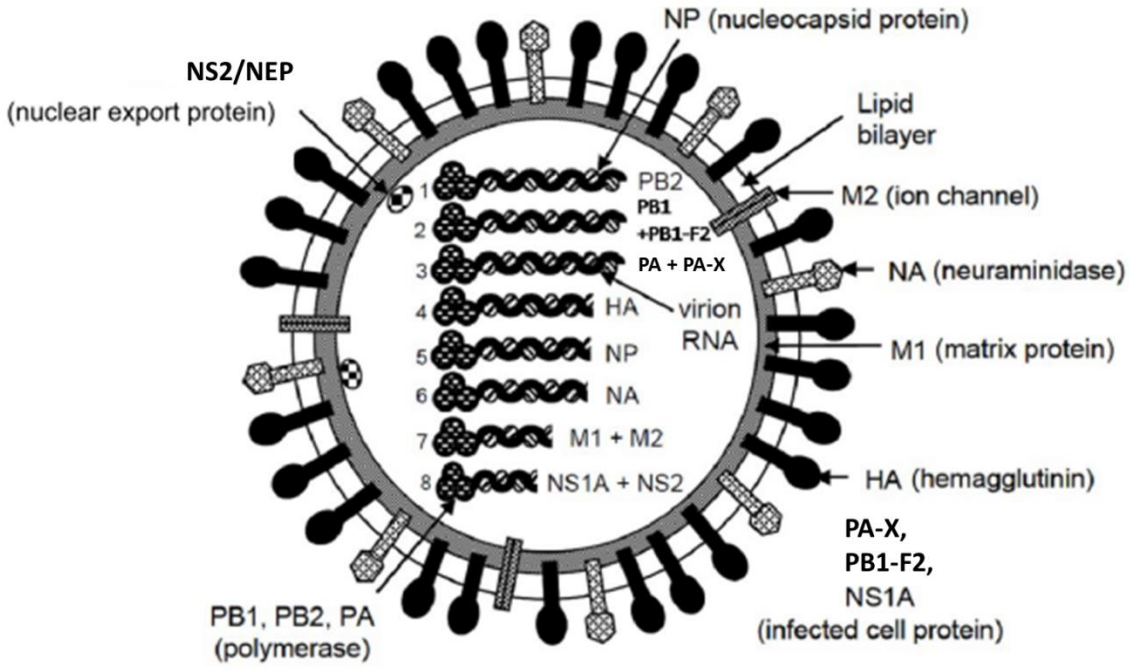

Figure 1.1 Schematic diagram of influenza A virion structure. The location of viral structural proteins, envelope, and eight RNA gene segments are indicated. The PA-X, PB1-F2, and NS1A protein are expressed and found only in infected cells, but not in vrions (Modified from (Noah and Krug, 2005)).

1.1.2 Structure of influenza A virus

Schematic diagram of influenza A vrion structure is shown in Figure 1.1. The influenza A virus genome is comprised of eight viral RNA segments (vRNAs), which encode thirteen or fourteen proteins (Krug and Fodor, 2013; Wise et al., 2012). The three largest vRNA segments 1~3 encode three viral polymerase subunits PA, PB1 and PB2, respectively. Segment 2 also encodes PB1-F2 from alternative reading frame, which serves a virulence factor to regulate host cell apoptosis (Chen et al., 2001). Segment 3 through ribosomal frameshift also encodes another protein, PA-X, to modulate virulence (Jagger et al., 2012). Segment 5 encodes NP that coats all eight vRNA segments, together with a single copy of the viral polymerase consisting of the PA, PB1 and PB2 proteins, to form viral ribonucleoprotein (vRNP) complexes. The NP protein is a monomer that nonspecifically and repeatedly binds to single-stranded vRNA every 24 bases. The 5' and 3' ends of vRNA form a partially double-stranded structure that serves as a "promoter" for the viral polymerases. The three polymerases with NP proteins are required for viral genome replication and RNA transcription (Figure 1.2). Segment 4 and 6 encodes HA and NA, respectively. The HA and NA are glycoproteins that are anchored on the viral bilayer phospholipid envelope to form spike-shaped outer layer. The HA protein is a homotrimer that binds the sialic acid receptors on the cells, which mediates virus-host cell membrane fusion and entry into the cell. The NA protein is a homotetramer that helps virus progeny release from cells by hydrolyzing sialic acid on receptors. Segment 7 encodes M1 and M2 through alternative splicing. The M1 proteins form a layer under the lipid envelope and serves structural function inside viral particle. In the infected

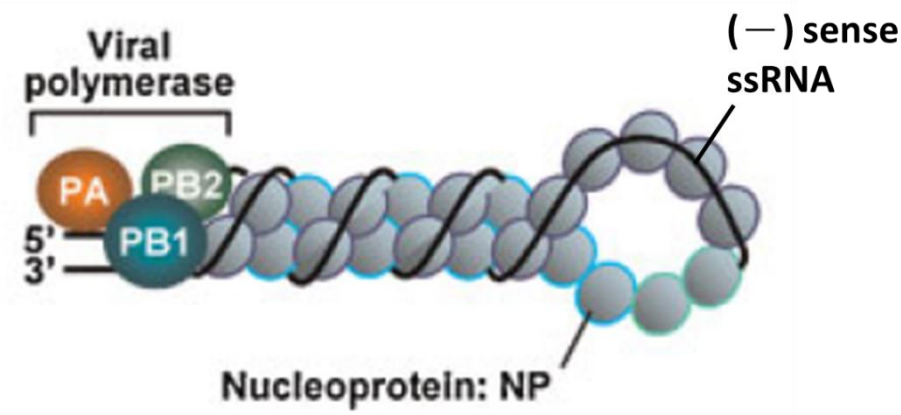

Figure 1.2 Schematic diagram of influenza A vRNP structure. The influenza A viral ribonucleoprotein complex (vRNP) is comprised of three viral polymerases PA, PB1 and PB2 (3P), and nucleoprotein NP. The viral (−) sense ssRNA forms a hairpin structure with 5' and 3' ends forming a supercoil structure where 3P binds to. The NP proteins bind nonspecifically along the vRNA (Modified from (Nagata et al., 2008)).

cells, the M1 mediates the encapsidation of vRNP into the viral envelope, which is essential for virus packaging and budding. The M2 homotetramer forms an ion channel, which pumps hydrogen ions (H+) into viral particle when virus enters into endosome. This step is important for viral vRNP uncoating from M1 and later transfer into nucleus. The smallest segment 8 encodes NS1 and NS2 through alternative splicing. The NS2 protein, also known as NEP, functions as a nuclear export protein for vRNP in infected cells. It is associated with M1 in viral particles. The NS1 is a multifunctional protein that counteracts many host anti-viral responses and regulates other host and viral functions (reviewed in (Krug, 2015)). Among all influenza A viral proteins, NS1, PB1-F2, and PA-X are non-structural proteins, and known to only be present in infected cells.

1.1.3 Replication of influenza A virus

Figure 1.3 shows the schematic diagram of influenza A vrus life cycle in cells. The influenza virus particle through its HA proteins bind to sialic acid residues on glycoproteins or glycolipid on cell membrane, which induces receptor-mediated endocytosis. Following endocytosis, the viral particle is internalized and fused with endosome. The M2 ion channels pump hydrogen ions into viral particle/endosome and lower the pH, which leads to M1 dissociation from vRNPs, disruption of endosome and release of vRNPs into cytoplasm. The released vRNPs then migrate into nucleus (Martin and Helenius, 1991). Viral RNA replication and transcription take place in nucleus. The viral genome is negative sense RNA (vRNA), which serves as template for positive sense mRNA and cRNA. cRNA is the complimentary copy of

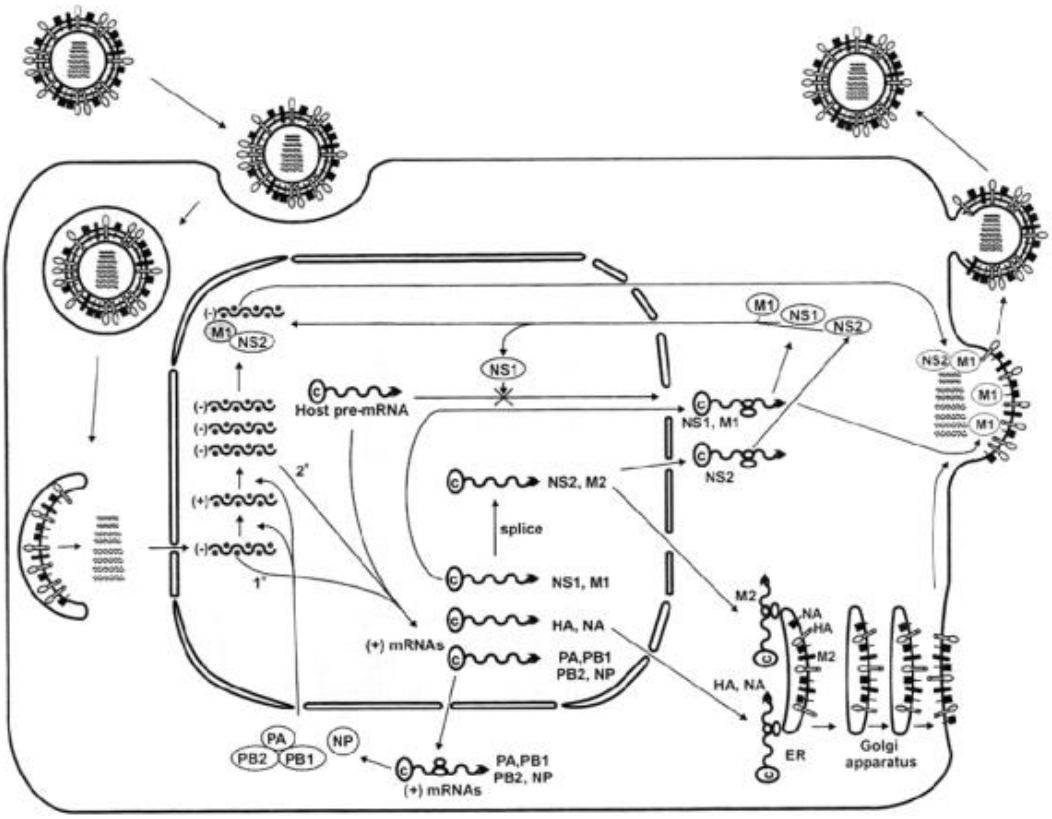

Figure 1.3 Schematic diagram of influenza A vrus life cycle in cells. Influenza A virus particle binds to sialic acid receptor on cell membrane, which leads to endocytosis and internalization into endosome. The vRNPs are then released into cytoplasm and migrated into nucleus. The viral genome is replicated and viral RNA is transcribed into mRNA by viral polymerase complexes in nucleus. The replicated viral genomes are assembled into vRNPs and exported into cytoplasm and packaged with other viral proteins on cell membrane. Finally, the progeny virion is released from cell membrane by budding process (Adapted from (Lamb and Krug, 2001)).

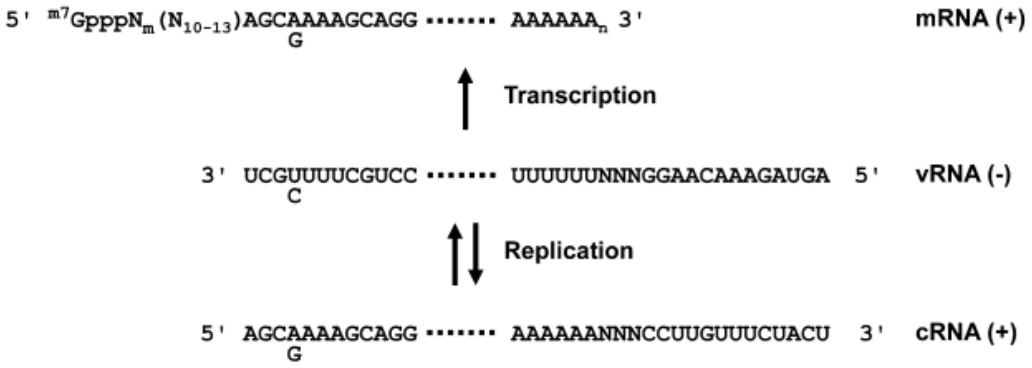

Figure 1.4 Transcription and replication of influenza virus genome segments. Negative sense viral RNA (vRNA) transcribed into positive sense mRNA with 5' cap and 3' poly-A tail. vRNA replicates by synthesis of positive sense complimentary RNA (cRNA) intermediates first, which then serve as template to synthesize vRNA (Adapted from (Krug and Fodor, 2013))

vRNA, which serves as template for further synthesis of vRNA (Figure 1.4).

Transcription of influenza A vRNA into mRNA is initiated by the “cap-snatching” mechanism (Figure 1.5). The vRNP contains the trimeric polymerase complex that binds to the partially double-stranded panhandle structure formed by the conserved 5’ and 3’ end of each vRNA segment (Figure 1.2). The viral mRNA synthesis is initiated by a primer “stolen” or “snatched” from host, which is a 10- to 13-bases-long capped RNA primer from cellular capped pre-mRNA bound by viral polymerase PB2 subunit and cleaved by endonuclease activity of the PA subunit (Dias et al., 2009; Guilligay et al., 2008; Plotch et al., 1981). A G residue is added to the 3’CA end of the capped primer to initiate the mRNA transcription. In addition, the PB1 subunit binding to the double-stranded panhandle structure is also required for for transcription (Fodor et al., 1994). Transcription elongation is catalyzed by the PB1 subunit, which contains the polymerase active site for nucleotide addition. The viral mRNA elongates until the polymerase reaches the 4-7 uridine (U) sequence located 16-20 nucleotides from the 5’ end of vRNA template. Then the polymerase reiteratively copies the U sequence (“sutters”), which generates the poly(A) tail for the viral mRNA in a host-independent process (Poon et al., 1999). The viral mRNAs then are exported into cytoplasm for translation.

Replication of influenza A vRNA occurs in two stages. In the first stage, the (−) sense vRNA is replicated into (+) sense full-lengh complimentary RNA (cRNA). In the second stage, the cRNA serves as a template to synthesize the progeny vRNA. Both cRNA and vRNA synthesis are

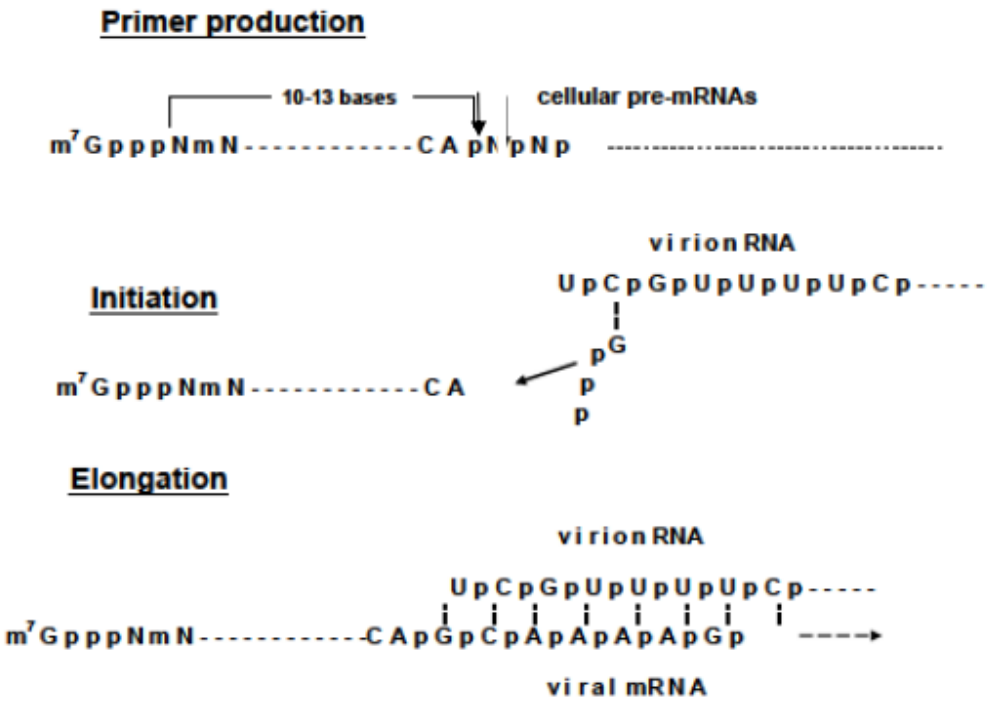

Figure 1.5 Cap-snatching mechanism to initiate viral mRNA synthesis. See text for details (Adapted from (Chen and Krug, 2000))

primer-independent (unprimed initiation), which is different from viral mRNA synthesis. The detail mechanism for cRNA and vRNA synthesis has not been definitely established. The structure of all three polymerase subunits bound with viral RNA promoter was not solved until recently. For the unprimed RNA replication, the PB1 protein contains an analogous putative priming loop (641-657aa) to stabilize the priming and incoming NTPs to facilitate unprimed initiation of RNA replication (Krug, 2014; Pflug et al., 2014; Reich et al., 2014).

Just like the other viruses, the gene expression of influenza virus is regulated during the infection. Immediately after the vRNA transportation into nucleus, all eight viral mRNAs are synthesized, and the vRNA, mRNA synthesis and protein synthesis are coupled. Afterwards, the infection can be divided into early and late stages. In general, the rate of both vRNA and mRNA synthesis increase and reach maximal during early stage; however, the mRNA synthesis rate is reduced dramatically during late stage, whereas the vRNA synthesis remains at similar maximal rate. The viral protein synthesis rate continues at maximal levels through the course of infection. To be specific, the vRNA, mRNA and protein synthesis of regulatory proteins NP and NS1 are preferentially occurred during early stage probably because NP regulates viral replication and transcription whereas NS1 regulates viral and host gene expressions required for viral replication. In contrast, the mRNA and protein synthesis of the structural proteins HA, NA and M1 preferentially occur during the late stage for the package of progeny viruses (Shapiro and Krug, 1988).

After viral genome replication and viral protein synthesis, the vRNP is assembled and exported into cytoplasm, which requires association with M1,

NS2/NEP (nuclear export protein) and cellular Crm1 export machinery (Akarsu et al., 2003). In the end of the viral life cycle, the vRNP is packaged with other viral proteins such as HA, NA, and M2 which are translated and transported through Golgi apparatus to the cell membrane. Finally, the progeny virion is released from cell membrane by the budding process (Figure 1.3).

1.1.4 Polymerase proteins of influenza A virus

The influenza A viral polymerase complex is consist of three subunits, PA (polymerase acidic), PB1 (polymerase basic 1) and PB2 (polymerase basic 2), which binds to the panhandle structure formed by the 5' and 3' end of each vRNA (Figure 1.2).

Figure 1.6 shows two domains of PA identified by proteolytic cleavage (Guu et al., 2008; Hara et al., 2006). The N-terminal domain of PA contains the endonuclease activity which cleaves the cellular capped pre-mRNA to generate a capped primer used for viral mRNA synthesis (the "cap-snatching" mechanism). Co-crystallization of PA C-terminal region interacting with N-terminus of PB1 was solved independently by two groups (He et al., 2008b; Obayashi et al., 2008). The structure of PA C-terminal region resembles the dragon head and its mouth clamps the small PB1 N-terminal region (Figure 1.6). Such interaction interface provides clues to the development of new antiviral drugs. In addition, the C-terminal region of PA contains a very basic groove that could interact with RNA, which is important in viral replication (Fodor et al., 2003). The PB1 contains the RNA dependent RNA polymerase (RdRp) domain and serves as the core polymerase in the trimeric polymerase

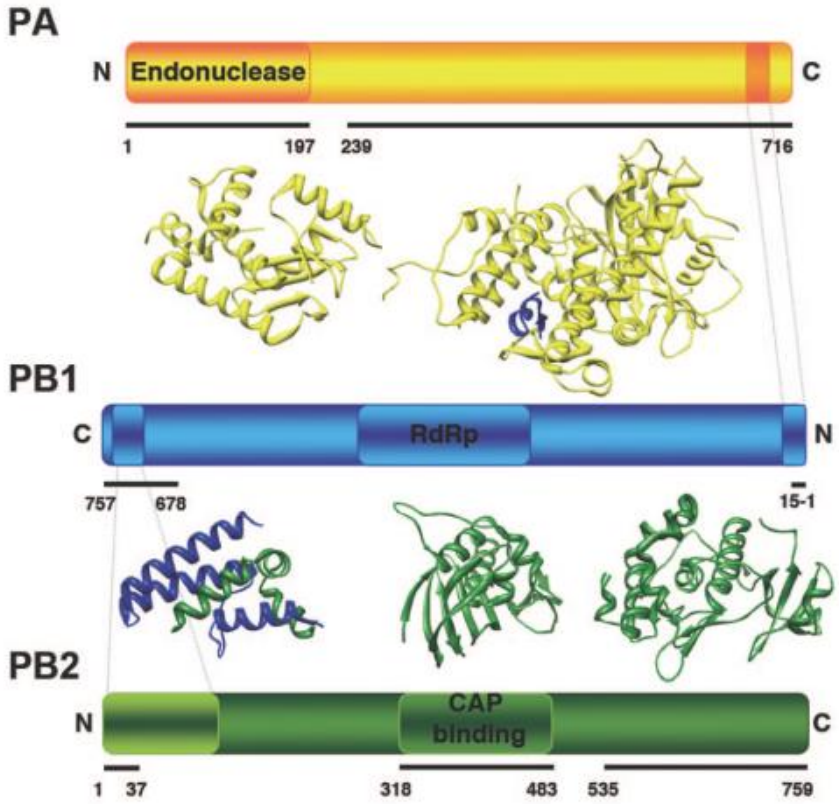

Figure 1.6 Diagram of influenza A viral polymerases PA, PB1, PB2, and their intersubunit interactions. Three polymerase proteins are shown as bar with N- and C-terminal region and functional domains are indicated. The regions with known structure are underlined and the corresponding structures are shown. The domains involved in intersubunit interactions are connected by dotted lines and the co-structures are presented (Adapted from (Resa-Infante et al., 2011)).

complex. In addition, the PB1 binding to the double-stranded panhandle structure of vRNA is required for transcription initiation (Fodor et al., 1994). PB1 N-terminal region 1-15 amino acids can interact with PA C-terminal domain. PB1 via its C-terminal 678-757 aa can also interact with the PB2 N-terminal region. The PB2 binds to the 5' cap of cellular capped pre-mRNA, which is required for viral mRNA transcription (Blaas et al., 1982; Ulmanen et al., 1981). It is important to understand how avian influenza virus adapts to human host. Few mutations on certain viral proteins could change host specificity. Some mutations are associated with the viral polymerase complex. One of the most well-known examples is the mutation of PB2 E to K at position 627 renders the avian influenza virus capable of replication in humans (Subbarao et al., 1993). However, the functional mechanism is not understood. One hypothesis is that, compared to PB2 with E627, the PB2 with K627 supports better viral replication in mammalian cells at lower temperature (33°C), which is the temperature of human upper respiratory tract; whereas the avian PB2 with E627 supports viral replication in birds intestinal tract with higher temperature (38–41°C) (Massin et al., 2001).

Recently, the Cusack research group just solved the crystal structures of complete bat influenza A polymerase complex and human influenza B polymerase complex, which contains vRNA promoter bound in both complexes (Pflug et al., 2014; Reich et al., 2014). Based on the complete crystal structure and by comparing with other known viral RNA polymerase structures, Cusack group proposed the structural mechanism by which influenza polymerases perform cap-snatching for transcription and unprimed initiation for replication, which was commented by Krug in the same issue

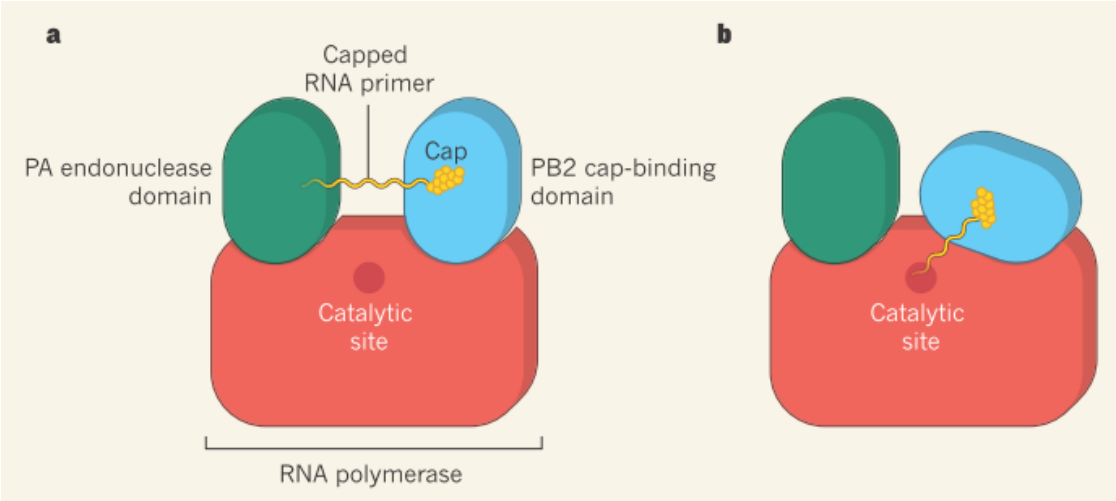

Figure 1.7 Diagram of RNA transcription by influenza polymerase. See text for details (Adapted from (Krug, 2014)).

(Krug, 2014). The polymerase proteins forms a U-shaped complex, in which PB1 locates in the bottom, and PA endonuclease domain and PB2 cap-binding domain locate in the two arms, as diagramed in Figure 1.7. Between the two arms of U-shaped complex there forms a channel with breadth corresponds to the length of the capped RNA primer that is cleaved by PA endonuclease from cellular pre-mRNA. The PB2 cap-binding domain binds cap of RNA primer, after cleavage by PA, the PB2 cap-binding domain rotates about 70° and directs the capped RNA primer to the PB1 catalytic site to initiate transcription. All three polymerase proteins are involved in binding two ends of viral RNA which is located close to the PB1 catalytic site for RNA synthesis. For the unprimed RNA replication, the PB1 protein contains an analogous putative priming loop (641-657aa) to stabilize the priming and incoming NTPs to facilitate unprimed initiation (Krug, 2014; Pflug et al., 2014; Reich et al., 2014).

All three polymerase proteins are translated in the cytoplasm and transported into nucleus for viral RNA replication/transcription. Although all three proteins contain nuclear localization signal, and they can interact with each other, they are transported in nucleus differently. The PA and PB1 protein interacts with each other in cytoplasm and transport into nucleus together, whereas PB2 protein transports with Hsp90 into nucleus. Finally, they form tripartite polymerase complex in nucleus (Deng et al., 2005; Fodor and Smith, 2004).

1.2 Cellular antiviral response against influenza virus

1.2.1 Antiviral response mediated by interferons

The viral infection triggers immune responses of host cells to counteract the viral invasion. The immune responses include the non-specific innate immunity and specific adaptive immunity. The innate immunity is the first line of antiviral response, where interferons (IFNs) play an essential role (reviewed in (Randall and Goodbourn, 2008; Sadler and Williams, 2008).

The IFNs are secreted cytokines, which are divided into three types, type I, II, and III based on their protein sequence. Type I IFNs is comprised of a large group of molecules, but the most well-known molecules are IFN-α and IFN-β, which are induced by viral infection. Type II IFNs contains IFN-γ, which is secreted from mitogenically activated T cells and natural killer (NK) cells, but are not induced directly by viral infection. Type III IFNs comprise three IFN-λ molecules, which is also induced by viral infection and shares the pathway as IFN-α/β response.

The most well established model of IFN-α/β-dependent antiviral response is through IFN-β. The induction of IFN-α is less well understood. In general, in the viral infected cells, the pattern-recognition receptors (PRRs) detect the viral nucleic acid such as the dsRNA and activate the signaling leading to activation of IFN regulatory factor-3 (IRF-3) and nuclear factor kappa B (NF-κB) in cytoplasm. The IRF-3 gets phosphorylated and dimerized, which is then transported into nucleus. Freed from its inhibitor IκB that is phosphorylated, ubiquitinated and degraded, the NF-kB is then transported into nucleus. The IRF-3, NF-κB and c-jun/ATF-2 forms complex called enhanceasome on the promoter of IFN-β and recruits transcription machinery, leading to transcription of IFN-β gene. The IFN-α/β proteins are then secreted and bind to the IFN-α/β

heterodimeric receptor (IFNAR1/IFNAR2) on self or the neighboring uninfected cells, which activates the JAK (tyrosine kinases associated with the receptor)-STAT (transcription factors that are phosphorylated by JAKs) signaling, leading to STAT1/2 heterodimer activation and translocation into nucleus. The STAT1/2 and IRF-9 form complex and bind to IFN-stimulated response element (ISRE) in the promoters of most IFN-stimulated genes (ISGs), leading to their transcriptions. The ISG proteins can either directly or indirectly counteract invading viruses so that the cells enter the antiviral state to prevent further viral replication and spread. The antiviral states against different viruses are established from combination of different ISGs. Some ISGs encode PRRs or transcription factors to increase IFN production. Some ISGs encodes proteins with direct antiviral functions. Some ISGs regulate translation arrest, or cell cycle arrest, or apoptosis, or cytoskeleton remodeling which is not favorable for viral replication. In addition to activating ISGs, IFN-α/β can also activate effector immune cells and promote acquired immune response.

1.2.2 Function of influenza A virus NS1 protein (NS1A protein) in counteracting antiviral response

The smallest influenza vRNA segment 8 encodes the nonstructural protein 1 (NS1A), and also NS2A protein through splicing. The NS1A and NS2A proteins share the same N-terminal 10 amino acids, and the subsequent sequence is different because NS2A uses the +1 reading frame after the 3’ splicing site. The expression level of NS1A to NS2A is around 10 to 1 due to inefficient splicing. The NS1A expresses in high level during viral

infection, and is not incorporated into virion. NS1A contains two functional domains: N-terminal 1 - 73 amino acids is the RNA-binding domain (RBD) and C-terminal 85 - 202~237 amino acids is the effector domain (ED). The NS1A RBD forms a symmetric homodimer with a unique six-helical chain fold (Chien et al., 1997; Liu et al., 1997; Yin et al., 2007), which binds dsRNA with relatively low affinity compared to cellular dsRNA-binding proteins (Tian and Mathews, 2001). The NS1A ED forms dimers with each monomer consisting of seven β-strands and three α-helices, which has several binding sites for viral and cellular proteins that are involved in many functions (Zhao et al., 2010b) (Figure 1.7).

NS1A is a multifunctional protein that counteracts many host antiviral responses and regulates viral and cellular functions. Overall speaking, one major function of NS1A is to inhibit the IFN production or to inhibit the IFN-mediated antiviral response. Previous study showed one function of NS1A RBD is to sequester the viral dsRNA away from being recognized by protein kinase R (PKR), thus inhibiting the activation of PKR signaling (Lu et al., 1995; Nemeroff et al., 1995). However, subsequent studies from our lab have elucidated the function of the NS1A RBD by using Influenza A/Udorn/72 virus expressing NS1A with R38A mutant that lose dsRNA binding activity. The main function of NS1A RBD is to counteract one of IFN-induced antiviral responses, the IFN-α/β-induced 2'-5'-oligo (A) synthetase (OAS)/RNase L pathway (Min and Krug, 2006). In addition, the PKR activation is inhibited by binding to NS1A ED (123-127 aa), but not due to sequestration of dsRNA by NS1A RBD. Further, the NS1A RBD is not involved in inhibition of IFN production (Li et al., 2006; Min and Krug, 2006; Min et al., 2007).

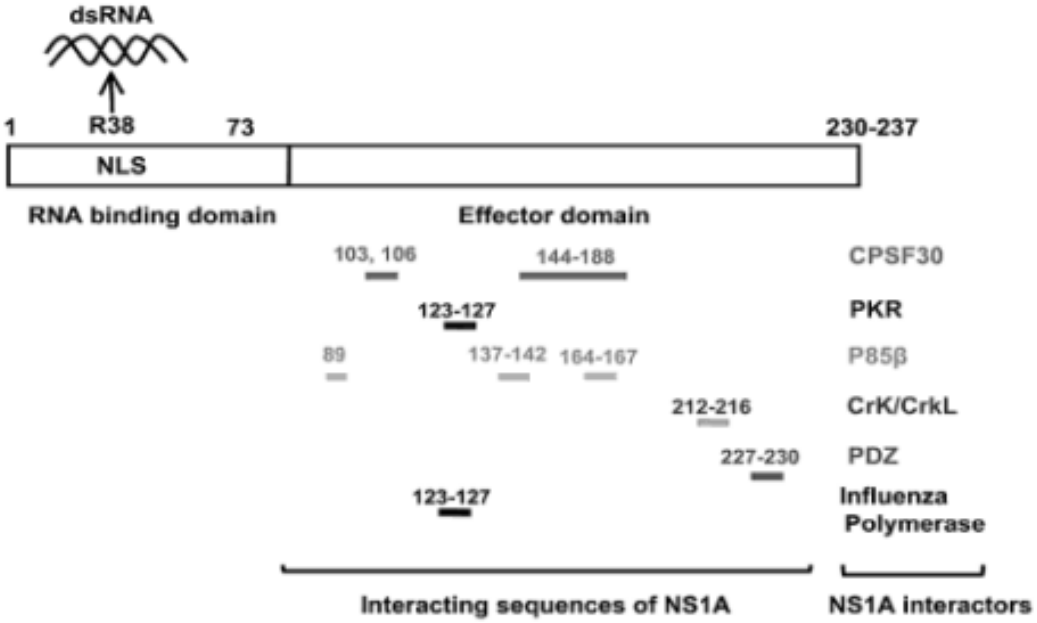

Figure 1.8 The NS1A protein and its interacting partners with corresponding binding regions. See text for details (Adapted from (Zhao et al., 2010b)).

The NS1A ED contains interaction regions for many cellular proteins to regulate their functions, which provides favorable environment for viral replication: (1) NS1A ED (103,106; 144-188 aa) binds the 30kD subunit of the cleavage and polyadenylation specificity factor (CPSF30), which inhibits the cellular pre-mRNA 3'-end processing, leading to reduced antiviral gene expression (discussed in detail in section 1.2.3) (Chen et al., 1999; Li et al., 2001; Nemeroff et al., 1998; Noah et al., 2003; Twu et al., 2006); (2) NS1A ED (123, 127 aa) binds N-terminal region of PKR to inhibit its activation by viral dsRNA, which then inhibits translation (Li et al., 2006; Min et al., 2007); (3) NS1A ED (89; 137-142; 164-167 aa) binds to p85β subunit of phosphatidylinositol-3-kinase (PI3K), leading to its activation and thus inhibiting viral-induced apoptosis (Ehrhardt et al., 2007; Hale et al., 2006; Shin et al., 2007); (4) The avian NS1A ED (213-216) binds to Crk/CrkL to promote PI3K activation (Heikkinen et al., 2008); (5) The avian NS1A ED (227-230) binds to PDZ to regulate virus pathogenicity in mice (Jackson et al., 2008; Obenauer et al., 2006); (6) Recently, the NS1A ED from human H3N2 virus was shown to have histone-like sequence (histone mimic, 226-229 aa) that binds to human PAF1 transcription elongation complex (hPAF1C) to suppress certain antiviral response (Marazzi et al., 2012). It should be noted that these NS1A interactions can be virus strain-specific.

In addition to the interactions described above, it has been proposed that NS1A interacts with retinoic acid-inducible gene I (RIG-I), a critical cytoplasmic viral RNA sensor, to inhibit the IFN production (Guo et al., 2007b; Mibayashi et al., 2007; Opitz et al., 2007; Pichlmair et al., 2006). RIG-I serves as a PRRs to recognize 5'-tri-phosphate on the dsRNA panhandle structure

from influenza vRNA, leading to RIG-I activation and interaction with the adaptor MAVS, which then serves as a platform to activate the IRF3 and NFκB pathway (Takeuchi and Akira, 2009). However, the NS1A binding to RIG-I to inhibit IRF-3 activation and IFN production is somewhat controversial because it is only established using laboratory-adapted influenza strain PR/8/34 (Krug, 2015).

1.2.3 NS1A protein binds to CPSF30 to block 3' end processing of cellular pre-mRNA

One major function of NS1A is to inhibit the IFN production. The NS1A through ED interacts with two cellular proteins, CPSF30 (Nemeroff et al., 1998) and poly(A)-binding protein II (PABII) (Chen et al., 1999) that are essential for cellular pre-mRNA 3'-end processing, to inhibit antiviral gene expression, including IFN production. The mechanism by which NS1A binds to CPSF30 and PABII to block 3' end processing of cellular pre-mRNA is in Figure 1.8 (Chen and Krug, 2000). CPSF30 binding site locates on a region centered at aa 186, whereas PABII binds to aa 223-237 on NS1A (Li et al., 2001). In cellular pre-mRNA 3'end processing, the binding of CPSF complex to the AAUAAA poly (A) signal is required for cleavage and polyadenylation of cellular pre-mRNAs (Colgan and Manley, 1997). The PABII stimulates the poly (A) polymerase (PAP)-catalyzed poly(A) tail synthesis (Chen et al., 1999). Therefore, the binding of NS1A to CPSF30 and PABII blocks their function in pre-mRNA 3'end processing, which results in accumulation of pre-mRNA with short poly(A) tail (~12 nts) in nucleus in influenza infected cells

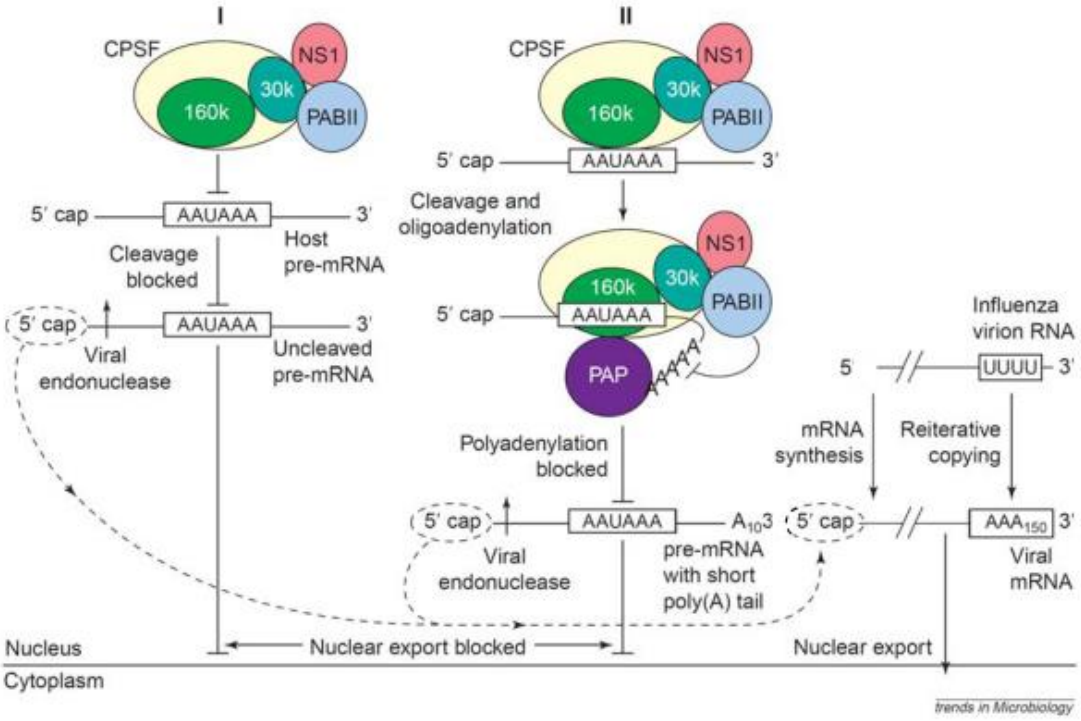

Figure 1.9 Mechanism by which NS1A binds to CPSF30 and PPABII to block 3' end processing of cellular pre-mRNA. See text for details (Adapted from (Chen and Krug, 2000)).

(Nemeroff et al., 1998). Further, the 5'cap of these accumulated pre-mRNAs in nucleus can be cleaved by viral polymerase and used for primer in viral mRNA synthesis (the "cap-snatch" mechanism). The inhibition of pre-mRNA 3'end processing does not affect viral mRNA maturation because the 3'poly(A) tail is added to viral mRNA by reiterative copying the U track in the virion RNA (Poon et al., 1999).

To sum up, there are two main mechanisms by which influenza A NS1 can inhibit IFN production: (1) to inhibit the RIG-I mediated IRF-3 and NFκB activation, thus blocking the IFN gene transcription; and (2) to bind to CPSF30/PABII, which inhibits the 3'end processing of IFN pre-mRNA. However, whether influenza virus requires both mechanisms to efficiently inhibit IFN production is controversial. The observation from our lab that only some influenza strains strongly inhibit IRF-3 activation and not all NS1A can bind CPSF30 to block pre-mRNA 3'end processing provides some clues. Specifically, NS1A from some seasonal H1N1, 2009 pandemic H1N1, and H5N1 can strongly inhibit IRF-3 activation, whereas NS1A from seasonal H3N2, H2N2, and some seasonal H1N1 does not inhibit IRF-3 activation. The NS1A of H3N2 and H2N2, which does not inhibit IRF-3 activation, can bind to CPSF30 and inhibit IFN pre-mRNA effectively (Kuo et al., 2010). In contrast, the NS1A from 2009 pandemic H1N1 that strongly inhibits IRF-3 activation does not bind to CPSF30 effectively (Figure 1.9). However, not all influenza viral strains fall into these two categories. For example, the NS1A from H5N1 after 1997 inhibits both IRF-3 activation and INF pre-mRNA 3'end processing. It remains a mystery why one mechanism is sufficient for some viruses whereas some viruses require both (Krug, 2015).

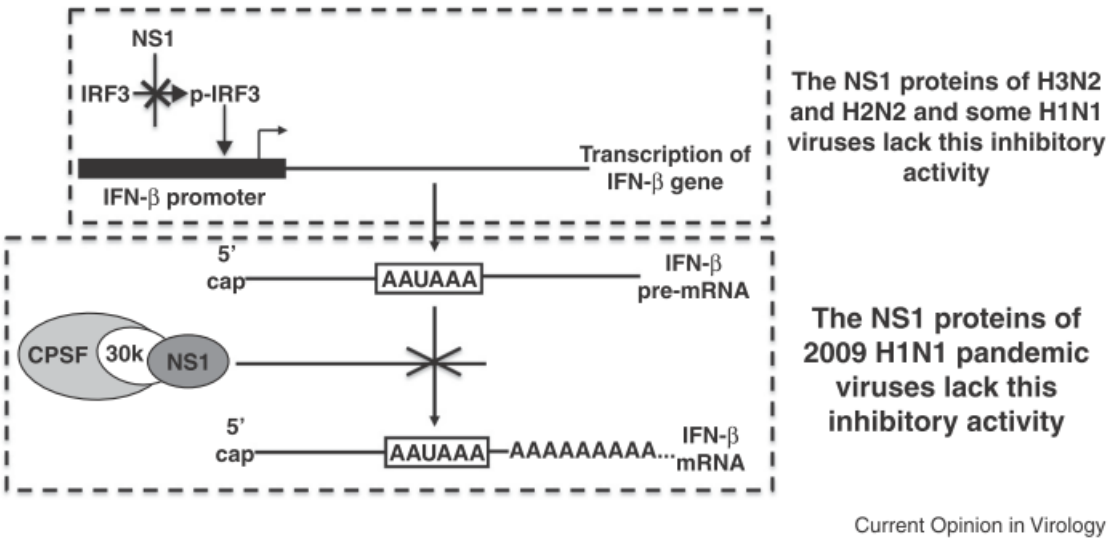

Figure 1.10 Two main mechanisms by which NS1A inhibit IFN production. For some influenza strains, their NS1A either blocks IRF-3 activation or blocks pre-mRNA 3'end processing to inhibit IFN production (Adapted from (Krug, 2015)).

Chapter 2: Identify the cellular proteins associated with infected cell NS1A-CPSF30 protein complexes

2.1 Introduction

Our lab established that NS1A binds to CPSF30 to block the cellular pre-mRNA 3'end processing. However, the ability of NS1A to bind CPSF30 is virus strain specific. The NS1A from 1997 Hong Kong H5N1 (HK97) does not bind to CPSF30 effectively in vitro because two hydrophobic amino acids F103 and M106 that are required for stabilization of NS1A-CPSF30 complex are mutated to L103 and I106. However, HK97-NS1A binds to CPSF30 to a significant extend in vivo because cognate internal viral protein(s) stabilize the NS1A-CPSF30 complex in infected cells (Twu et al., 2007). Subsequent study showed that viral polymerase complex (PA, PB1, PB2 and NP) serves as the cognate proteins to stabilize the NS1A-CPSf30 complexes. Further, the viral polymerase proteins were shown to be the integral component of the NS1A-CPSF30 complex even when the NS1A contains the F103 and M106 and thus can bind to CPSF30 effectively (Kuo and Krug, 2009). The study from Kuo et al. provided a useful platform to purify the functional NS1A-CPSF30 complexes from virus infected cells by affinity selectin of CPSF30 and found the association of viral polymerase proteins.

In this study, we further modified the purification procedure from study by Kuo et al., 2009 and purified CPSF30-NS1A complexes by sequential affinity selection of CPSF30 and NS1A from Influenza A/Udorn/72 virus (Ud) infected cells. Then the purified products were subjected to mass spectrometry analysis to identify the component proteins. Many host proteins were

identified. Several of them belong to the cellular RNA helicase family. We tested whether they have functional impact on influenza virus replication by knocking down each candidate protein with corresponding siRNA individually. Interestingly, knockdown of two RNA helicases (DDX21 and DHX30) out of four candidate RNA helicases (the other two are DHX9 and MOV10) enhanced viral replication, indicating that DDX21 and DHX30 restrict influenza virus replication.

Further experiments on DDX21 demonstrated that DDX21suppresses viral RNA synthesis at early time point of infection due to the ability of DDX21 binding to PB1, which inhibits assembly of the tripartite viral polymerase (PA, PB1 and PB2). At late time point of infection, the increasing amount of NS1A binds to DDX21 and displaces PB1 from DDX21, which counteracts the DDX21-mediated antiviral activity (Chen et al., 2014). These results demonstrated that identification of associated host proteins from purified CSPF30-NS1A complexes from infected cells provides a useful platform leading to discovery of important host proteins that regulate influenza virus replication.

Two types of anti-influenza drugs are currently available, which targets either NA (oseltamivir, zanamivir) or M2 (amantadine/rimantadine) (Das et al., 2010). However, most circulating influenza A viruses are resistant to amantadine/rimantadine and are developing resistance to oseltamivir (Deyde 2007, Bloom 2010). Thus the development of new anti-influenza drugs is required. The present study provides a way to identify associated host proteins that play important functions in influenza virus replication. One

approach for new antivirals development would be to target these host proteins and/or their interaction with specific viral proteins.

2.2 Materials and Methods

2.2.1 Cell-lines and recombinant viruses

HEK-293T human kidney cell-line (ATCC CRL-11268), HeLa human cervix adenocarcinoma cell-line (ATCC CCL-2), A549 human lung carcinoma cell-line (ATCC CCL-185), Madin-Darby canine kidney cell-line (MDCK) (ATCC CCL-34), and Calu3 human lung adenocarcinoma cell-line (ATCC HTB-55) were purchased from ATCC. 293T, HeLa, A549 and MDCK cells were grown in Dulbecco's modified Eagle's medium (DMEM) (GIBCO) supplemented with 10% heat-inactivated fetal bovine serum (FBS) (GIBCO), 2 mM l-glutamine, 100 units/ml penicillin, and 100 µg/ml streptomycin (1% PSG) (GIBCO) at 37°C under a 5% CO2/95% air atmosphere. Calu3 cells were grown in Advanced MEM (GIBCO) supplemented with 10% FBS and 1% PSG at 37°C under a 5% CO2/95% air atmosphere.

H3N2 Influenza A/Udorn/72 (Ud) virus stocks were grown in 10-day fertilized eggs, and virus titers were determined by plaque assays in MDCK cells. Recombinant influenza A viruses were generated using 12 plasmids based reverse genetics (Figure 2.1) (Takeda et al., 2002). The negative-strand viral genomic RNAs are encoded in eight pHH21 plasmids under the control of a polymerase I promoter. Eight pHH21 plasmids containing full-length cDNA for each vRNAs of Ud virus, and four pcDNA plasmid expressing PA, PB1, PB2 and NP were provided by Makoto Takeda (Dr. Lamb’s lab,

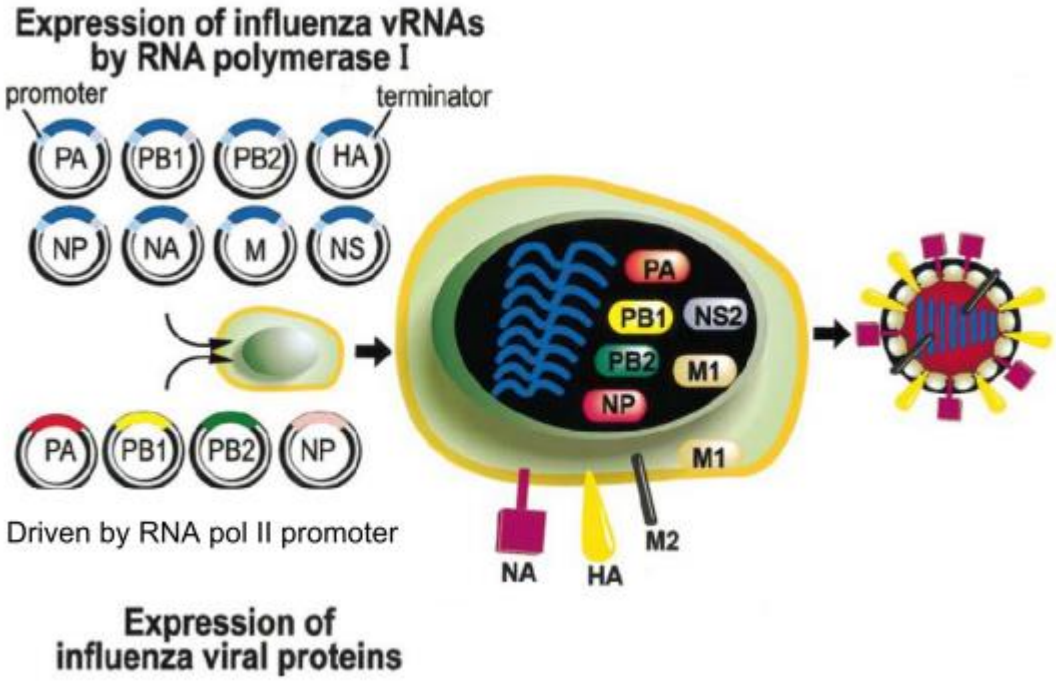

Figure 2.1 The procedure of generating recombinant influenza A Ud viruses by 12 plasmids based reverse genetics. See text for details (Adapted from (Neumann and Kawaoka, 2001)).

Northwestern University). In brief, recombinant Ud virus was generated by co-transfection of 8 pHH21 plus 4 pcDNA plasmids into 293T cells in serum- and antibiotics-free Opti-MEM I medium (GIBCO). Medium was changed to Opti-MEM I supplemented with 2.5μg/ml N-acetylated-trypsin (Sigma) and 1% PSG at 8 hours post transfection. The 293T cells were overlaid onto MDCK cells for viral amplification at 18 hours after medium change. If the recombinant viruses are generated, the cells will show cytopathic effect (CPE), which leads to cell death. Then the supernatant containing the recombinant viruses was collected and stored at -80°C. Plaque assay in MDCK cells was performed to isolate individual viral plaques. Individual viral plaque was picked and injected into the allantoic cavity of 10-day fertilized chicken eggs for further virus amplification (Charles River Laboratories) at 34°C. Allantoic fluid containing virus was harvested at 48 hours after injection, and stored at -80°C. Virus titer (plaque forming units (PFU) /ml) was determined by plaque assays in MDCK cells. The viral genomic RNAs were extracted by Trizol reagent (Invitrogen) and chloroform method and subjected to RT-PCR using specific primers. The cDNAs of each viral RNAs were sequenced for confirmation.

To generate Ud viruses expressing 1xFLAG-tagged NS1A proteins, a FLAG sequence was inserted between the 5'UTR and coding sequence of NS reading frame in the pHH21 plasmid by standard cloning procedure. All eight genomic RNA segments of the recombinant viruses were sequenced (Zhao et al., 2010a).

2.2.2 Purification of NS1A-CPSF30 complexes from infected cells

To purify the NS1A-CPSF30 protein complex by sequential affinity

selection of CPSF30 and NS1A from Ud infected cells, $4x10^7$ of 293T cells (2x 150mm dishes) were transfected with a pcDNA3 plasmid encoding N-terminal glutathione *S*-transferase (GST) tagged CPSF30 (GST-CPSF30) using the Mirius TransIT-LTR Transfection reagent (Kuo and Krug, 2009), and 24 hours later were infected with 2 plaque-forming units/cell of either wild-type Ud virus or the Ud virus expressing a 1xFlag-tagged NS1 protein (Zhao et al., 2010a). Cells were collected 12 hours after infection, and were disrupted by suspension in a lysis buffer containing 50 mM Tris-HCl pH 7.5, 150 mM NaCl, 5 mM EDTA, 2.5 mM MgCl2, 1% NP40, 10% glycerol, 1 mM PMSF, and 1x Protease inhibitor (Roche), followed by passage through a 25 gauge needle several times for further disruption. The extracts were diluted with a buffer containing 50 mM Tris-HCl pH 7.5, 150 mM NaCl, 1 mM PMSF, and 1x Protease inhibitor to make the 0.5% final concentration of NP40, and affinity purified using glutathione sepharose beads (Amersham). The glutathione sepharose beads that bound to GST-CPSF30 complexes were washed in a solution containing 50 mM Tris-HCl pH 7.5, 150 mM NaCl and 0.5% NP40, and eluted by 10mM glutathione. The eluate was then bound to agarose beads conjugated with the M2 monoclonal Flag antibody (Sigma), washed four times with a buffer containing 50 mM Tris-HCl pH7.5, 150 mM NaCl, 0.25% NP40, and Flag-NS1A containing protein complexes were eluted with 500 ng/ml of 3xFlag peptides (Sigma). Immunoblots confirmed that the purified product contains GST-CPSF30 and 1xFlag-NS1A (Chen et al., 2014).

2.2.3 Mass spectrometry analysis of the purified NS1A-CPSF30 complexes

The purified product was then concentrated using Amicon centrifugal filter units with 10kD cut-offs (Millipore). An aliquot of the concentrated purified product was analyzed by SDS-PAGE gel, which was stained with colloidal blue (Invitrogen) to visualize the purified proteins. Gels from several molecular weight regions were cut out and sent for mass spectroscopy analysis by Harvard Taplin Mass Spectrometry Facility. Another aliquot of the concentrated purified product was analyzed by immunoblots probed with the indicated antibodies. Repeated rounds of purification and mass spectrometry have been done and the identified proteins associated with GST-CPSF30 and 1xFlag-NS1A complexes were very consistent (Chen et al., 2014).

2.2.4 SiRNA knockdown of DDX21 or DHX30

Four RNA helicases were identified associated with the GST-CPSF30 and 1xFlag-NS1A complexes. Knockdown of each helicases by corresponding siRNA was performed to screen whether they have functional impact on influenza virus replication in cells. All siRNA duplexes were designed and synthesized by Invitrogen (Stealth RNAi™ siRNA), and re-suspended in DEPC-treated water to a final concentration of 20μM for storage at -80°C. SiRNA sequences used in this study (chapter 2) are shown in Table 2.1.

For preliminary screening, three siRNAs from Invitrogen were mixed and tested for knockdown efficiency of target gene in HeLa cells. To further test functional impact of candidate genes on influenza virus replication, siRNA knockdowns were performed in HeLa cells followed by infection of Ud virus at 2-5 pfu/cell for detection of viral protein synthesis in single cycle of viral growth.

Table 2.1 siRNA sequences used in this study

Target	Oligo#	Sequence (complimentary sequence not shown)
DDX21	1	5’- CCA GCG CUC CUU GAU CAA CUC AAA U
DDX21	2	5’- GCU GGG CGA GGA GAU UGA UUC CAA A
DHX30	1	5’- CAA GGU GAU UCA GAU UGC AAC GUC A
DHX30	2	5’- GCG GCA GCU GAA UCC AGA GAG UAU U
Control		5’- UUG AUG UUG AGC AAU UCA CGU UCA U

Table 2.2 Primer sequences used in this study

Target	Strand	Sequence
DDX21	Forward	5’- CCA GCA AAG ATG CCA TCA GGC TTT
DDX21	Reverse	5’- CCA GCG TCG TGA ATC ATG CCA TTT
DHX30	Forward	5’- AAT GCG CAC TCG ATT TGG ACC TTG
DHX30	Reverse	5’- GCT GTC ATG GCT CAA CAG TGC TTT
DHX9	Forward	5’- TCG AGC CAT CTC TGC TAA AGG CAT
DHX9	Reverse	5’- TTC CAT TGT CGT ATC GGG CCA TCT
MOV10	Forward	5’- GGC AAT TAA GCA GGT GGT GAA GCA
MOV10	Reverse	5’- AAG CGT TCT CGA TCC ACG ACA TCA

The candidate genes that had effect on viral protein synthesis in single cycle growth were then tested for their effect in Calu-3 cells with siRNA knockdown followed by Ud virus infection at 0.001 pfu/cell for analysis of infectious virus produced in multiple cycle of viral growth.

To perform siRNA knockdown in HeLa cells, the Xtreme ® siRNA transfection reagent (Roche) was diluted in Opti-MEM I (Invitrogen) for 5 minutes, whereas the siRNA was diluted in Opti-MEM I and then mixed with the diluted transfection reagent in a ratio of 2.5µl reagent per 20nM final concentration of siRNA in cell culture. The siRNA mixture was incubated for another 20 minutes before gently added into cell culture that have been changed with fresh DMEM containing 10% FBS and 1% PSG. 20nM final concentration of siRNA was used for knockdown in HeLa cells for 36 - 48 hours before virus infection. For maximal knockdown efficiency in Calu-3 cells, cells were trypsinized, washed and re-suspended in serum- and antibiotics-free Advanced MEM. At 8 - 18 hours after addition of siRNA mixture into re-suspended Calu-3 cell cultures, medium was replaced with fresh Advanced MEM with 10% FBS and 1% PSG. 80 - 100nM final concentration of siRNA was used for knockdown in Calu-3 cells for 36 - 48 hours before virus infection.

2.2.5 RNA Extraction and Semi-quantitative Reverse Transcription (RT)-PCR

For preliminary screening the siRNA knockdown efficiency, mRNA level of target genes (DDX21, DHX30, DHX9 and MOV10) were determined. Cells transfected with siRNA against each target for 36-48 hours were extracted

and total RNA was extracted with the Trizol reagent (Invitrogen) and chloroform according to manufacturer's instructions. A mixture of the RNA and the oligo-dT primer was incubated at 65°C for 10 minutes, and then added to the reverse transcription mixture containing reverse transcriptase (Roche), dNTP, and RNaseOut (Invitrogen). After incubation at 55°C for 30 minutes, the generated cDNA was PCR amplified using PCR supermix (Invitrogen) with specific primers for each candidate target genes (Table 2.2). Amplified PCR products were separated by electrophoresis on 1% agarose.

2.2.6 Antibodies and Immunoblotting

Antibody against the major structural proteins of Ud virus, which detects NP as well as HA and M1, was provided by Robert A. Lamb (Chen et al., 2007). NS1 antibody was generated against GST tagged NS1A protein from our lab. Actin and tubulin antibodies were obtained from Sigma and Cell Signaling, respectively. DDX21 and DHX30 antibodies were obtained from Abcam.

Cells harvested at indicated time were extracted in a lysis buffer containing 50 mM Tris-HCl pH 7.5, 150 mM NaCl, 5 mM EDTA, 2.5 mM MgCl2, 1% NP40, 10% glycerol, 1 mM PMSF, and 1x Protease inhibitor (Roche). Proteins were separated by SDS-PAGE and transferred to nitrocellulose membrane (Bio-Rad) by semi-dry transfer method. Membrane was blocked in TBS containing 0.2% Tween (TBST) and 5% non-fat milk, and then incubated with the primary antibody against the protein of interest. After washing away unbound primary antibody with TBST, the membrane was incubated with the corresponding secondary antibody. After another wash with

TBST, proteins on the membrane were detected with enhanced chemiluminescence (ECL) western blotting substrate (Pierce) and exposed to CL-Xposure film (Pierce).

2.2.7 Virus infection and plaque assays

For single cycle virus replication, HeLa cells were infected with Ud virus at 2-5 pfu/cell (high multiplicity of infection or high M.O.I.). HeLa cells were washed with PBS to remove serum in the medium. Ud virus was diluted in serum-free DMEM containing 1% BSA and 1% PSG, and added onto cells at 2-5 pfu/cell. Cells were incubated at 37°C for 1 hour to let virus binds to cells. After wash with PBS and change with fresh serum-free DMEM and 1% PSG, cells were incubated for the indicated times. For multiple cycle virus replications, Calu-3 cells were infected with Ud virus at 0.001 pfu/cell (low M.O.I.). Calu-3 cells were washed and incubated with diluted Ud virus in serum-free Opti-MEM I containing 1% BSA and 1% PSG. After 1 hour incubation, cells were washed with PBS and replaced with Advance MEM containing 2.5μg/ml N-acetylated trypsin and 1% PSG. At indicated time post infection (usually 12, 24, 36 and 48 hours), small amount of supernatant from cell culture was harvested and the virus titer was determined by plaque assays.

For plaque assays, confluent monolayer MDCK cells were washed and infected with serial 10-fold dilutions of virus in serum-free DMEM containing 1% BSA and 1% PSG. After 1 hour virus absorption, medium was replaced with serum-free DMEM containing 1% PSG and 2.5μg/ml N-acetylated trypsin pre-mixed with 1% (final conc.) non-solidified agarose at 42°C. The solidified

cell culture was incubated for 48 hours and formation of viral plaques against viable cells was stained and visualized with crystal violet.

2.3 Results

2.3.1 Purification of NS1A-CPSF30 complexes from influenza A virus infected cells

The basic experimental procedure for purification of NS1A-CPSF30 complexes from influenza virus infected cells is diagrammed on in Figure 2.2 (A). To scale-up the purification to get enough product for mass spectrometry analysis, $4x10^7$ of 293T cells (2 x 150mm dishes) were transfected with GST-CPSF30 for 24 hours, and infected with either wild-typed Ud virus (as a control) or Ud virus expressing 1xFlag-NS at 2 pfu/cell. 12 hours after infection, cells were collected and extracted. Cell lysate was first selected with GST beads to pull down GST-CPSF30-containing protein complexes, which was subsequently selected with beads conjugated with anti-Flag M2 antibody to immuneprecipitate 1xFlag-NS-containing protein complexes.

During the purification procedure, aliquots of each step were analyzed by immunoblots to monitor the purification specificity and efficiency (Figure 2.2). The immunoblot with antibody against NS1A shows similar expression of wt-NS1A and 1xFlag-NS1A in cells. After binding to GST beads, there were some unbound GST-CPSF30 and 1xFlag-NS1A remaining in the cell lysate (lane 2 and 3 in Figure 2.2 (B)). Complexes containing GST-CPSF30 and wt-NS1A or 1xFlag-NS1A were successfully selected and eluted from GST-beads (lane 4 and 5). Elution efficiency was high because there was not much left in the

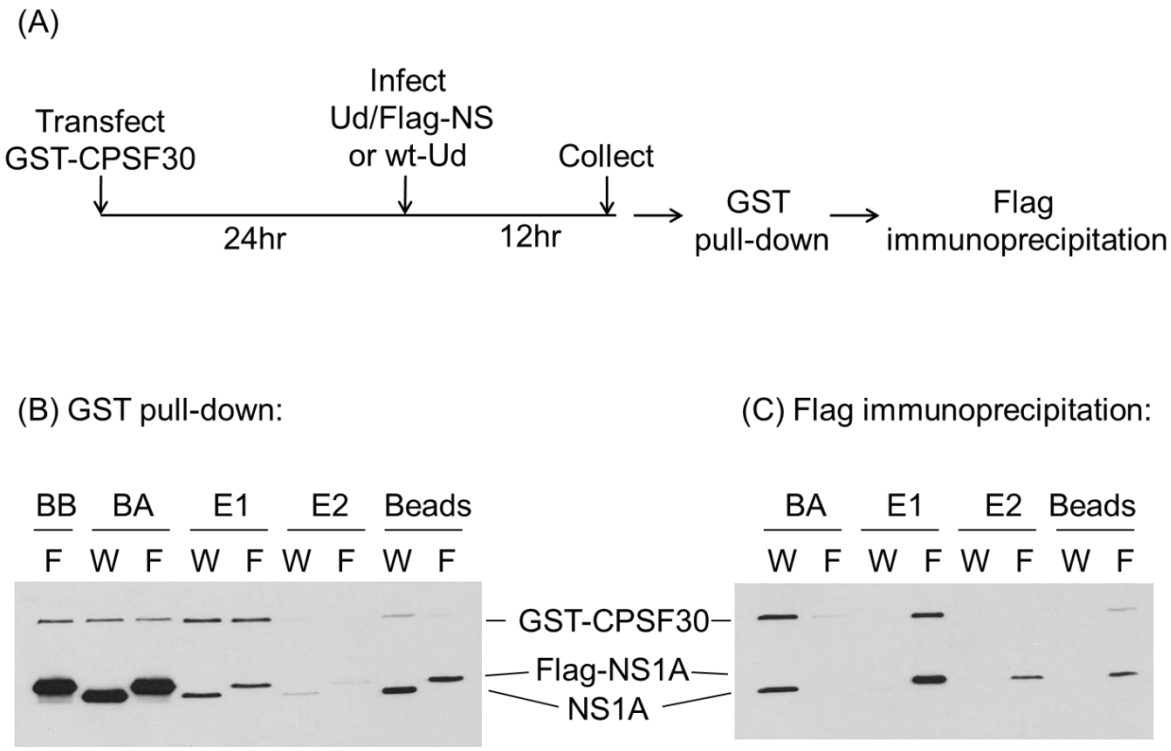

Figure 2.2 Purification of NS1A-CPSF30 complexes from infected cells. **(A)** 293T cells were transfected with GST-CPSF30 for 24 hours and then infected with either wt Ud or Ud expressing 1xFlag-NS. 12 hours after infection, cells were collected and extracted for sequential selection with GST pull-down followed by Flag immunoprecipitation. **(B)** Immunoblot of GST pull-down. Cells infected with wt-Ud (W) or Ud expressing 1xFlag NS (F) were selected with GST beads. BB: cell extract before binding to GST-beads; BA: cell extract after binding to GST-beads; E1: first elution from GST-beads; E2: second elution from GST-beads; Beads: GST-beads after two rounds of elution. **(C)** Immnoblot of Flag selection. Eluate from GST pull-down was selected with beads conjugated with Flag M2 antibody. BA: eluate after binding to anti-Flag-beads. E1: first elution from anti-Flag-beads; E2: second elution from anti-Flag-beads; Beads: anti-Flag-beads after two rounds of elution.

second elution and on the beads (lane 6 - 9). The eluate from GST beads was subsequently selected with anti-Flag M2 beads. After binding to anti-Flag-beads, the complexes containing GST-CPSF30 and wt-NS1A were still in the eluate (lane 1 and 3 in Figure 2.2 (C)), whereas the complexes containing GST-CPSF30 and 1xFlag-NS1A were effectively selected and eluted from anti-Flag-beads, indicating the high specificity and efficiency of Flag selection (lane 2 and 4). Elution efficiency was high because there was not much left in the second elution and on the beads (lane 5 - 8) (Chen at al. 2014).

2.3.2 Identification of the cellular proteins associated with the NS1A-CPSF30 complexes by mass spectrometry

The purified complexes containing CPSF30 and NS1A were immunoblotted with antibody against the known associated viral proteins. The immunoblots in Figure 2.3 (A) showed that the purified complexes contain not only NS1A and GST-CPSF30, but also viral polymerase proteins PA, PB1, PB2 and NP, confirming previous results from our lab (Kuo and Krug, 2009). Notably, 1xFlag-NS2A/NEP protein (15 kDa) was not detected, presumably because it does not bind to CPSF30 and hence was not co-purified by GST pull-down. The purified CPSF30-NS1A product from either wt-NS1 control or 1xFlag-NS1 sample were resolved by SDS-PAGE electrophoresis, and visualized by Colloidal blue staining (Figure 2.3 (B)). Two major bands on gel correspond to GST-CPSF30 (~50 kDa) and 1xFlag-NS1A (~27 kDa). The Flag-NS1 sample contains proteins larger than 65 kDa that were absent in the control wt NS1 sample. Therefore, the gel pieces of region of high molecular weight (region of interest, 70 - 170 kDa) were cut out and sent to Harvard for

(A) (B)

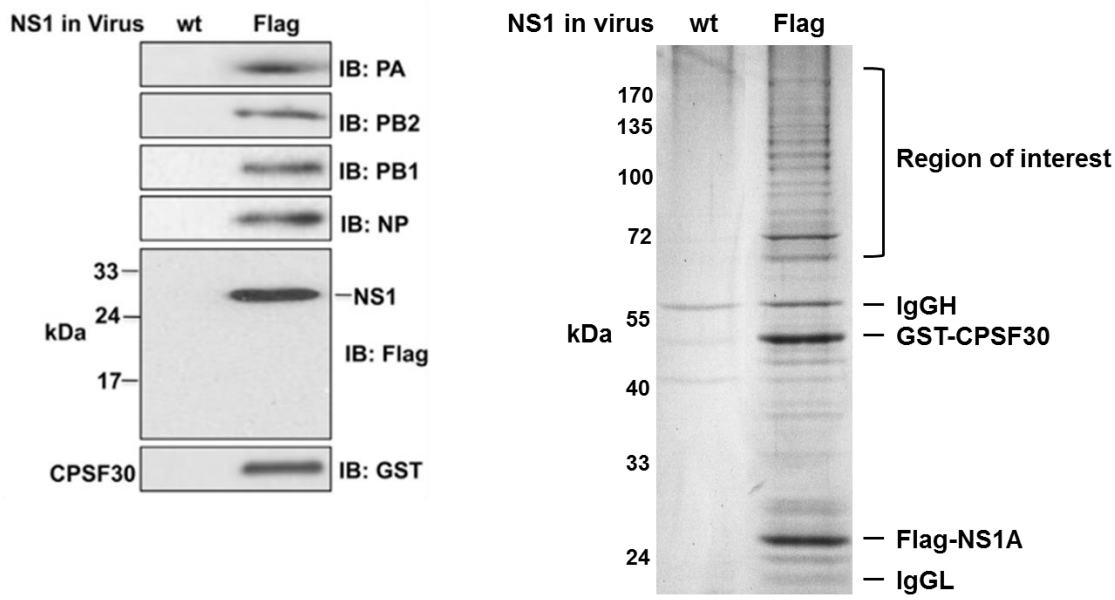

Figure 2.3 The purified NS1A-CPSF30 complexes contains many other proteins. (A) Immunoblot for the viral PA, PB1, PB2, NP and NS1 proteins and for CPSF30 in the purified CPSF30-NS1A complexes from Flag-NS1 sample or the control wt NS1 sample (Adapted from (Chen et al., 2014)). **(B)** SDS-PAGE electrophoresis followed by Colloidal blue staining of the proteins in the purified CPSF30-NS1A complexes from Flag-NS1 sample or the control wt NS1 sample.

Table 2.3 Mass spectrometry result of associated proteins in purified CPSF30-NS1A complexes

70-90 kDa		90-110 kDa		110-140 kDa		140-170 kDa	
Protein	Matches	Protein	Matches	Protein	Matches	Protein	Matches
PABP4	10	**DDX21**	27	**DHX9**	21	MYH9	20
HNRPM	10	Nucleolin	27	**DHX30**	18	**CPSF160**	18
PABP3	5	**Mov10**	23	Matrin3	16	LaRP1	11
FIP1	5	**PB1**	14	LaRP1	11	Q65ZQ1	6
Y00305	3	**ZAP**	13	Nucleolin	10	DDX21	6
PB2	3	ILF3	11	HNRPU	8	MYH10	4
		CPSF100	8	Q65ZQ1	6	WDR33	3
		Q65ZQ1	6	Rent1	6	O14654	3
		DHX36	6	CL010	6		
		HNRL1	6	DDX21	5		
		HNRPU	4	SF3B3	5		
		RBM28	4	Q9Y687	3		
		XRN2	4				

mass spectrometry analysis. Repeated rounds of purification and mass spectrometry analysis were done and the results were very consistent. Hence only one representative result from mass spectrometry is shown and summarized in Table 2.3. Four different regions based on molecular weight were analyzed. Number of peptides that matched the protein sequence was indicated as “Matches”. Several influenza viral polymerase proteins were identified associated with NS1-CPSF30 complexes: PB2 in 70 - 90 kDa region, and PB1 in 90 - 110 kDa region, which was consistent with and confirmed the immunoblot result. Importantly, several CPSF subunit proteins (FIP1 in 70 - 90 kDa, CPSF100 in 90 - 110 kDa; CPSF160 in 140 - 170 kDa) and PABP proteins (PABP3 and PABP4 in 90 - 110 kDa) were identified, which validated our purification procedure and demonstrated that we purified functional active NS1-CPSF30 complexes from infected cells (Chen and Krug, 2000).

Interestingly, four cellular RNA helicases were identified as top candidates associated with NS1-CPSF30 complexes. DDX21 (27 matches) and MOV10 (23 matches) were in the 90 - 110 kDa region, and DHX9 (21 matches) and DHX30 (18 matches) were in the 110 - 140 kDa region. The other top candidates were nucleolin (27 matches, 70 - 90 kDa) which is major nucleolar protein, and ZAP (13 matches, 70 - 90 kDa) which is a zinc-finger antiviral protein (the main project of my thesis, presented in chapter 3), and MYH9 (20 matches, 140 - 170 kDa) which is heavy-chain of a non-muscle myosin.

Among the four candidate four RNA helicases, DHX30 was reported to have a role in HIV-1 gene expression (Zhou et al., 2008). DHX9 was reported

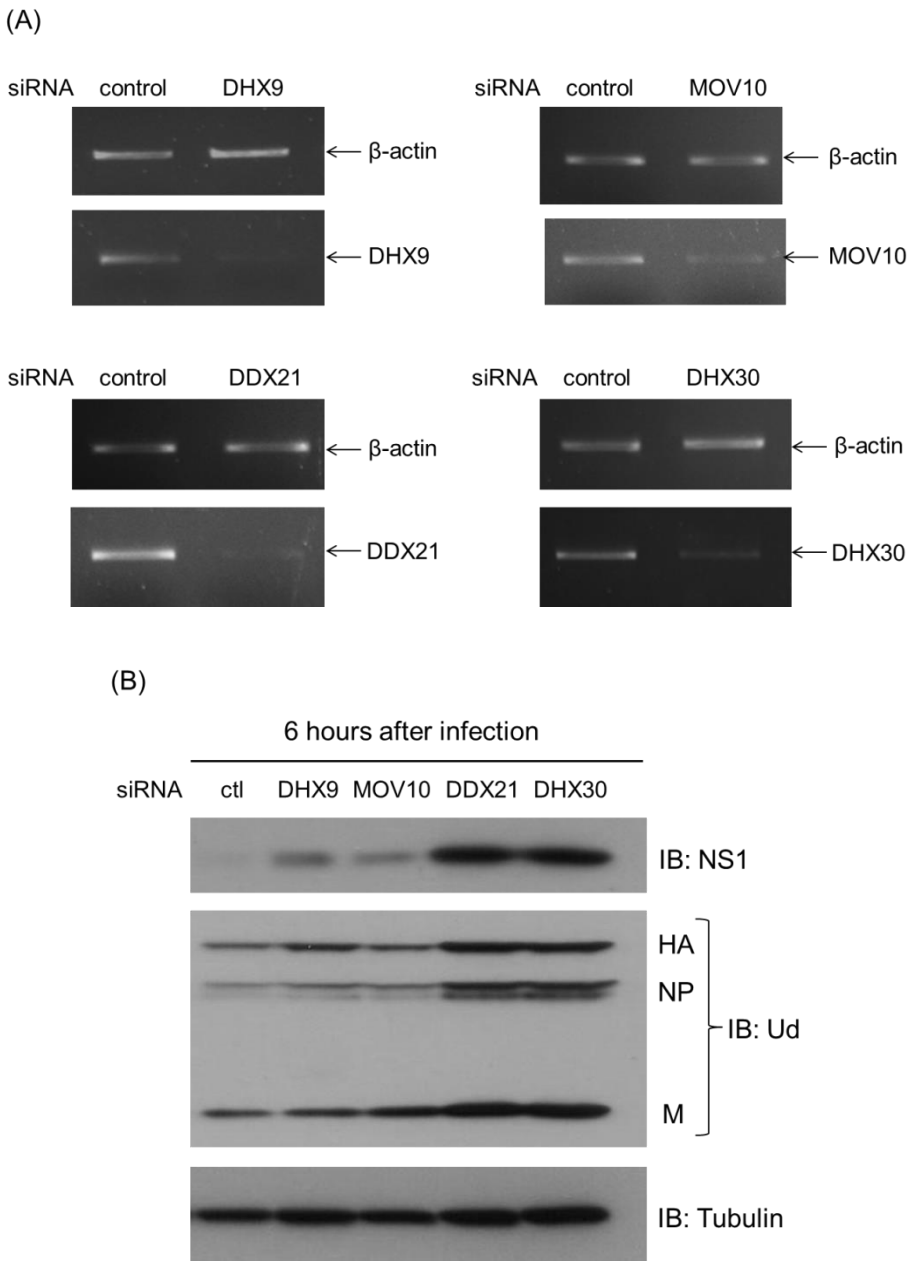

Figure 2.4 siRNA knock down of four candidate RNA helicases and their effect on viral replication. (A) Semi-quantitative RT-PCR for the knockdown of DHX9, MOV10, DDX21 and DHX30 mRNA by mixture of three siRNA (Invitrogen) in HeLa cells, respectively. β-actin mRNA served as an internal loading control. **(B)** Immunoblot for the effect of knocking down each RNA helicase on virus replication. HeLa cells were transfected with siRNA against each RNA helicase separately for 48 hours, and then infected with Ud virus at 2 pfu/cell. Cells were collected 6 hours post infection and immunobloted with antibody against NS1A, and Ud structural proteins (HA, NP and M). (Done by Guifang Chen)

to have roles in HCV replication (He et al., 2008a) , and have role in promoting HIV-1 replication at both reverse transcription and translation stages (Xing et al., 2010). DDX21 was reported to regulate translation of polycistronic mRNA of Borna disease virus (Watanabe et al., 2009). MOV10 was reported to be involved in hepatitis delta virus replication (Haussecker et al., 2008). However, no known functions were reported for these four candidate RNA helicases in influenza virus replication. We were interested in whether these RNA helicases play any role in influenza virus replication.

2.3.3 SiRNA knocking down of the identified RNA helicases DDX21 or DHX30 enhances influenza A virus replication in cells

To determine whether the four candidate RNA helicases play roles in influenza A virus replication, we knocked down each of them by siRNA and determined whether this knockdown impacted Ud virus replication. HeLa cells were transfected with a mixture of three siRNAs against each RNA helicase for 48 hours, and then infected with Ud virus at high M.O.I. (2 pfu/cell). Cells were collected at 6 hours post infection, and viral proteins were measured by immunoblot. Figure 2.4 (A) shows that mRNA of each RNA helicase could be knocked down by the mixture of siRNA with high efficiency. The measurement of viral protein expression in single cycle growth is a good estimate of the extent of virus replication. We found that knockdown of DHX9 or MOV10 only slightly increased NS1 protein expression, and did not affect protein expression of the major structural proteins HA, NP and M1 (Lane 2, 3 compared to lane 1). However, knockdown of DDX21 or DHX30 significantly increased protein expression of NS1, HA, NP and M1, indicating that DDX21

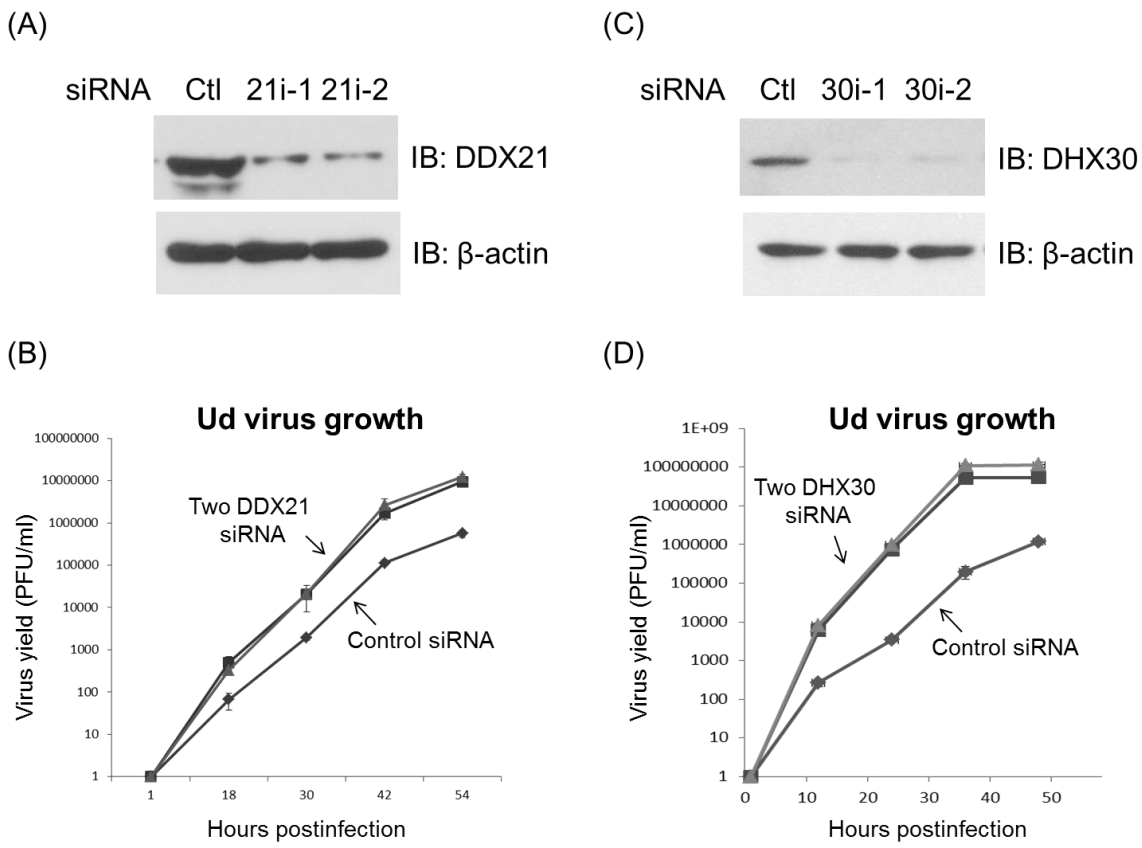

Figure 2.5 Knockdown of DDX21 or DHX30 by siRNA significantly increases influenza Ud virus replication. (A) Immunoblot for knockdown of DDX21 protein by two different siRNA (denoted as 21i-1 and 21i-2). β-actin protein served as an internal loading control. **(B)** Multiple cycle growth curve of Ud virus in Calu-3 cells. Calu-3 cells were transfected with siRNA against DDX21 (21i-1 or 21i-2) or control siRNA for 36 hours, and then infected with Ud virus at 0.001 pfu/cell. Supernatant containing released virus were collected at indicated time points post infection and virus yield was determined by plaque assay in MDCK cells. **(C)** Immunoblot for knockdown of DHX30 protein by two different siRNA (denoted as 30i-1 and 30i-2). **(D)** Multiple cycle growth curve of Ud virus in Calu-3 cells. Calu-3 cells were transfected with siRNA against DHX30 (30i-1 or 30i-2) or control siRNA for 36 hours, and then infected with Ud virus at 0.001 pfu/cell. (Done by Guifang Chen)

and DHX30 inhibit influenza virus replication (Lane 4, 5 compared to lane 1).

To further confirm that DDX21 and DHX30 inhibit influenza virus replication, we performed multiple cycle growth of Ud virus in Calu-3 cells which is human airway epithelial cell-line. Calu-3 cells were transfected with siRNA against DDX21 or DHX30 for 36 hours (Figure 2.5 (A) and (C)), and then infected with Ud virus at low M.O.I (0.001 pfu/cell). At the indicated time points post infection, small aliquots of supernatant containing released virus were collected and virus yield was determined by plaque assay in MDCK cells. Replication of Ud virus was significantly enhanced in either DDX21 or DHX30 knockdown cells, approximately 30-fold increase compared to control cells for DDX21 knockdown (Figure 2.5(B)) and 2-log increase compared to control cells for DHX30 (Figure 2.5(D)), demonstrating that DDX21 and DHX30 inhibit influenza A virus replication in human cells. Similar results were also obtained in HeLa cells and also with different influenza A virus strain (H1N1 influenza A/WSN/33) (Chen et al., 2014).

2.3.4 Mechanism for antiviral activity of DDX21 against influenza A virus

Further studies on DDX21 from our lab have revealed the mechanism of the antiviral activity of DDX21 against influenza A virus (Chen et al., 2014). We showed that DDX21 inhibits influenza A virus replication by binding to PB1 protein and blocking viral polymerase complex formation, leading to reduced viral RNA synthesis and protein expression at early times of infection. At later times of infection when sufficient NS1 proteins have been synthesized, the DDX21 antiviral activity is counteracted by NS1 protein, which binds to DDX21 and displaces PB1 from DDX2. As a consequence, viral polymerase

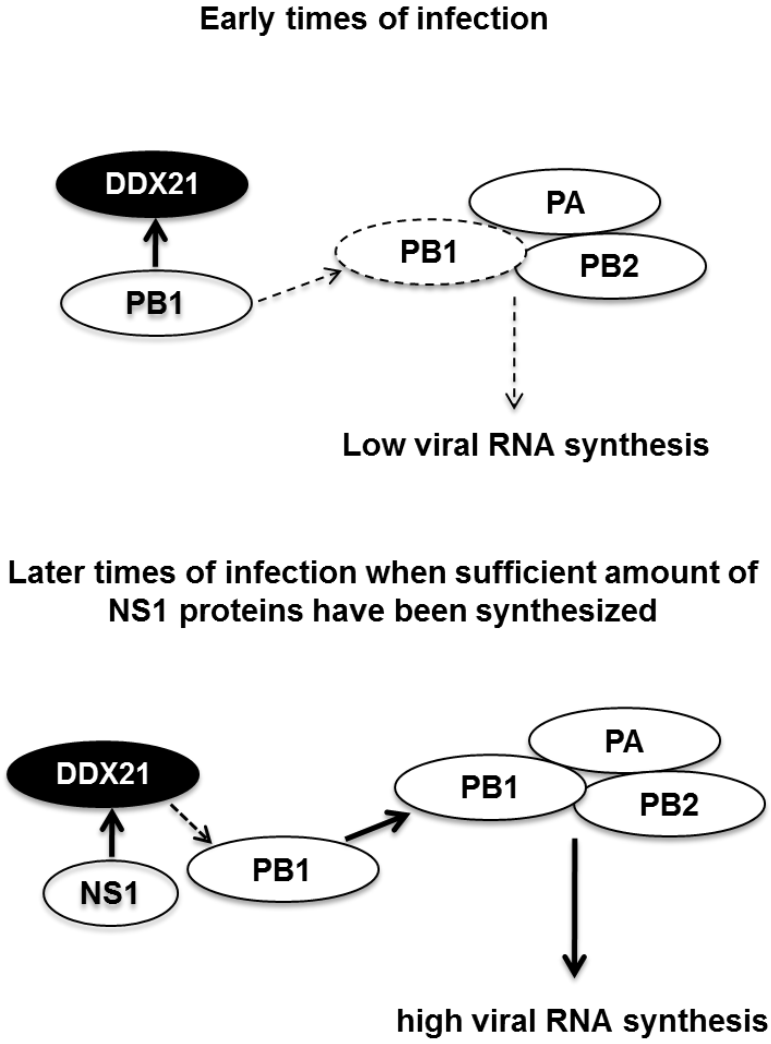

Figure 2.6 Mechanism for DDX21 regulation of influenza A virus RNA synthesis. At early times of infection, DDX21 inhibits viral RNA synthesis by binding to PB1 protein thus reducing the formation of viral polymerase complex. However, at later times of infection when sufficient amount of NS1 protein have been made, this antiviral activity is counteracted by the NS1 protein, which binds to DDX21 and displaces PB1 from DDX21. (Modified from (Chen et al., 2014))

complex formation is not blocked and viral RNA synthesis is no longer inhibited (Figure 2.6).

Chen et al. further showed that DDX21 binds to the RNA binding domain of the NS1 protein and identified amino acids K41 and R44 were required for DDX21 binding. However, K41 and R44 are also involved in binding dsRNA, α-importin, and NP (Cheng et al., 2009; Chien et al., 2004; Gack et al., 2009; Melen et al., 2007; Robb et al., 2011). To prove the mechanism, a NS1-K41A/R44A double mutant virus (41/44 virus) was generated. The virus with mutant NS1 that cannot bind to DDX21 showed reduced viral protein expression at both early and later times of infection. Knockdown of DDX21 rescued the phenotype of mutant 41/44 virus to that of wild-type virus, demonstrating the 41/44 virus was attenuated due to antiviral activity of DDX21, but not the other K41/R41-involved-functions.

2.3.5 Mechanism for antiviral activity of DHX30 against influenza A virus

The study of mechanism by which DHX30 inhibits influenza A virus is still in progress in our lab. Unpublished data from our lab showed that, just like DDX21, DHX30 can inhibit viral RNA synthesis at early times of infection. In addition, DHX30 was found to interact with NS1A but not PB1 or the other viral polymerases. Interestingly, amino acids K41 and R44 of NS1A are also required for DHX30 binding. While DDX21 requires full-length protein to be functional, DHX30 N-terminal RNA-binding domain is sufficient to inhibit virus. Currently two hypotheses are under tested: (1) DHX30 binds to viral RNA directly, which affects viral RNA synthesis; and (2) because region around K41 and R44 of NS1A is involved in many other functions, DHX30 binding to NS1A

may affect NS1A's function in regulation of viral replication.

2.4 Discussion

Replication of virus in host cells involves the interplay between viral and host cellular proteins. One important field for influenza A virus research is to identify host proteins that regulate viral replication through interaction with specific viral proteins. Our previous findings that NS1A forms complex with CPSF30 to block the pre-mRNA 3' end processing, and that viral polymerase proteins are associated with the NS1A-CPSF30 complexes led us to purify these macromolecular complexes to determine whether additional cellular proteins are associated with these complexes. Our current approach is to purify such macromolecular complexes from influenza virus infected cells, and identify host proteins that are associated with these complexes, and then determine whether the identified host proteins have any role in virus replication.

We modified the purification procedure from single selection of GST-CPSF30 reported in study by Kuo et al. to sequential selection of GST-CPSF30 and Flag-NS1A. The only proteins that are present in the purified protein complexes should be CPSF30, NS1A and proteins interacting with CPSF30 and/or NS1A. The associated cellular proteins could either directly or indirectly interact with CPSF30 and/or NS1A. In the present study, we showed that the double purification procedure was efficient and specific (Figure 2.2). The macromolecular complexes containing CPSF30 and NS1A were purified. The presence of not only CPSF30 and NS1, but also viral polymerase protein PA, PB1, PB2 and NP was confirmed, which was consistent with our previous

results. The NS2A was not found in the purified protein complexes, which provides a way to separate NS1A from NS2A in determining interaction partners (Figure 2.3). The mass spectrometry analysis of the purified product indeed identified many associated proteins, including viral polymerase proteins and CPSF subunit proteins that should be present in the protein complex, which validated our purification of functional active protein complexes from viral infected cells (Table 2.3). In addition, four host RNA helicases were identified as top associated proteins on the list, and siRNA knockdown screening showed that two out of four, DDX21 and DHX30 inhibit virus replication (Figure 2.4 and 2.5).

We showed that DDX21 RNA helicase that is associated with the CPSF30-NS1A complexes is a host factor that regulates viral RNA synthesis via interaction with PB1 at early time points and with NS1A at later time points (Figure 2.6). The interaction of DDX21 with NS1A explains how DDX21 is associated with the CPSF30-NS1A complexes. Interestingly, DDX21 was not identified in previous study that aimed to determine the host proteins involved in influenza A virus replication by RNAi screening (Watanabe et al., 2010). Another study reported that DDX21 interacts with transfected PA-PB1 hetero-dimer protein in RNase-sensitive manner, suggesting RNA-mediated interaction (Bradel-Tretheway et al., 2011). However, our results showed that DDX21 binds to PB1 but not PA in RNase-resistant manner, indicating protein-protein interaction, which emphasizes the validity of identifying specific viral-host protein interaction from viral infected cells.

The NS1A protein has binding sites for many cellular proteins, and some

of these interactions may be mutually exclusive (Krug and Garcia-Sastre, 2013). It is very likely that multiple NS1-CPSF30 complexes exist due to different cellular protein bound to NS1A. Further, while some NS1-CPSF30 complexes contain viral polymerase proteins as confirmed by immunoblot and mass spectrometry (Figure 2.3, Table 2.3), some of the NS1-CPSF30 complexes from Ud infected cells probably do not have association of viral polymerase proteins because Ud NS1A can stably interact with CPSF30 without stabilization from cognate viral polymerase proteins (Kuo and Krug, 2009). The NS1-CPSF30 complexes that interact with DDX21 most likely do not contains viral polymerase proteins as integral components, particularly because DDX21 binds to only PB1 but not PA and PB2 at early times and binds to NS1A at later times of infection. Hence the purified NS1-CPSF30 complexes containing DDX21 were most likely the complexes formed at later time of infection, consistent with the procedure that the infected cells were collected at 12 hours post-infection.

To determine the function of NS1A-DDX21 interaction, Chen et al., identified the binding site of DDX21 on NS1A protein, and demonstrated that the Ud virus expressing mutant NS1A that cannot bind to DDX21 cannot counteract the antiviral activity of DDX21. This result showed that endogenous DDX21 inhibits viral RNA synthesis, which is in turn suppressed by NS1A in infected cells. Additional proof for antiviral activity of DDX21 would be to determine the binding site of DDX21 on PB1 and generated a virus expressing mutant PB1 that cannot be targeted by DDX21. Since PB1 structure was solved recently (Reigh et al., 2014; Pflug et al., 2014), further study is needed to determine whether it is feasible to generate such PB1

mutant virus whose primary defect is in DDX21 binding.

DDX21 probably interacts with PB1 in the cytoplasm before it forms complex with PA and being transferred into nucleus for tripartite viral polymerase formation (Fodor and Smith, 2004). Although DDX21 is a nucleolar protein, studies have shown that DDX21 participates in cytoplasmic functions. DDX21 was reported to regulate translation of polycistronic mRNA of Borna disease virus (Watanabe et al., 2009); and DDX21 forms complex with another two RNA helicases to sense dsRNA in dendritic cells (Zhang et al., 2011b). On the other hand, the interaction between DDX21 and PB1 or NS1 may interfere with DDX21's cellular function. DDX21 was recently reported to regulate transcription and ribosomal RNA processing (Calo et al., 2014). It would be interesting to determine whether influenza virus regulates cellular transcription and ribosomal RNA processing through binding and sequestering DDX21.

For the anti-influenza viral drugs development, the binding sites of DDX21 on NS1A have been determined, which are around the region (R37, R38, K41 and R44) also participates in binding dsRNA, α-importin, TRIM25 and NP (Cheng et al., 2009; Chien et al., 2004; Gack et al., 2009; Melen et al., 2007; Robb et al., 2011). Since this region on NS1A is crucial for multiple functions required for virus replication in cells, inhibitors against this region would be expected to strongly inhibit virus replication. Actually, our lab and others have been shown that influenza virus expressing NS1 with mutations in this region are highly attenuated (Donelan et al., 2003; Gack et al., 2009; Min and Krug, 2006).

Ch.3 Identification of a novel battle between influenza A virus and a newly identified ZAPL antiviral activity

3.1 Introduction

In addition to the four host RNA helicases identified associated with the purified CPSF30-NS1A complexes, we surprisingly found the association of the host antiviral protein ZAP, which was with 13 matches identified in the 90 - 110 kDa region (Table 2.3). We were very curious about the presence of an antiviral protein in the host-viral complex.

3.1.1 ZAP is a CCCH-type zinc-finger antiviral protein

ZAP is a CCCH-type zinc-finger antiviral protein. There are two dominant isoforms of ZAP in human cell: one is a longer 902 amino acids protein (denoted as ZAPL) that contains an N-terminal zinc-fingers domain, an internal TPH and WWE domains, and a C-terminal PARP-like domain. The other one is a shorter 699 amino acids protein (denoted as ZAPS) with identical N-terminal and internal domains but lacks the C-terminal PARP-like domain of ZAPL (Figure 3.1) (Kerns et al., 2008). By screening the mammalian cDNA library for genes that confer antiviral activity, Steven Goff Lab has identified that the zinc-finger antiviral protein (ZAP) was a host factor to prevent retroviral Moloney murine leukemia virus (MLV) infection in 2002 (Gao et al., 2002). The minimum required region is the rat N-terminal ZAP (rZAP) that contains only the zinc-finger domain (Figure 3.1). Subsequent studies showed that, in addition to retroviral MLV, overexpression of ZAP inhibits replication of many viruses in cells, including several members in the

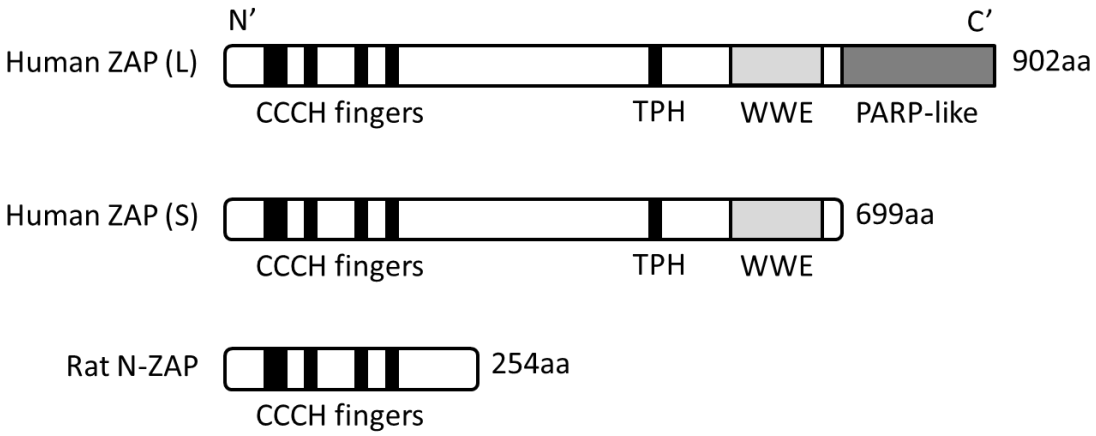

Figure 3.1 The diagram showing domains in different ZAP isoforms. There are two dominant ZAP isoforms in human cells. The longer isoform ZAPL contains N-terminal zinc fingers domain, internal TPH and WWE domain, and C-terminal PARP-like domain. The shorter isoform ZAPS contains identical C-terminal and internal domains, but lacks the C-terminal PARP-like domain. Rat cell contains one major shorter isoform the N-ZAP which is mainly the zinc fingers domain (Kerns et al., 2008).

positive-sense ssRNA Alphavirus (Sindbis virus, Semliki Forest virus, Ross River birus and Venezuelan equine encephalitis virus) (Bick et al., 2003), and negative-sense ssRNA Filovirus (Ebola virus and Marburg virus) (Muller et al., 2007). Recent studies showed ZAP also inhibits HIV-1 (positive-sense ssRNA) and Hepatitis B virus (partial dsDNA) (Mao et al., 2013; Zhu et al., 2011). However, ZAP does not have universal antiviral activity since ZAP does not inhibit replication of vesicular stomatitis virus (negative-sense ssRNA), poliovirus (positive-sense ssRNA), yellow fever virus (positive-sense ssRNA) and herpes simplex virus type 1 (dsDNA) (Bick et al., 2003). It looks like ZAP has antiviral activity to retroviruses and some ssRNA viruses and only few DNA virus. In addition, the inhibition of viral replication can be up to 3 to 4 log units when cells are infected with high multiplicity of infection (MOI) and even more in low MOI, suggesting very robust inhibition of viral replication.

3.1.2 ZAP binds specifically to the cytoplasmic viral mRNA and leads to its degradation

The N-terminal zinc-fingers of ZAP is the major antiviral functional domain. Before the discovery of human ZAP in 2008 (Kerns et al., 2008), most studies used rat N-terminal ZAP (rZAP) as a model to study its antiviral functions. ZAP was found to block Sindbis virus replication after the virus binding to cells, penetration and uncoating, but before the amplification of newly synthesized positive strand genomic RNA. In addition, the translation of incoming viral RNA was found to be blocked by ZAP (Bick et al., 2003). The MLV experiments showed that the cytoplasmic viral mRNA level is decreased in the presence of ZAP while the nuclear viral mRNA level is not affected (Gao et al.,

2002). Later, ZAP was further shown to directly bind to and downregulate specific viral mRNAs through mainly the second and fourth zinc fingers (Guo et al., 2004; Muller et al., 2007). However, no specific consensus mRNA sequence could be mapped so far since different virus mRNAs have different ZAP binding regions (ZAP responsive element, or ZRE). Further sequence analysis of different ZAP binding mRNA fragments did not identify any common characteristics structures, so it remains unclear how ZAP recognizes specific viral mRNA (Guo et al., 2004).

For the mechanism by which ZAP downregulates viral mRNA, study has demonstrated that ZAP can recruits the RNA processing exosome to degrade the target viral mRNA (Guo et al., 2007a). Because mRNA is highly structured, ZAP may need other factors for efficient mRNA degradation. Further study showed that certain RNA helicase (p72 DEAD box RNA helicase), as a ZAP-interacting protein, is required to promote ZAP-mediated RNA degradation (Chen et al., 2008). In addition, in HIV-1 infected cells the 5' decapping complex through association with RNA helicase p72, and 3' poly(A)-specific ribonuclease (PARN) were recruited by ZAP to promote the viral mRNA degradation (Zhu et al., 2011). Based on these studies, the current working model for ZAP antiviral activity is that ZAP specifically binds to target viral mRNA containing ZAP-responsive element (ZRE) through mainly the second and fourth zinc-finger motifs, and recruits many cellular proteins involved in RNA degradation including p72 RNA helicase to resolve RNA structure for efficient degradation, and decapping complex (DCP) to degrade mRNA from 5'end, and poly(A)-specific ribonuclease (PARN) to degrade 3' poly A tail, and RNA exosome to degrade RNA body from 3'end (Figure 3.2).

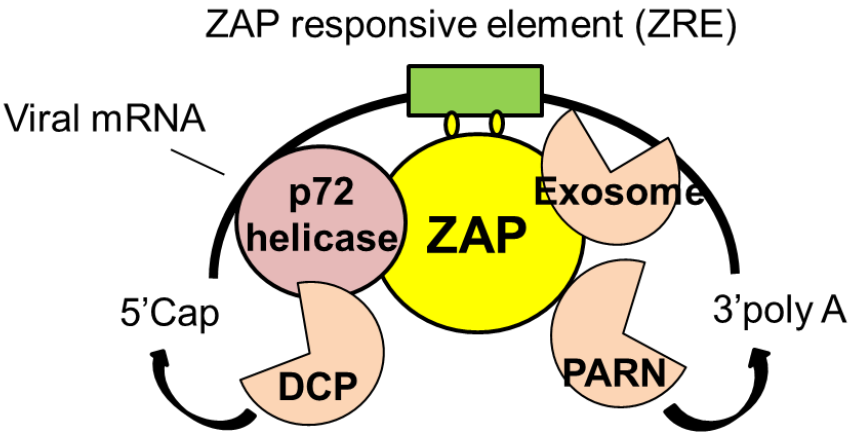

Figure 3.2 Diagram showing the mechanism of ZAP-mediated viral mRNA degradation. ZAP via its zinc fingers targets ZAP-responsive element (ZRE)-containing viral mRNA, and then recruits many cellular proteins including p72 RNA helicase to resolve RNA structure, and decapping complex (DCP) to degrade mRNA from 5'end, and poly(A)-specific ribonuclease (PARN) to degrade 3' poly A tail, and RNA exosome to degrade RNA body from 3'end.

In addition to its antiviral activity, the cellular function of ZAP zinc-finger domain is unclear. Since ZAP can promote degradation of specific viral mRNA, it is reasonable that ZAP may also regulate or be involved in specific cellular mRNA processing or metabolism. Recently a study showed that human ZAPL, also known as PARP13, destabilizes cellular mRNAs including TRAILR4 post-transcriptionally to regulate TRAIL-mediated apoptosis in the absence of viral infection (Todorova et al., 2014), indicating ZAP and its specific ZAP binding sequence may represent a novel mechanism to regulate cellular mRNA stability.

3.1.3 The mechanism by which ZAPL PARP domain contributes to antiviral activity is unclear

The antiviral function of ZAP N-terminal zinc finger domain has been well-established; however, much less is known about how ZAPL PARP domain is involved in antiviral functions. ZAP, also known as PARP13, belongs to the poly(ADP-ribose) polymerase (PARP) protein family. The primary function of PARP is to post-translationally modify its target protein with poly(ADP-ribose), or pADPr, which is also known as poly(ADP-ribosylation) or PARylation. However, it was reported that ZAPL PARP domain lacks the poly(ADP-ribosylation) activity possessed by other cytoplasmic PARP proteins (Kleine et al., 2008). Interestingly, compared to ZAPS, ZAPL was shown to have stronger RNA degradation activity and stronger antiviral activity against Semliki Forest virus and Moloney murine virus. However, the underlying mechanism for how PARP domain enhances antiviral activity remains unclear (Kerns et al., 2008). Subsequent study showed that S-farnesylation of a Cys

in the PARP domain leads ZAPL to associate with endo/lysosomes, which contributes the enhanced ZAPL antiviral activity against Sinbis virus. However, the mechanism by which endo/lysosomes association contributes to stronger RNA degradation activity and antiviral activity of ZAPL remains to be further investigated (Charron et al., 2013). Another study showed although the ZAPL PARP domain lacks the poly(ADP-ribosylation) activity due to inactive catalytic triad motif, such inactive triad motif are required for its antiviral activity against Sindbis virus. Mutation of the inactive triad motif to triple alanines or catalytic active triad motif possessed by other functional active PARPs abolished ZAPL's antiviral activity (Glasker et al., 2014). To conclude, the mechanism by which ZAPL PARP domain contributes to antiviral activity is still unclear. Further, whether such antiviral activity is dependent on zinc-finger antiviral activity or not is also unknown.

3.1.4 ZAP serves as a PARP protein that regulates stress responses and microRNA activity in cells

ZAP serves as a PARP protein which is also involved in other cellular function. Poly(ADP-ribosylation) was best known for its functions in the nucleus to regulate transcription, chromosome structure, and DNA damage repair (Krishnakumar and Kraus, 2010). Accumulated studies showed Poly(ADP-ribosyaltion) is also involved in cytoplasmic functions. Recent study from Phillip Sharp and Paul Chang Lab showed that poly(ADP-ribosylation) is required for the assembly of cytoplasmic stress granules (SG), which regulates mRNA stability and translation upon stress. Several PARP proteins including ZAP (PARP13) were identified associated with SG. Although

PARP13 is lack of PARP activity, PARP13 probably cooperates with other PARP proteins (PARP12 and 15) to poly-ADP-ribosylate the microRNA-binding Argonaute proteins upon stress, which inhibits microRNA-mediated translation repression and microRNA-directed mRNA cleavage (Leung et al., 2011).

In the present study, we revealed the antiviral role of ZAPL C-terminal PARP domain against influenza A virus. We showed that the ZAPL PARP domain targets the viral polymerase PA and PB2 proteins. These two viral polymerases are poly(ADP-ribosylated), presumably by other PARP protein(s), which enhances the ZAPL-PA and ZAPL-PB2 interaction. The ZAPL-associated, poly(ADP-ribosylated) PA and PB2 are then ubiquitinated and proteasomally degraded. Such ZAPL antiviral activity is counteracted by the binding of polymerase PB1 protein to an adjacent WWE region, which displaces PA and PB2 from ZAPL and thus escape degradation. Because PB1 displaces PA and PB2 and protects them from ZAPL-mediated degradation, endogenous ZAPL only moderately inhibits influenza A virus replication (20-30-fold), as determined by siRNA knockdown experiment. These results indicate that influenza A virus has partially won the battle against the newly identified ZAPL antiviral activity.

3.2 Materials and Methods

3.2.1 Cell-lines and recombinant viruses

HEK-293T human kidney cell-line (ATCC CRL-11268), HEL299 human lung fibroblast cells (ATCC CCL-137), Madin-Darby canine kidney cell-line

(MDCK) (ATCC CCL-34), and Calu3 human lung adenocarcinoma cell-line (ATCC HTB-55) were purchased from ATCC. 293T, HEL299 and MDCK cells were grown in Dulbecco's modified Eagle's medium (DMEM) (GIBCO) supplemented with 10% heat-inactivated fetal bovine serum (FBS) (GIBCO), 2 mM l-glutamine, 100 units/ml penicillin, and 100 µg/ml streptomycin (1% PSG) (GIBCO) at 37°C under a 5% CO2/95% air atmosphere. Calu3 cells were grown in Advanced MEM (GIBCO) supplemented with 10% FBS and 1% PSG at 37°C under a 5% CO2/95% air atmosphere.

Influenza A wild-type Ud virus, and Ud virus encoding NS1 and NS2 proteins with a N-terminal 1xFlag tag were generated by plasmid-based reverse genetics as described in details in Section 2.2.1. All eight genomic RNA segments of recombinant viruses were sequenced. Virus stocks were grown in 10-day-old fertilized eggs, and virus titers were determined by plaque assays in MDCK cells.

3.2.2 Plasmids and antibodies

Human ZAPL and ZAPS cDNAs were cloned by RT-PCR of RNA isolated from human HEL299 cells. The primers used to generate these two cDNAs are shown in Table 3.1. The ZAPL C88R mutation was introduced into ZAPL using standard oligonucleotide mutagenesis methods. Each cDNA was cloned into the pcDNA3 mammalian expression vector. All constructs were confirmed by sequencing. The LlucSN plasmid was provided by Harmit Malik to assay the mRNA degradation activity of ZAP (Kerns et al., 2008). Rabbit antibody against PB1 was provided by Krister Melen and Ikka Julkunen. Monoclonal antibodies against PA and PB2 were provided by Juan Ortin

Table 3.1 Primer sequences used in this study

Target	Purpose	Strand	Sequence
ZAPL		Forward	5’- ATG GCG GAC CCG GAG GTG
ZAPL		Reverse	5’- CTA ACT AAT CAC GCA GGC
ZAPS		Forward	5’- ATG GCG GAC CCG GAG GTG
ZAPS		Reverse	5’- CTA TCT CTT CAT CTG CTG
PA	RT-PCR	Forward	5’- GAA ATG GGG AAT GGA GAT GA
PA	RT-PCR	Reverse	5’- CAT GCT CTC GAT TTG TTG GA

Table 3.2 siRNA sequences used in this study

Target	Sequence (complimentary sequence not shown)
ZAPL	5’- AAA UUU AUC CAG GAG CUC UGA GUU C
PARG	5’- GAA AUA UUU CUA GCC UGA AUG UAG A
Control	5’- UUG AUG UUG AGC AAU UCA CGU UCA U

(Ochoa et al., 1995). Antibody against the major structural proteins of Ud virus, which detects NP as well as HA and M1 (denoted as Ub Ab), was provided by Robert A. Lamb (Chen et al., 2007). The antibody against amino acids 300 - 400 of human ZAPS and ZAPL was from Abcam. Tubulin antibody was from Cell Signaling, and polyclonal antibody against poly(ADP-ribosylation) was from BD-Pharmingen (LP96-10) (Leung et al., 2011).

3.2.3 siRNA knockdown of ZAPL and PARG

Knockdown of ZAPL by siRNA was performed to determine whether ZAPL has functional impact on influenza Ud virus replication in A549 cells. The siRNA duplexes specifically against ZAPL (but not ZAPS) was designed and purchased through Invitrogen (Stealth RNAi™ siRNAs) using sequence of ZAPL C-terminal PARP domain. The sequence of ZAPL siRNA is shown in Table 3.2. To determine the role of poly(ADP-ribosylation) in ZAPL's antiviral function, siRNA knockdown of PARG which is an enzyme to hydrolyze poly(ADP-ribose) chain was performed in 293T cells, and the siRNA sequence is shown in Table 3.2. The control siRNA is a scrambled siRNA sequence with no known human gene target. The knockdown experiment was performed using either siRNA against target gene or control siRNA mixed with X-tremeGENE siRNA Transfection Reagent (Roche) according to the manufacturer's protocol.

In brief, for maximal knockdown efficiency in A549 cells, cells were trypsinized, washed and re-suspended in serum- and antibiotics-free Opti-MEM I. At 6 - 8 hours after addition of siRNA mixture into re-suspended A549 cell cultures, medium was replaced with fresh DMEM with 10% FBS and 1%

PSG. Final concentration of 40 nM siRNA was used for ZAPL knockdown in A549 cells for 36 - 48 hours before virus infection. For siRNA knockdown in 293T cells, no trypsinization and resuspension of cells are needed. The siRNA and transfection reagent mixture was added into cell culture that have been replaced with fresh DMEM containing 10% FBS and 1% PSG. Final concentration of 50 - 80nM siRNA was used for PARG knockdown in 293T cells for 36 - 48 hours.

3.2.4 RNA Extraction, Semi-quantitative Reverse Transcription (RT)-PCR, and Quantitative RT-PCR

Total RNA in cells is harvested by using Trizol reagent (Invitrogen) and chloroform according to manufacturer's instructions. cDNA is generated from reverse transcription of total mRNA with oligo-dT primer, which is then PCR amplified with specific primers to each candidate target genes (shown in Table 3.1). Amplified PCR products are separated by electrophoresis on 1% agarose. To quantitate PA mRNA levels in the transfection assay to determine whether ZAP leads to PA mRNA degradation, RNA was extracted from cell, polyadenylated mRNA was isolated using oligo(dT)-coated beads (Qiagen), and reverse transcribed using an oligo-dT primer. PCR amplification of PA mRNA and β-actin mRNA was carried out using Ud PA specific primers (shown in Table 3.1), and β-actin specific primers, respectively, and the FastStart Universal Probe Master Mix (Rox) with Universal Probe Library #134 for Ud PA or #64 for human β-actin. Analysis was carried out using the Perkin-Elmer/Applied Biosystems 7900HT sequence detector. The C-T value for PA mRNA was normalized to the C-T value of β-actin mRNA. The

quantitative RT-PCR reactions were performed in triplicate.

3.2.5 Luciferase assay of mRNA-degrading activity of ZAP

To determine the different ZAP constructs are functional active in targeting viral mRNA for degradation, a reporter luciferase assay established by others was performed (Kerns et al., 2008). 293T cells were transfected using the Mirius TransIT-LTR Transfection reagent with 50 ng of the LlucSN plasmid, 25 ng of the pcDNA3 plasmid expressing renilla luciferase, and either an empty pcDNA3 vector (No ZAP control) or one of the following plasmids: ZAPL (0.5 μg), ZAPS (0.2 μg), or ZAPL-C88R (1.2 μg). These levels of the different ZAP plasmids resulted in equal expression of the encoded proteins, as shown by an immunoblot probed with the ZAP antibody. The total amount of transfected plasmids was equalized by the addition of the empty pcDNA3 plasmid. After 24 hours of transfection, cells from triplicate transfections were collected, and the activities of the two luciferases activity in cell extracts were determined using a Mithras microplate luminometer.

3.2.6 Virus infection and plaque formation assay

To determine the multiple cycle growth of Ud virus in ZAPL knockdown cells, A549 cells with ZAPL knockdown for 36 - 48 hours were infected with Ud virus at 0.05 pfu/cell (low M.O.I.). A549 cells were washed and incubated with diluted Ud virus in serum-free DMEM containing 1% BSA and 1% PSG. After 1 hour incubation, cells were washed with PBS and replaced with DMEM containing 1 μg/ml N-acetylated trypsin and 1% PSG. At indicated time post infection, small amount of supernatant from cell culture was harvested and the

virus titer was determined by plaque formation assay as described in section 2.2.7.

3.2.7 Co-immunoprecipitation experiment

To study protein-protein interaction, co-immunoprecipitation experiment was performed. Cells were co-transfected using the Mirius TransIT-LTR transfection reagent with the two or three plasmids indicated in the text, and were extracted with lysis buffer containing 50 mM Tris-HCl pH 7.5, 150 mM NaCl, 5 mM EDTA, 2.5 mM MgCl2, 1% NP40, 10% glycerol, 1 mM PMSF, and 1x Protease inhibitor (Roche). Cell extracts were diluted with lysis buffer containing 50 mM Tris-HCl pH7.5, 150 mM NaCl, 1 mM PMSF, and 1x Protease inhibitor to make final concentration of 0.5% NP40 and then immunoprecipitated with the antibody against one of the expressed proteins or tubulin antibody as a negative control, followed by binding to mixture of Protein A/G Sepharose beads (GE Health). After washing the Sepharose beads four times with wash buffer containing 50 mM Tris-HCl pH7.5, 150 mM NaCl, 0.5% NP40, proteins were eluted by heating the beads at 95℃ in a sample buffer containing 50 mM Tris-HCl pH6.8, 2% SDS, 6% glycerol, 2% β-mercaptoethanol. The eluate was resolved by electrophoresis on a SDS-PAGE gel, which was then analyzed by immunoblots probed with the antibody against the protein(s) expressed by each plasmid(s) or with tubulin Ab as internal loading control.

3.2.8 Ubiquitination assay

To study whether certain protein is ubiquitinated and proteasomally

degraded, ubiquitination assay was performed. 293T cells were co-transfected with the plasmids indicated in the text, and, where indicated, were then treated with 40uM MG132 (Biomol International) which is a proteasome inhibitor to block proteasome function. Cells were extracted with lysis buffer supplemented with three deubiquitinase inhibitors: 5mM NEM (Sigma), 20uM PR-169, 5mM 1,10-phenanthroline (LifeSensors). Cell extracts, after reducing the NP40 concentration to 0.5%, were incubated with agarose beads conjugated with tandem ubiquitin-binding domains (TUBE-2, LifeSensors) to select for ubiquitinated proteins. After washing the TUBE-2 beads four times with wash buffer containing 50 mM Tris-HCl pH7.5, 300 mM NaCl, 0.5% NP40, proteins were eluted by heating the beads for 5 minutes at 95℃ in sample buffer containing 50mM Tris-HCl pH6.8, 2% SDS, 6% glycerol, 2% β-mercaptoethanol. The eluate was subjected to electrophoresis on a SDS-PAGE gel, followed by immunoblots probed with the indicated antibodies.

3.2.9 Poly-(ADP-ribosylation) assay

To study whether certain protein is poly-ADP-ribosylated, a poly-(ADP-ribosylation) assay with modified pADPr lysis buffer and procedure from previous study was performed (Leung et al., 2011; Seo et al., 2013). At least $2x10^7$ of 293T cells were co-transfected with the plasmids indicated in the text, and, where indicated, were then treated with 40uM MG132 to block proteasome function. Cells were extracted with a modified pADPr lysis buffer containing 50 mM HEPES pH7.4, 150 mM NaCl, 1 mM EGTA, 1 mM MgCl2, 1% TX-100, 1 mM DTT, 10 uM nocodazole (Sigma), 10 ug/mL cytochalasin D (Enzo Life Science), 1 uM PARG inhibitor ADP-HPD (EMD millipore), 1mM

NAD+ (Sigma), 1 mM PMSF, and 1x Protease inhibitor (Roche). Cell extracts were incubated with Flag-antibody-conjugated agarose M2 beads (Sigma) to immunoprecipitate Flag-PA or Flag-PB2; or Flag-Z2 ZAP fragment. After washing the agarose beads three times with the pADPr buffer containing a higher concentration of NaCl (300mM), proteins were eluted by incubating the beads with 500ug/mL 3xFlag peptides (Sigma) for Flag-tagged protein elution. The Flag eluate or the V5-immunoprecipitates was heated at 70℃ for 8 minutes in sample buffer containing 60mM Tris-HCl pH6.8, 2% SDS, 10% glycerol, 1.25% β-mercaptoethanol, and was then subjected to electrophoresis on a SDS-PAGE gel, which was then analyzed by immunoblots probed with an antibody against pADPr (LP96-10, BD-Pharmingen) or the antibody against the indicated protein (Leung et al., 2011; Seo et al., 2013).

3.2.10 Generation of pseudo-retrovirus

Instead of plasmid transfection into cells for protein expression, some experiments in present study employed pseudo-retrovirus infection to express specific viral protein in cells (i.e. PA and PB2 in this study). To make the retrovirus expressing indicated proteins in cells, the influenza Ud virus PA, PB2 or PB2 with C-terminal 1xFlag were cloned into a modified pQCXIP retroviral vector provided by Steven Goff Lab using either standard cloning or a modified SLIC procedure (done by Mark Collin) (Li and Elledge, 2007).

For PA the primers were:

Forward: 5’- ATGGAAGATTTTGTGCGACAATGCTTCAATTCGATG-3’; and

Reverse: 5’- CTATCTTAATGCATGTGTTAGGAAGGAGTTGAACCAAG-3’

For PB2 the primers were:

Forward: 5’- ATGGAAAGAATAAAAGAACTACGGAATCTGATGTCGC-3’; and
Reverse: 5’- TTAATTGATGGCCATCCGAATTCTTTTGGTCGCTG-3’

All constructs were confirmed by sequencing. To generate retrovirus, 293T cells were co-transfected with indicated retroviral vector, pcDNA3-Gag-pol and pcDNA3-VSV-G for 48 hours to generate pseudo-retrovirus. The supernatant containing the released pseudo-retrovirus were collected, filtered by 0.22μm PES membrane and applied to the target cells for 24 hours to express desired proteins (Naldini et al., 1996).

3.2.11 Immunofluorescence by confocal microscopy

To determine the cellular localization where ZAPL interacts with PA, PB2 and PB1, immunofluorescence by confocal microscopy was performed (done by Ligang Zhou). In brief, 293T cells were transfected with GFP-PB1, PA-GFP, V5-ZAPL plasmid, where indicated, for 36 hours. The cells were then fixed with 4% paraformaldehyde and permeabilized with 0.5% Triton X-100. V5-ZAPL was visualized using mouse anti-V5 antibody and Alexa fluor 546 conjugated goat anti-mouse antibody (Life technologies). Cell nuclei were stained with DAPI. Images were obtained using a Zeiss LSM 710 Confocal microscope, and data were processed with ZEN 2012 software. For PB2 localization, Split-GFP strans-1-10 (Sandia Biotech) was cloned on to the C-terminus of PB2, split-GFP strand-11 was cloned on to the N-terminus of ZAPL or ZAPS. 293T cells transfected with indicated plasmids were fixed,

permeabilized and stained with DAPI before they were used for direct fluorescence with the confocal microscope. All images were acquired using the same settings.

3.3 Results

3.3.1 ZAPL, which is associated with purified CPSF30-NS1 complexes, inhibits influenza A virus replication.

The CPSF30-NS1A protein complexes were purified from Ud virus infected cells as described in chapter 2 (Chen et al., 2014). 293T cells were transfected with GST-CPSF30 and then infected with wild-type Ud or Ud virus expressing Flag-NS1. The complexes were purified by GST pull down followed by Flag immunoprecipitation. Mass spectrometry analysis on the purified complexes has identified a list of associated host proteins. We have shown that the viral polymerase proteins PA, PB1, PB2, NP, and the cellular DDX21 RNA helicase are associated with the CPSF30-NS1A complexes. In addition, we surprisingly found substantial number of peptides of the cellular ZAP protein (13 peptide matches) in the 90 - 110 kDa region but not in the other molecular weight region from mass spectrometry results (Table 2.3). These results suggested that the CPSF30-NS1A complexes contain the longer ZAPL isoform (100 kDa), but not the shorter ZAPS isoform (78 kDa) lacking the C-terminal PARP domain (Figure 3.3A). To verify it is the ZAPL isoform that associates with the CPSF30-NS1A complexes, immunoblotting with ZAP antibody raised against N-terminal region (Abcam) shared by two isoforms was performed. Consistent with mass spectrometry results, only the ZAPL protein, but not the ZAPS protein, was detected in the purified CPSF30-

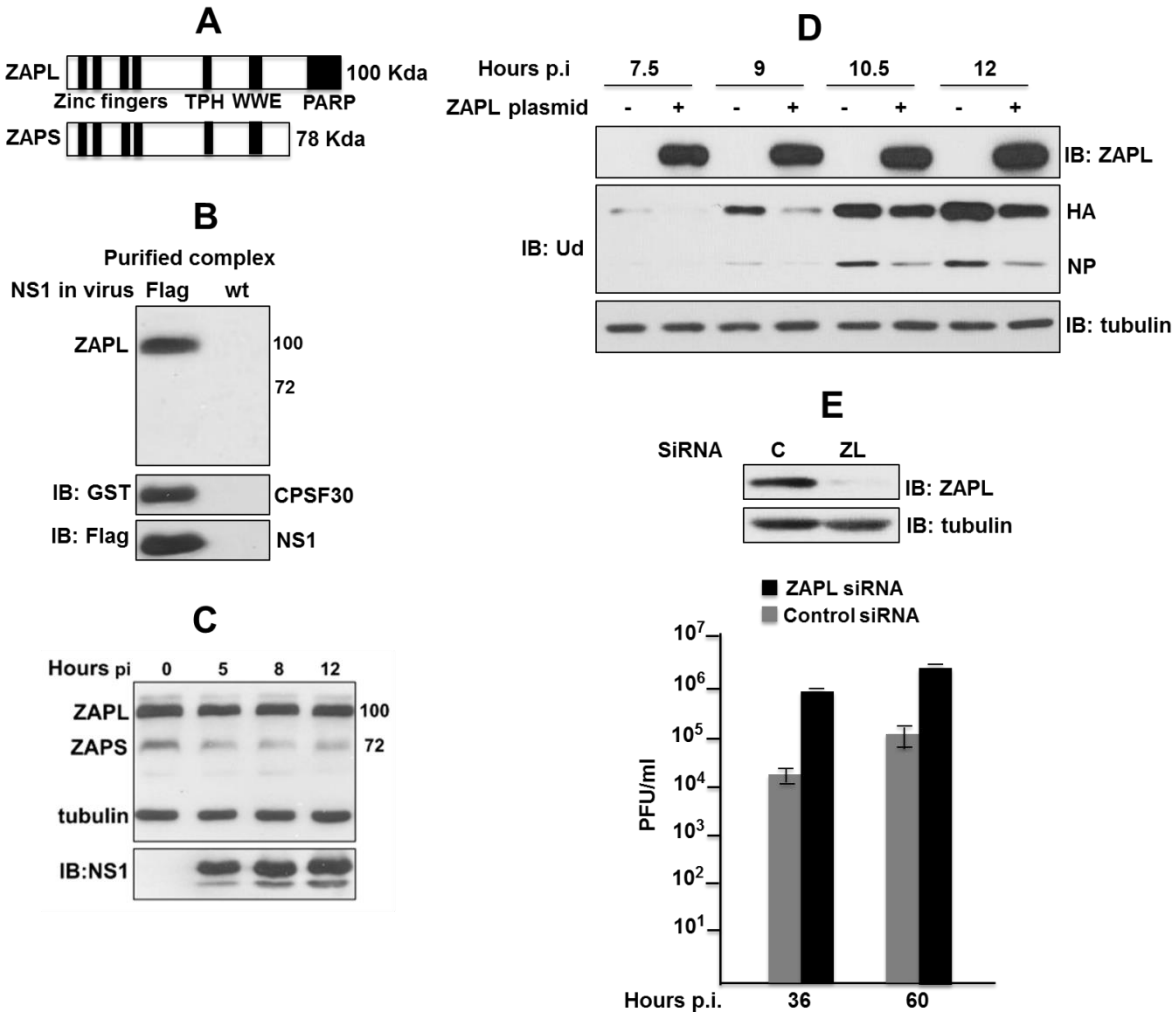

Figure 3.3 ZAPL, which is associated with purified CPSF30-NS1 complexes, inhibits influenza A virus replication. (A) The domains in human ZAPL and ZAPS. **(B)** Immunoblot to confirm ZAPL association in purified CPSF30-NS1 complexes. **(C)** Immunoblot to measure the amounts of ZAPL and ZAPS in cells after Ud virus infection. **(D)** 293T cells were transfected with the ZAPL plasmid or a control plasmid for 40 hours, followed by infection with 0.1 pfu/cell of Ud virus. At the indicated times after infection, cell extracts were immunoblotted with ZAPL, Ud or tubulin Ab. **(E)** A549 cells were transfected with a ZAPL-specific or a control siRNA for 36 hours, followed by infection with 0.05 pfu/cell of Ud virus. Virus production at the indicated times after infection was determined by plaque assays. The bars show the standard deviation of triplicate of virus production. The efficiency of ZAPL knockdown is shown in the immunoblot of cell extracts probed with ZAPL Ab.

NS1A complexes (Figure 3.3B), but not in the control sample, indicating ZAPL is associated with the CPSF30-NS1A complexes. Endogenous ZAP expression level during Ud virus infection was determined in 293T cells. Both ZAPL and ZAPS are expressed in virus infected cells, and ZAPL expression predominates whereas ZAPS expression is reduced about 2-fold over virus infection. In addition, ZAPL protein level remains similar through virus infection (Figure 3.3C).

To establish whether endogenous ZAPL plays a role in virus replication, we first determine whether overexpression of ZAPL affects viral protein synthesis in 293T cells. No effect was seen when cells were transfected with low amount of ZAPL and infected with high M.O.I. of Ud virus (data not shown). However, overexpression of high amount of ZAPL reduced viral protein synthesis approximately 2-4 fold when infected with low M.O.I. of Ud virus (0.1 pfu/cell) (Figure 3.3D), suggesting ZAPL inhibits Ud virus replication. To verify whether endogenous ZAPL inhibits Ud virus replication, we transfected A549 human lung cells with ZAPL-specific siRNA to efficiently knock down endogenous ZAPL. Multiple cycle growth of Ud virus from low M.O.I. infection (0.05 pfu/cell) in A549 cells with ZAPL knockdown or control knockdown were performed, and viral productions were determined at 36 and 60 hours after infection (Figure 3.3E). Interestingly, replication of Ud virus was enhanced by 20-30 fold in ZAPL knockdown cells compared to cells transfected with control siRNA, demonstrating that endogenous ZAPL moderately inhibits influenza A virus replication in human cells.

3.3.2 ZAPL binds to PB1 protein and reduces protein levels of PA and

PB2.

As the first approach to study the mechanism by which ZAPL inhibits influenza virus replication, we determined which protein(s) that ZAPL interacts with in the CPSF30-NS1A complexes. Co-immunoprecipitation experiment was performed to study protein-protein interaction. 293T cells were transfected with plasmid expressing each component protein in the CPSF30-NS1A complexes, i.e. PA, PB1, PB2, NP and NS1 individually, with or without co-transfection with ZAPL plasmid. Cell extracts were then immunoprecipitated with ZAPL, followed by immunoblots probed with Abs against each protein. Among the proteins tested, ZAPL only interacts with PB1 and NP (Figure 3.4A-B), suggesting that ZAPL likely through binding to these two proteins associates with CPSF30-NS1A complexes. Further RNase treatment showed that ZAPL interacts with PB1 in a RNase-resistant manner, indicating involvement of protein-protein interaction (Figure 3.4A, lane 2). In contrast, RNase treatment disrupted ZAPL-NP interaction, indicating this interaction is RNA-mediated and likely nonspecific (Figure 3.4B, lane 2). For this reason, we only focused on ZAPL-PB1 protein-protein interaction in subsequent experiments. The interaction of ZAPL with PB1 is not limited to PB1 from Ud virus, ZAPL also interacts with PB1 from pandemic H1N1 influenza A/CA/04/09 virus in a RNase-resistant manner, indicating the ZAPL-PB1 interaction is not Ud-specific (Figure 3.4C). To confirm that ZAPL interacts with PB1 in infected cells, cells were transfected with ZAPL and then infected with Ud virus. The ZAPL immunoprecipitates verifies the ZAPL-PB1 interaction in infected cells (Figure 3.4D).

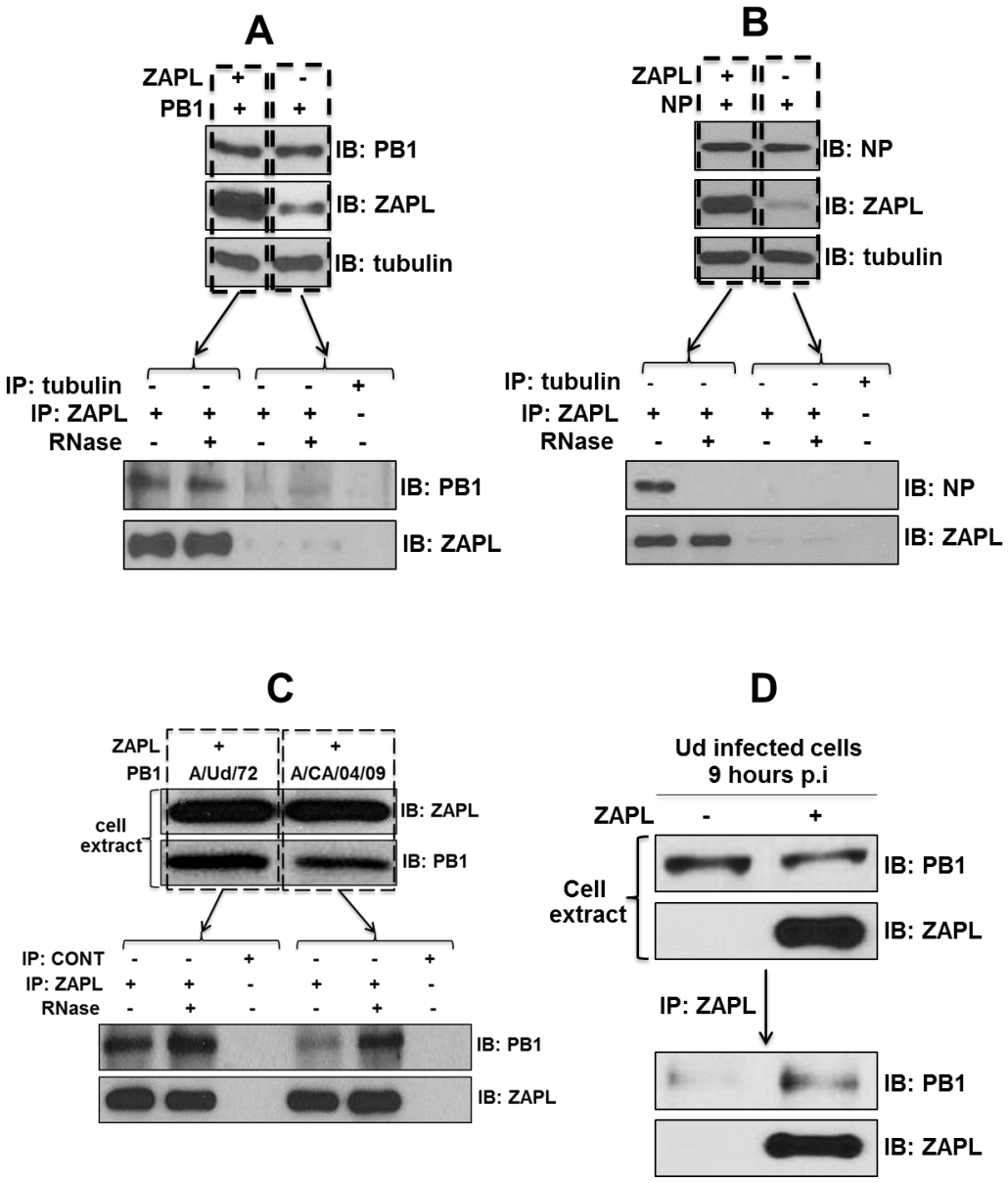

Figure 3.4 ZAPL interacts with PB1 in a RNase-resistant manner and interacts with NP in a RNase-sensitive manner. (A) 293T cells were transfected with PB1 and with or without ZAPL plasmid. Cell extracts were immunoprecipitated with ZAPL Ab or tubulin Ab as a control, and were then treated with or without RNase A (5 μg/ml). The immunoprecipitates were then immunoblotted with ZAPL or PB1 Ab. **(B)** Cells were transfected with NP and with or without ZAPL plasmid. Cell extracts were immunoprecipitated with ZAPL Ab or tubulin Ab, and were then treated with or without RNase A. The immunoprecipitates were then immunoblotted with ZAPL or NP Ab. **(C)** Cells were transfected with ZAPL and a PB1 plasmid of H1N1 influenza A/CA/04/09

virus. Same immunoprecipitation and immunobloting were performed. **(D)** Cells transfected with or without ZAPL plasmid were then infected with Ud virus at 0.1 pfu/cell. Cell extracts collected at 9 hours post infection were immunoprecipitated with ZAPL. The immunoprecipitates were then immunoblotted with ZAPL or PB1 Ab.

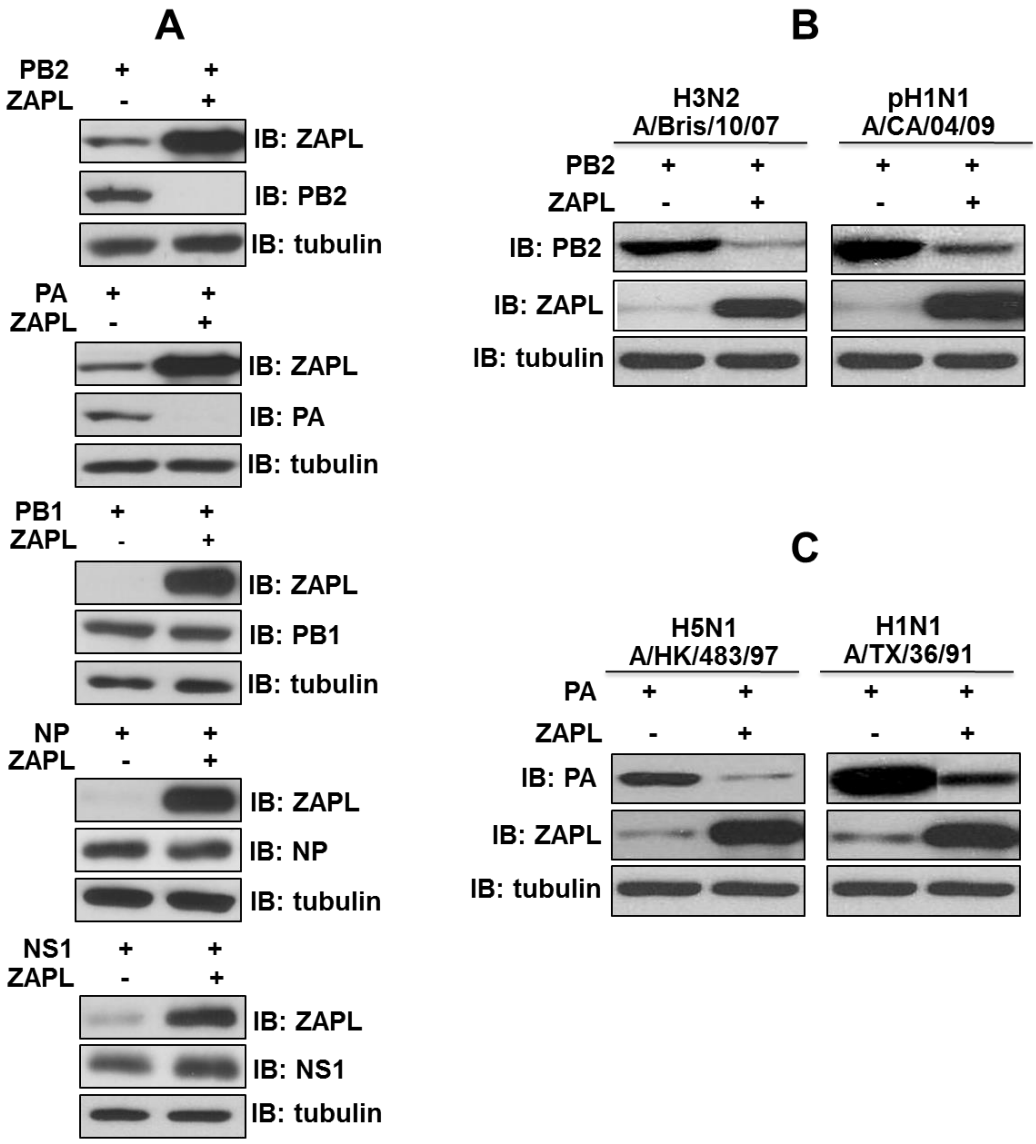

Figure 3.5 Plasmid-expressed ZAPL leads to protein reduction of PA and PB2, but not PB1, NP and NS1. (A) 293T cells were transfected with NS1, PB1, NP, PB2 or PA and with or without ZAPL plasmid, respectively, and cell extracts were immunoblotted with Ab against ZAPL, tubulin and the indicated co-expressed proteins. **(B-C)** Cells were transfected with PB2 or PA of the indicated influenza A virus strain and with or without ZAPL plasmid. Cell extracts were immunoblotted with PB2, PA, ZAPL, or tubulin antibody.

We did not detected ZAPL interaction with the other tested proteins (PA, PB2 and NS1). Interestingly, when we checked the cell extracts prior to co-immunoprecipitation experiments, we found PA and PB2 protein level were significantly and consistently reduced when co-transfected with ZAPL, suggesting ZAPL may play an inhibitory role against influenza virus. In contrast, co-transfection of ZAPL did not lead to reduction of PB1, NP or NS1 protein level (Figure 3.5A). PA and PB2 from different influenza virus strains were also tested. Figure 3.5B showed that ZAPL overexpression led to reduction of PB2 from both H3N2 influenza A/Bris/10/07 and pandemic H1N1 A/CA/04/09 strains. Figure 3.5C showed that ZAPL overexpression led to reduction of PA from both H5N1 influenza A/HK/483/97 and H1N1 A/TX/36/91 strains. These results indicate the effect of ZAPL on PA and PB2 protein reduction is not Ud-specific, and ZAPL may play a general inhibitory role against multiple influenza A viruses.

3.3.3 The C-terminal PARP domain, but not the RNA-binding activity of the N-terminal zinc-fingers of ZAPL is required for PA protein reduction

Previous studies have established the working model for ZAP's antiviral activity against other viruses. ZAPL specifically binds to target viral mRNAs via N-terminal zinc-fingers domain and promotes degradation of these viral mRNAs, thus inhibits viral replication (Bick et al., 2003; Gao et al., 2002; Guo et al., 2004; Guo et al., 2007a; Kerns et al., 2008; Muller et al., 2007; Zhu et al., 2011). We first tested whether viral mRNA degradation is the underlying mechanism by which ZAPL leads to PA and PB2 protein reduction. To test this, ZAPL with second zinc-finger C88R mutation that has been shown to lose

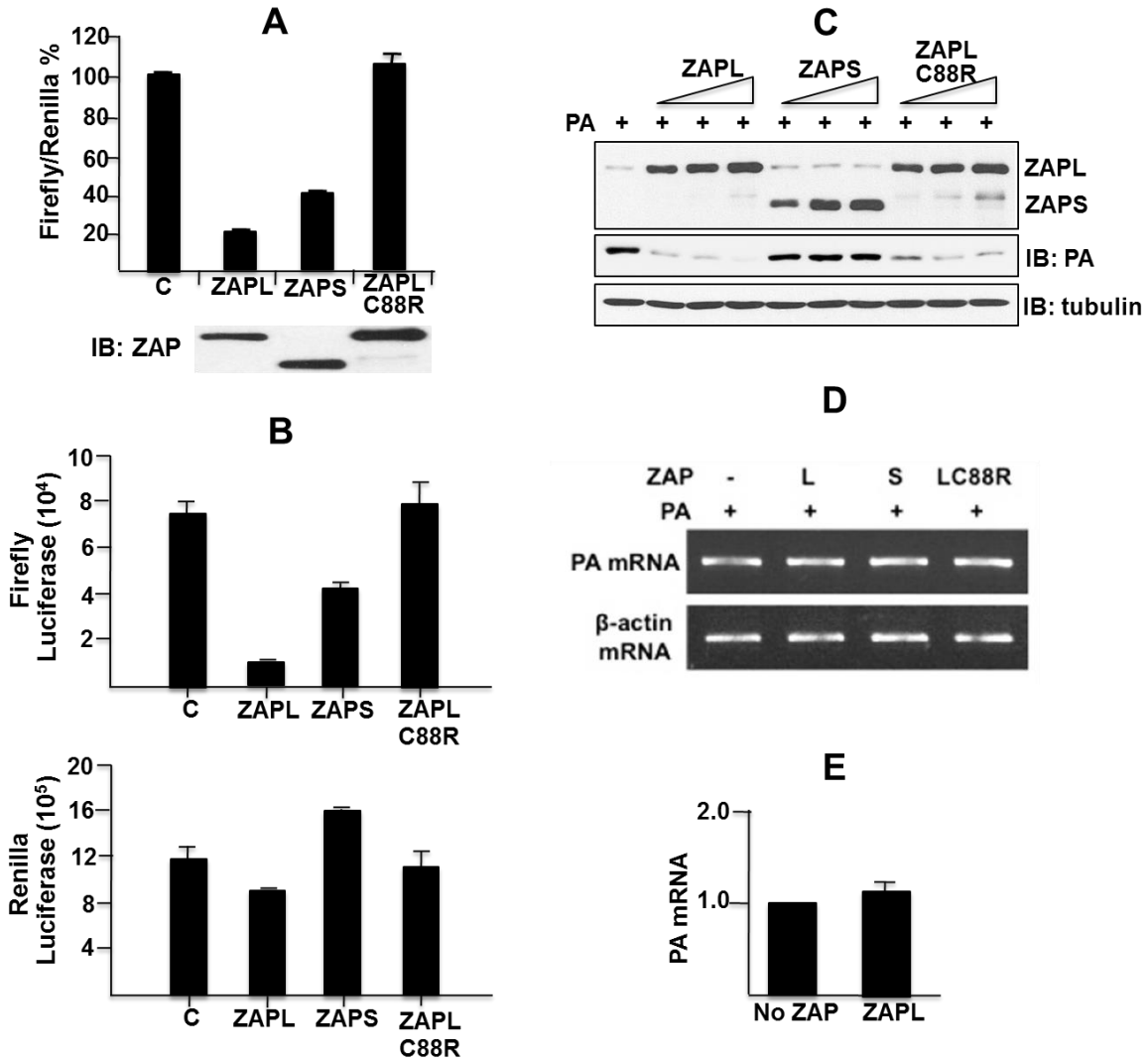

Figure 3.6 The RNA-degradation activity of the ZAPL N-terminal zinc-fingers is not involved in protein reduction of PA. (A-B) Luciferase reporter assay of mRNA degradation activity of ZAP proteins. 293T cells were transfected with 50ng of the LlucSN luciferase reporter plasmid and either ZAPL, ZAPS, ZAPL-C88R, or control plasmid. To determine transfection efficiency, 50ng of Renilla luciferase plasmid was included. After 24 hours of transfection, cells were collected, and the activities of the two luciferases in cell extracts were determined. The Firefly/Renilla ratio is shown as a percent of the control (C=No ZAP). Transfections were carried out in triplicate, and error bars are shown. The ZAP immunoblot shows that equal amounts of the three ZAP proteins were produced. **(C)** Effect of increasing amounts of ZAPL, ZAPS, or ZAPL-C88R plasmid on the protein expression of PA plasmid. **(D)**

Semi-quantitative RT-PCR of PA mRNA in cells transfected with the PA with either ZAPL, ZAPS, ZAPL-C88R, or control plasmid. Polyadenylated mRNA was isolated using oligo-dT-conjugated beads (Qiagen), and the amount of PA mRNA was determined by RT-PCR using specific primers. **(E)** Quantitative RT-PCR of PA mRNA in cells transfected with the PA and with or without ZAPL plasmid. Reactions were carried out in triplicate. The PA mRNA level in the presence of ZAPL was normalized to that without ZAPL. Error bars are shown.

RNA-binding and RNA degradation activities was constructed (Guo et al., 2004) and tested whether such mutant ZAPL can reduce PA and PB2 protein level. We first verified that the ZAPL-C88R zinc-finger mutant indeed lose ability to degrade its target viral mRNA by using an luciferase reporter assay for ZAP-mediated RNA degradation established in study by Kerns et al., 2008. The LlucSN reporter used in this assay contains a MLV sequence which can be targeted by ZAP, and once targeted and degraded, the luciferase activity decreases. Figure 3.6A showed that ZAPL with C88R mutation indeed lose ability to target mRNA. Consistent with results from study by Kerns et al., 2008, ZAPL shows strong activity against viral mRNA, whereas ZAPS also causes RNA degradation with less efficiency than ZAPL. Figure 3.6B showed the transfection efficiency was similar between these different plasmids by measuring the activity of Renilla luciferase which does not contain target sequence of ZAP. We next tested these different ZAP proteins on their ability to affect PA protein level. Cells were transfected with PA and increasing amounts of either ZAPL, ZAPL-C88R mutant or ZAPS plasmid (Figure 3.6C). Surprisingly, the wild-type ZAPL and ZAPL-C88R mutant effectively reduced the amount of PA protein to essentially the same extent, showing that the RNA degradation activity of N-terminal zinc-finger domain of ZAPL is not involved in reducing PA protein level. Furthermore, ZAPS, which causes RNA degradation but lacks the C-terminal PARP domain, did not reduce PA protein level, demonstrating that the PARP domain has an important role in the reduction of PA, which is confirmed below. To further verify that RNA degradation was not involved in ZAPL-mediated inhibition of PA protein production, we determined the level of PA mRNA from cells transfected with

PA and and with or without different ZAP plasmids. The mRNAs with poly-A tail were purified with oligo-dT-beads (Qiagen) and RT-PCR with specific primers was performed. Semi-quantitative RT-PCR showed that level of PA mRNA was not affected by all tested ZAP proteins (Figure 3.6D), consistent with the conclusion from immunoblots in Figure 3.6C. Further quantitative RT-PCR showed that ZAPL did not decrease the level of PA mRNA (Figure 3.6E). We conclude that ZAPL-mediated PA protein reduction is not due to the mRNA degradation mechanism by ZAPL zinc-finger.

3.3.4 PB2 and PA bind to the ZAPL PARP domain and undergo proteasomal degradation, whereas PB1 binds to an adjacent region of ZAPL that contains the WWE domain and is not degraded.

The above results indicate that it is unlikely that the RNA-binding activity of the N-terminal zinc fingers of ZAPL is involved in its antiviral activity against influenza A virus. Accordingly, we next tested an alternative mechanism, whether plasmid-expressed ZAPL promotes proteasomal degradation of PA and PB2 proteins. To test this, cells were transfected with PA or PB2 and with or without ZAPL plasmid for 18 hours and then treated with the proteasome inhibitor MG132 or DMSO as control for 24 hours (Figure 3.7A-B). In cells co-transfected with ZAPL, very low amount of PA or PB2 protein was detected in the absence of MG132 (lane 3 and 7). However, the protein levels of these two proteins were significantly increased by when proteasome function was blocked by MG132 (lane 4 and 8), suggesting the plasmid-expressed ZAPL leads to proteasomal degradation of PA and PB2. Interestingly, co-immunprecipitation of these cells extracts with ZAPL showed that the PA and

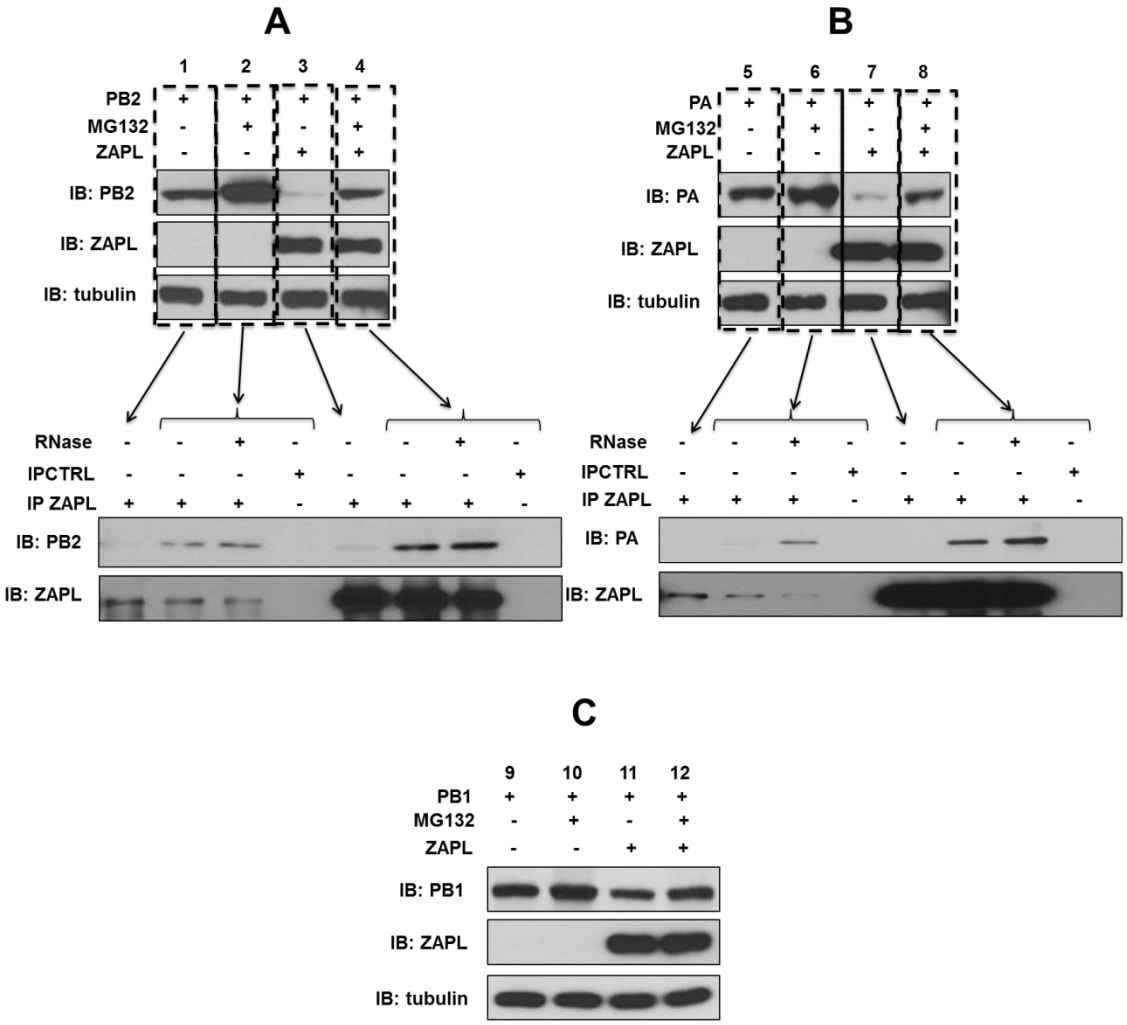

Figure 3.7 PA and PB2 protein reduction by ZAPL can be rescued by MG132 treatment, in which ZAPL interacts with MG132-stabilized PA and PB2. (A-C) 293T cells were treated with 40μM MG132 or as 0.1% DMSO as a control after transfection with PB2 (A), PA (B) or PB1 (C) and with or without ZAPL plasmid as described in the text. For the PB2 and PA transfections (lanes 1-8), the extracts from DMSO-treated cells were immunoprecipitated with ZAPL Ab, followed by immunoblots with ZAPL and PA or PB2 Ab. The extract from MG132-treated cells was immunoprecipitated with ZAPL Ab or tubulin Ab as immunoprecipitation control, with or without subsequent RNase treatment. The imunoprecipitates were immunoblotted with ZAPL and PA or PB2 Ab. For the PB1 transfection (lanes 9-12), the cell extracts were immunoblotted with PB1, ZAPL and tubulin Ab.

PB2 protein that were rescued from proteasomal degradation by MG132 treatment were bound to ZAPL in a RNase-resistant manner, suggesting that ZAPL binds to PA and PB2 to promote their degradation. Plasmid-expressed ZAPL was largely responsible for reducing PA and PB2 proteins, because PA and PB2 levels were lower than that in the absence of ZAPL plasmid, both with or without MG132 treatment (compare lane 1 and 2 to lane 3 and 4; lane 5 and 6 to lane 7 and 8), suggesting MG132 treatment only partially rescued PA ad PB2 protein from plasmid-expressed ZAPL. Furthermore, in the absence of plasmid-expressed ZAPL, the PA and PB2 protein also rescued by MG132 treatment (lane 1 and 2; lane 6 and 7), and the MG132-stablized PA and PB2 proteins were bound to endogenous ZAPL in a RNase-resistant manner, suggesting endogenous ZAPL targets PA and PB2 to promote their proteasomal degradation in the absence of plasmid-expressed ZAPL, which was verified in the subsequent further experiments. On the other hand, the level of PB1 protein was not increased by MG132 treatment in the absence of plasmid-expressed ZAPL, and was only slightly increased less than 2-fold by MG132 treatment in the presence of plasmid-expressed ZAPL (Figure 3.7C), indicating that ZAPL specifically targets PA and PB2, but not PB1, for degradation.

Based on the result that the C-terminal PARP domain of ZAPL is required for PA protein degradation, we next determined whether ZAPL PARP domain is also required for binding to PA and PB2. We constructed two different ZAP fragments, Z1 that contains PARP domain and Z2 that contains WWE and PARP domain, and tested their ability to bind PA, PB2 and PB1 protein (Figure 3.8A). Cells were transfected with PB2 (Figure 3.8B), PA (Figure 3.8C)

or PB1 (Figure 3.8D) and V5-tagged wild-type ZAPL or ZAP fragments, and then treated with MG132 for PB2 and PA expressed cells to minimize PB2 and PA degradation caused by endogenous or plasmid-expressed ZAPL. Cell extracts were immunoprecipiated with V5 antibody and immunoblotted with indicated Abs. The results showed that Z1 ZAP fragment comprising the PARP domain was sufficient for binding PB2 and PA, but not PB1, demonstrating that the PARP domain is responsible for binding PB2 and PA, but not PB1. The Z2 ZAP fragment comprising both WWE and PARP domains bound to PB1 almost as efficiently as the full-length ZAPL, indicating that PB1 presumably binds to the ZAPL region containing WWE domain. Because the ZAP fragment containing WWE domain alone (580-700 aa) did not express well in cells, thus it was not available for further verification of PB1 binding in this approach. We conclude that the PARP domain is responsible for binding PB2 and PA, and is required for their degradation, whereas PB1 binds primarily to the adjacent ZAPL region containing WWE domain and is not degraded.

Furthermore, we found that Z2 fragment bound significantly more PB2 and PA than full-length ZAPL and Z1 fragment, and some of the Z2-bound PB2 and PA proteins were larger in size (lane 3 in Figure 3.8B, C), suggesting they were post-translationally modified. Compared to Z1, Z2 fragment contains one more domain, WWE domain, which has been shown to interact with poly-ADP-ribosylated chains (Wang et al., 2012), it is therefore likely that the PB2 and PA proteins associated with the Z2 fragment are poly-ADP-ribosylated, which was verified in subsequent experiment. We hypothesized that the PB2 and PA proteins bound to the Z2 fragment are poly-ADP-

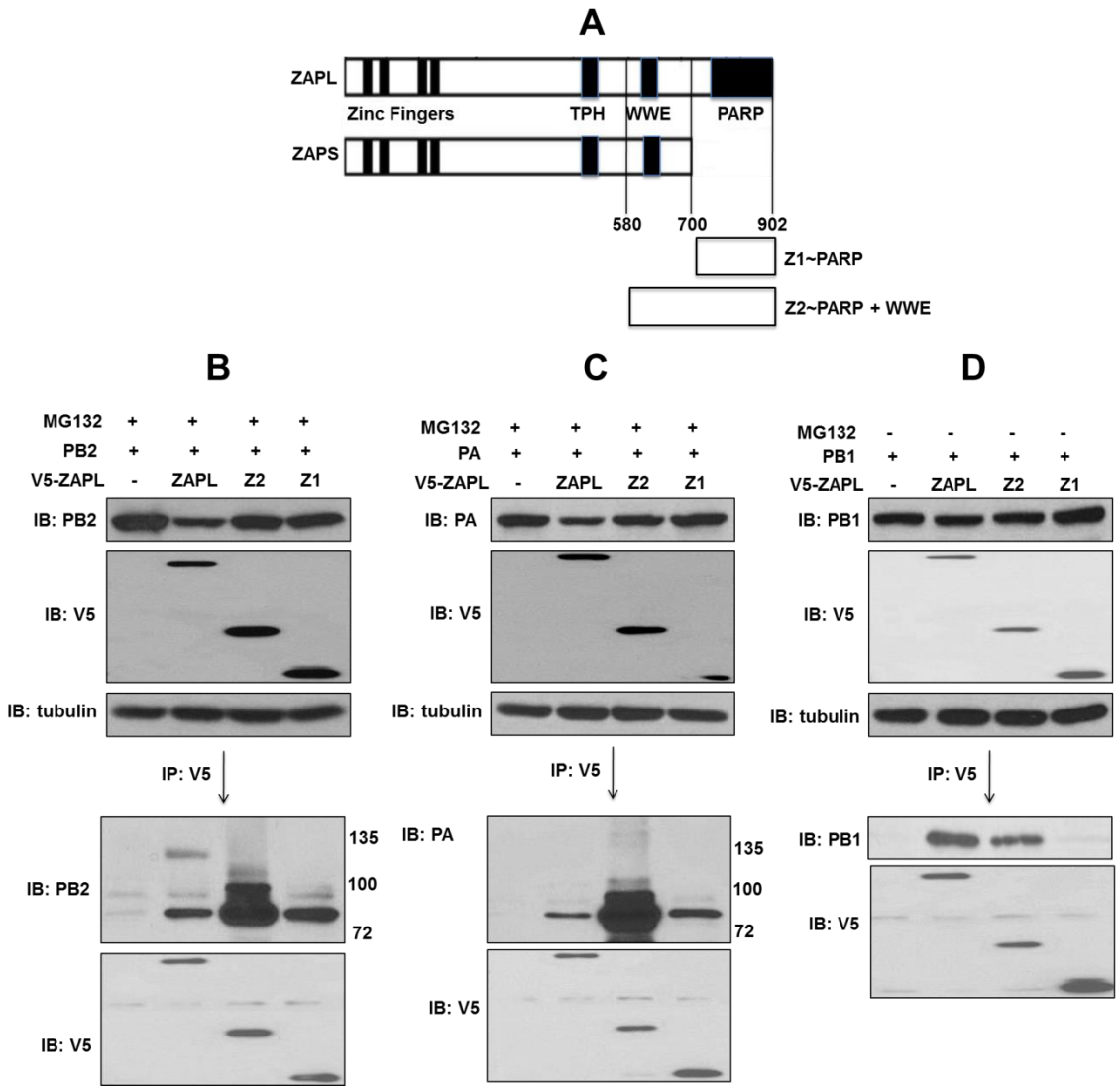

Figure 3.8 PB2 and PA bind to the ZAPL PARP domain, whereas PB1 binds to an adjacent region of ZAPL that contains the WWE domain. (A) Diagram of the Z1 and Z2 fragments of ZAPL. Z1 (700–902 aa) contains PARP domain whereas Z2 (580–902aa) contains PARP and WWE domain. **(B-D)** 293T cells were transfected with PB2 (B), PA (C) or PB1 (D) with V5-ZAPL, V5-Z2, or V5-Z1 or control plasmid. The PB2 and PA transfections were followed by MG132 treatment. Aliquots of the cell extracts were immunoblotted with the indicated Abs as input for immunoprecipitation. After immunoprecipitation with V5 Ab, the immunoprecipitates were immunoblotted with the indicated Abs.

ribosylated intermediates that require the full-length ZAPL protein for subsequent processing, i.e. ubiquitination that then leads to proteasomal degradation (see detail in Discussion).

ZAPL, also known as PARP13, has been shown to participate in cellular functions in cytoplasm (Leung et al., 2011), where ZAPL binds to endosomal membranes and/or is associated with stress granules (Charron et al., 2013; Leung et al., 2011). As a result, ZAPL would be expected to target PA, PB2 and PB1 proteins in the cytoplasm. To verify that is the case, immunofluorescence by confocal microscopy was performed on cells transfected with PA, PB2 or PB1 and low amount of ZAPL to minimize degradation of PA and PB2 (Figure 3.9). Individually expressed PA and PB1 proteins are localized primarily in the cytoplasm, whereas PB2 is mainly in the nucleus (Fodor and Smith, 2004). Figure 3.9A showed that ZAPL indeed interacts with PA or PB1 in the cytoplasm. To investigate that ZAPL also targets PB2 in the cytoplasm, split-GFP approach was used. Split-GFP strans-1-10 (Sandia Biotech) was cloned on to the C-terminus of PB2, split-GFP strand-11 was cloned on to the N-terminus of ZAPL or ZAPS (as a negative control). In Figure 3.9B, GFP signal only can be seen in the cytoplasm when cells were co-transfected with PB2 and ZAPL, but not ZAPS, indicating ZAPL interacts with PB2 in the cytoplasm and confirming that PARP domain is required for binding PB2.

3.3.5 Plasmid-expressed and endogenous ZAPL binds to PA and PB2, leading to their ubiquitination and proteasomal degradation.

Because proteins are ubiquitinated before they get proteasomal

degraded, we tested whether PA and PB2 are ubiquitinated prior to proteasomal degradation, and whether the ubiquitination requires ZAPL. Cells were transfected with PB2 or PA and with or without ZAPL plasmid. Where indicated, the transfected cells were then treated with MG132 or DMSO as shown in Figure 3.10. Ubiquitinated protein species in cell extracts were affinity selected by beads conjugated with tandem ubiquitin-binding domains (TUBE-2, LifeSensors), followed by immunoblot probed with PA or PB2 Ab. Multiple ubiquitinated protein species larger in size than PA or PB2 were detected in the cells transfected with ZAPL (Lane 2 in Figure 3.10A and B). Most of these ubiquitinated protein species were absent when PA and PB2 were not protected against proteasomal degradation by MG132 treatment (Lane 3 in Figure 3.10A and B), indicating that the observed ubiquitinated proteins are PA and PB2 ubiquitin conjugates.

Interestingly, ubiquitinated PA and PB2 proteins were also detected from the cells without plasmid-expressed ZAPL and treated with MG132 (Lane 1 in Figure 3.10A and B). To determine whether endogenous ZAPL is responsible for the ubiquitination and degradation of PA and PB2, two different approaches were carried out. In the first approach, endogenous ZAPL was knocked down by specific siRNA. Cells were transfected with either control siRNA or siRNA specifically targets the ZAPL PARP domain so that only ZAPL but not ZAPS is knocked down. To avoid second exposure of the cells to transfection reagent, PB2 and PA were expressed from pseudo-retrovirus. Compared to control samples, siRNA knockdown of endogenous ZAPL effectively rescued PB2 and PA from degradation (Figure 3.11A). As a negative control, GFP expression from the same pseudo-retrovirus was not

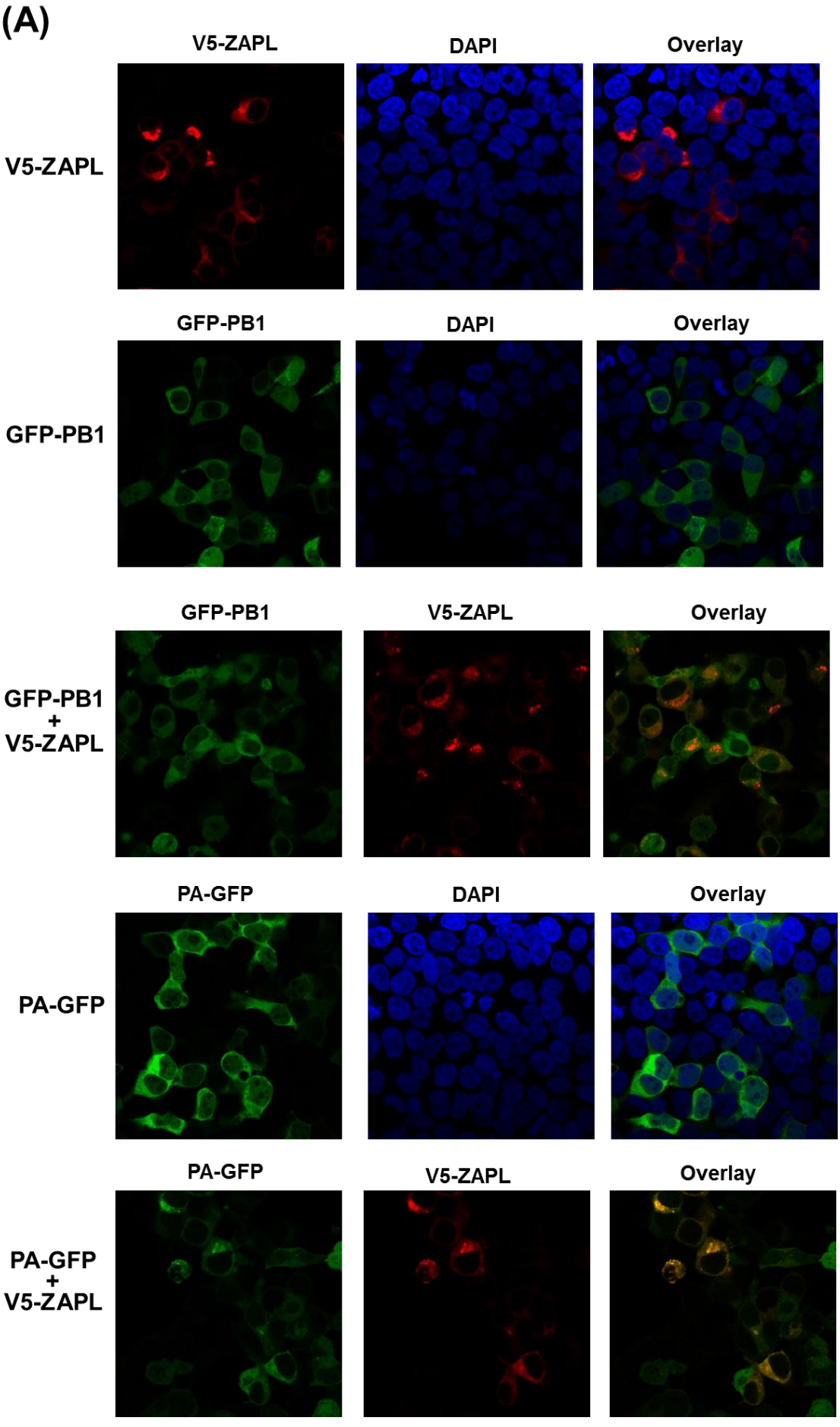
(A)
V5-ZAPL
DAPI
Overlay
V5-ZAPL
GFP-PB1
DAPI
Overlay
GFP-PB1
GFP-PB1
V5-ZAPL
Overlay
GFP-PB1
+
V5-ZAPL
PA-GFP
DAPI
Overlay
PA-GFP
PA-GFP
V5-ZAPL
Overlay
PA-GFP
+
V5-ZAPL

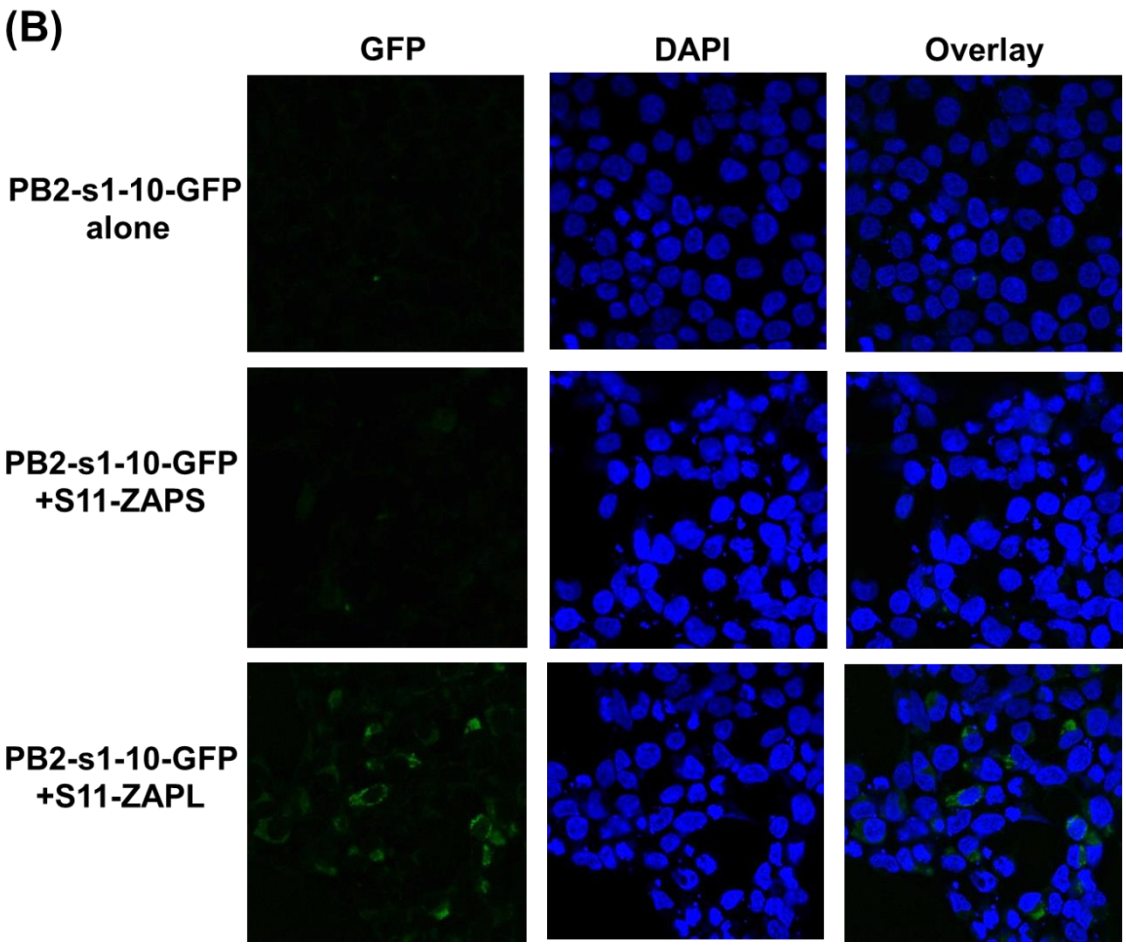

Figure 3.9 ZAPL interacts with PB1, PA or PB2 in the cytoplasm. (A) 293T cells were transfected with GFP-PB1, PA-GFP, V5-ZAPL plasmid, where indicated, for 36 hours. The cells were then fixed with 4% paraformaldehyde and permeabilized with 0.5% Triton X-100. V5-ZAPL was visualized using mouse anti-V5 antibody and Alexa fluor 546 conjugated goat anti-mouse antibody (Life technologies). Cell nuclei were stained with DAPI. Images were obtained using a Zeiss LSM 710 Confocal microscope, and data were processed with ZEN 2012 software. **(B)** Split-GFP strans-1-10 (Sandia Biotech) was cloned on to the C-terminus of PB2, split-GFP strand-11 was cloned on to the N-terminus of ZAPL or ZAPS (as a negative control). 293T cells transfected with indicated plasmids were fixed, permeabilized and stained with DAPI before they were used for direct fluorescence with the confocal microscope. All images were acquired using the same experimental settings. (Done by Ligang Zhou)

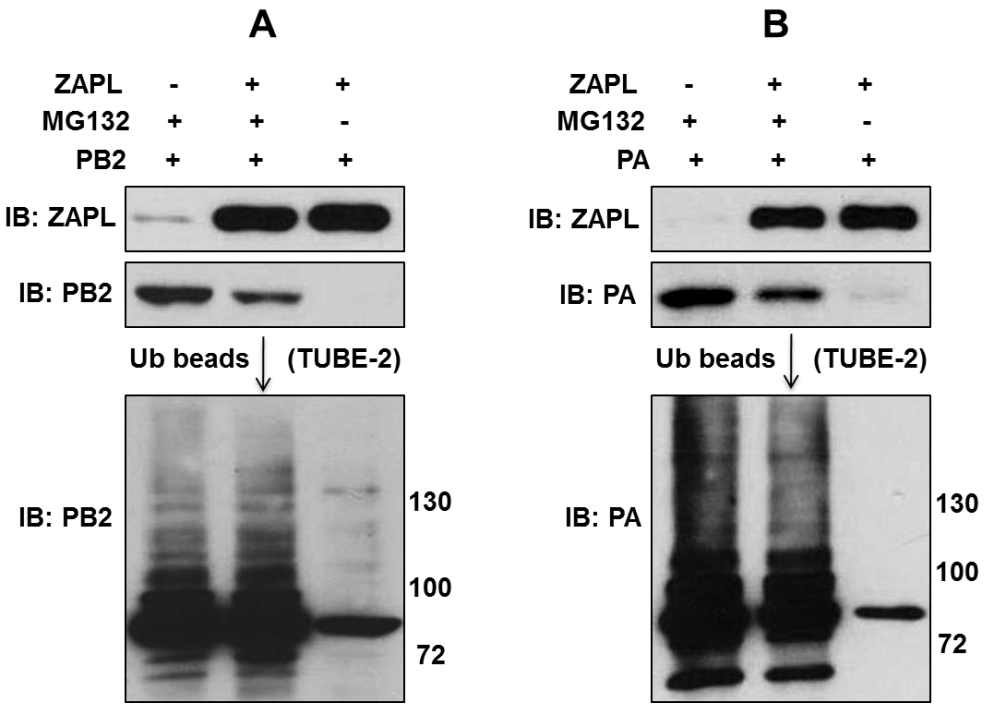

Figure 3.10 PA and PB2 protein are ubiquitinated under MG132 treatment. **(A-B)** 293T cells were transfected with PB2 (A) or PA (B) and with or without ZAPL plasmid. Where indicated, the transfected cells were treated with MG132 or DMSO. Aliquots of the cell extracts were immunoblotted with the indicated Abs as input for immunoprecipitation. After binding the cell extracts to beads conjugated to tandem ubiquitin-binding domains (TUBE-2, LifeSensors), the bound proteins were eluted and immunblotted with PB2 or PA Ab.

affected by ZAPL knockdown. As the second approach, the Z2 ZAP fragment was overexpressed to interact and occupy PB2 and PA so that endogenous ZAPL cannot target them. Cells were transfected with increasing amounts of Z2 fragment and treated with retrovirus expressing PA or PB2. As shown in Figure 3.11B, overexpression of Z2 fragment rescued PB2 and PA protein from endogenous ZAPL-mediated degradation in a dose-dependent manner. As a negative control, Z2 overexpression did not affect the protein level of GFP expressed from pseudo-retrovirus.

These results provide further evidences that ZAPL PARP domain binds to PB2 and PA to promote their degradation. The siRNA knockdown of ZAPL and Z2 overexpression results indicate that endogenous ZAPL is responsible for the degradation of PB2 and PA in the absence of plasmid-expressed ZAPL. We next determined whether endogenous ZAPL is also responsible for PB2 and PA ubiquitination prior to proteasomal degradation. Cells were transfected with or without Z2 fragment, followed by infection with retrovirus expressing PB2 and then MG132 treatment. Total ubiquitinated proteins in cell extracts were selected with TUBE-2 beads. The overexpression of Z2 fragment significantly reduced the ubiquitination of PB2 that occurs in the absence of plasmid-expressed ZAPL without affecting the total protein ubiquitination in cells (Figure 3.12A). These results establish that endogenous ZAPL and plasmid-expressed ZAPL promote the ubiquitination and proteasomal degradation of PB2 and PA.

We then determined whether ubiquitinated PB2 and PA proteins are bound to ZAPL. Cells were transfected with PB2 and with or without ZAPL plasmid, and

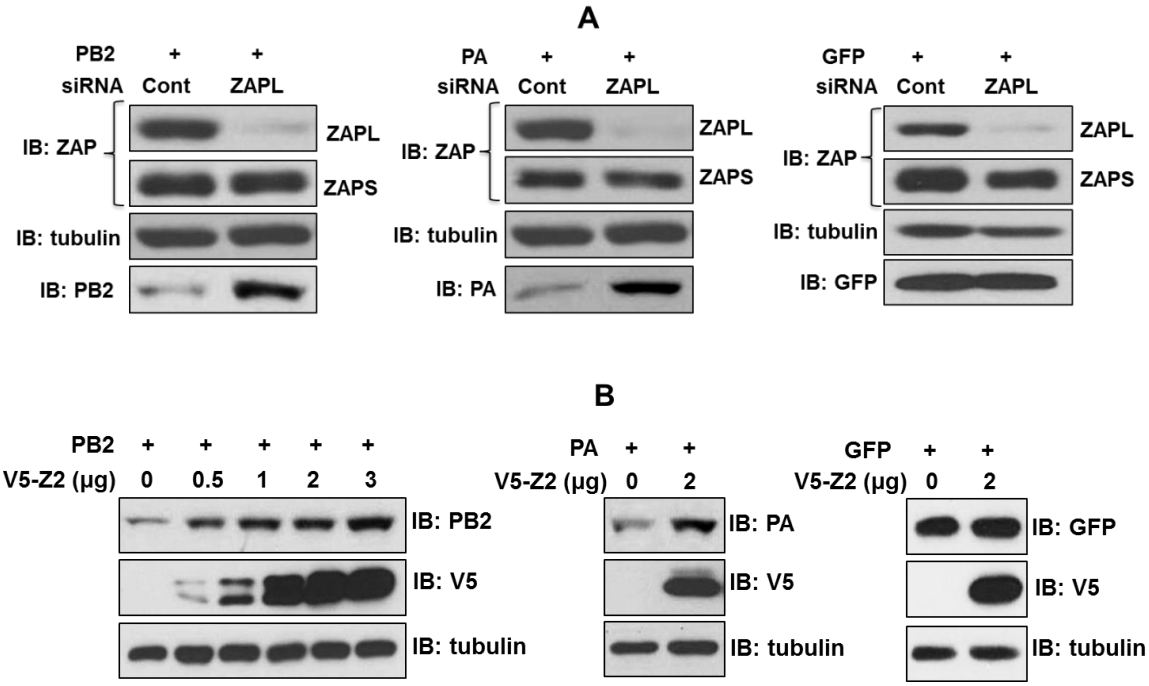

Figure 3.11 Endogenous ZAPL is responsible for PB2 degradation. (A) 293T cells were transfected with control siRNA or ZAPL-specific siRNA for 36 hours, and were then infected with retrovirus expressing either PB2, PA or GFP as control for 24 hours. Cell extracts were immunoblotted with the indicated Abs. **(B)** 293T cells were transfected with the indicated amounts of the V5-Z2 ZAP fragment plasmid for 48 hours, followed by infection with a retrovirus expressing PB2, PA or GFP for 24 hours. The cell extracts were immunoblotted with the indicated Abs.

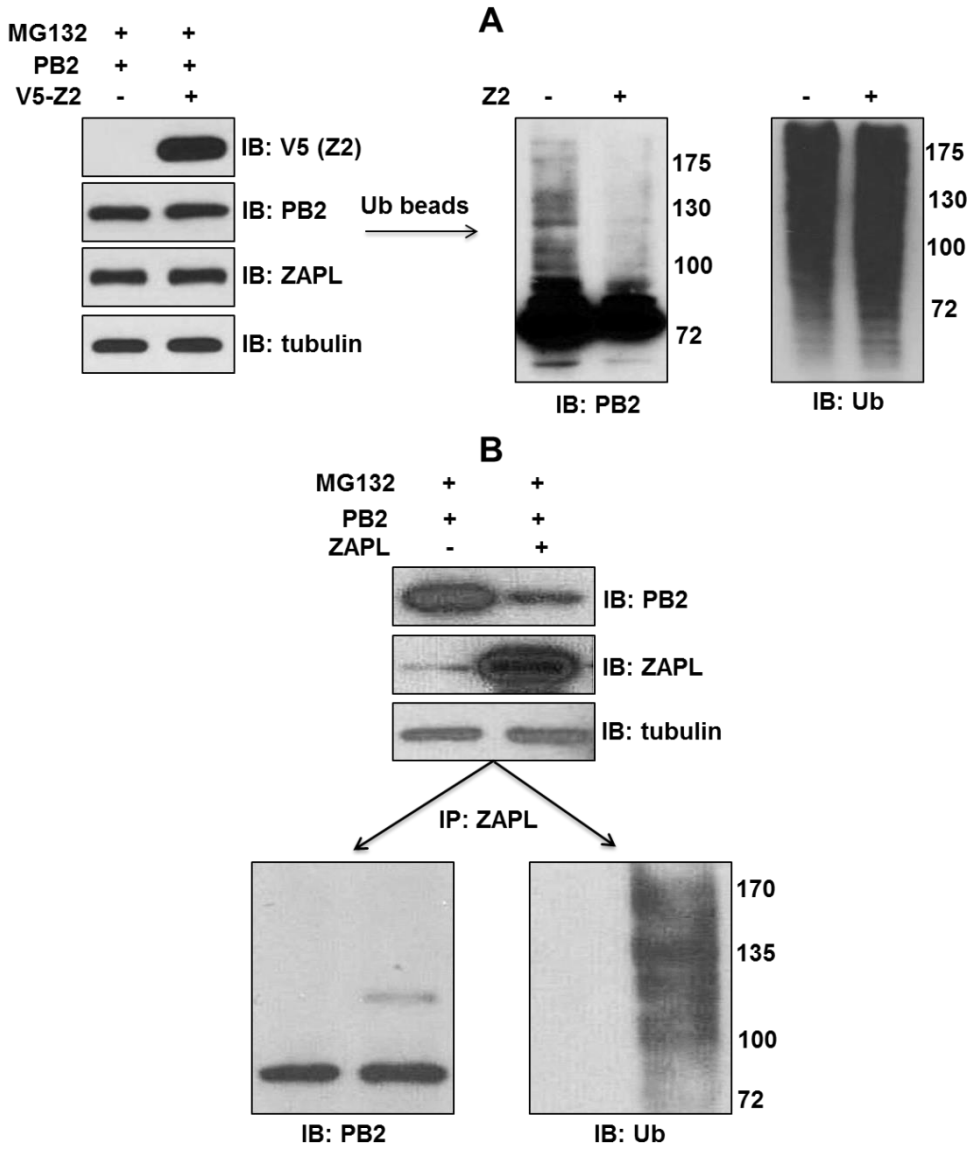

Figure 3.12 ZAPL binds to PB2 and leads to its ubiquitination. (A) 293T cells were transfected with or without V5-Z2 plasmid for 40 hours, followed by infection with a retrovirus expressing PB2 and then MG132 treatment. An aliquot of the cell extracts was immunoblotted with the indicated Ab as input for immunoprecipitation. The cell extracts were selected on beads conjugated to tandem ubiquitin-binding domains (TUBE-2), and the eluate was immunoblotted with either PB2 or Ub Ab. **(B)** 293T cells were transfected with PB2 and with or without ZAPL plasmid, and then treated with MG132. Aliquots of the cell extracts were immunoblotted with the indicated Abs as input for immunoprecipitation. Cell extracts were immunoprecipitated with ZAPL Ab, and the immunoprecipitate was immunblotted with PB2 or Ub Ab.

then treated with MG132. Cell extracts were immunoprecipitated with ZAPL, and immunblotted with presence of PB2 and ubiquitination (Figure 3.12B). The result showed that PB2 and ubiquitinated protein species larger in size than PB2 were detected in ZAPL immunoprecipitates, indicating that ubiquitinated PB2 is bound to ZAPL. Taken together, these results indicate that PB2 and PA are ubiquitinated while they are bound to ZAPL.

3.3.6 PB2 and PA are poly(ADP-ribosylated), but not by ZAPL, which is involved in ZAPL-mediated degradation.

Now we established that ZAPL PARP domain targets PA and PB2, leading to their ubiquitination and proteasomal degradation. We were wondering how PARP domain is involved in protein degradation pathway. Recent studies have provided some clues. The primary function of PARP protein is to post-translationally modify its target protein with poly-(ADP-ribose) chain, a process known as poly(ADP-ribosylation) or PARylation. Poly(ADP-ribosylation) was best known for its functions in the nucleus to regulate transcription, chromosome structure, and DNA damage repair (Krishnakumar and Kraus, 2010). Accumulated studies showed poly(ADP-ribosylation) is also involved in cytoplasmic functions. One of which is that cytoplasmic PARP-containing proteins can initiate proteasomal degradation by poly(ADP-ribosylating) their target proteins, followed by ubiquitination catalyzed by an E3 ubiquitin ligase that recognize poly-ADP-ribose and the PARP protein to which the poly-ADP-ribosylated target protein is bound (DaRosa et al., 2014; Leung et al., 2011; Wang et al., 2012; Zhang et al., 2011a). However, the PARP domain of ZAPL (also known as PARP13.1) lacks the catalytic activity

for poly(ADP-ribosylation) (Kleine et al., 2008). It is likely that ZAPL cooperates with other PARP proteins to perform this activity, as previously shown by others (Leung et al., 2011).

To study the underlying mechanism by which ZAPL PARP domain targets PA and PB2 for proteasomal degradation, we first determine whether PA and PB2 are poly(ADP-ribosylated). Cells were transfected with Flag-PB2 or Flag-PA and with or without ZAPL plasmid, and then treated with MG132 or DMSO. Cell extracts were immunoprecipitated with Flag-antibody-conjugated beads, and then the immunoprecitates were eluted and immunoblotted with Ab against poly(ADP-ribose) chains (Figure 3.13) (Leung et al., 2011; Seo et al., 2013). Multiple poly(ADp-ribosylated) protein species larger in size than PB2 and PA were detected in cells expressed with ZAPL when proteasome degradation of PB2 and PA was inhibited with MG132 (Lane 2 and 4 in Figure 3.13). These poly(ADP-ribosylated) protein species appeared as a smear larger in size of PB2 and PA because of the heterogeneity in the length of the poly(ADP-ribose) chain that were added, as previously shown by others (Leung et al., 2011; Seo et al., 2013). Most of these poly(ADP-ribosylated) protein species were absent when PB2 and PA were degraded in the absence of MG132 treatment (Lane 3 and 6 in Figure 3.13), indicating the observed poly(ADP-ribosylated) protein species are primarily poly(ADP-ribosylated) PB2 and PA proteins.

Poly(ADP-ribosylated) PB2 and PA proteins were also detected from the M132-treated cells without plasmid-expressed ZAPL (Lane 1 and 4 in Figure 3.13). To determine whether endogenous ZAPL is responsible for the

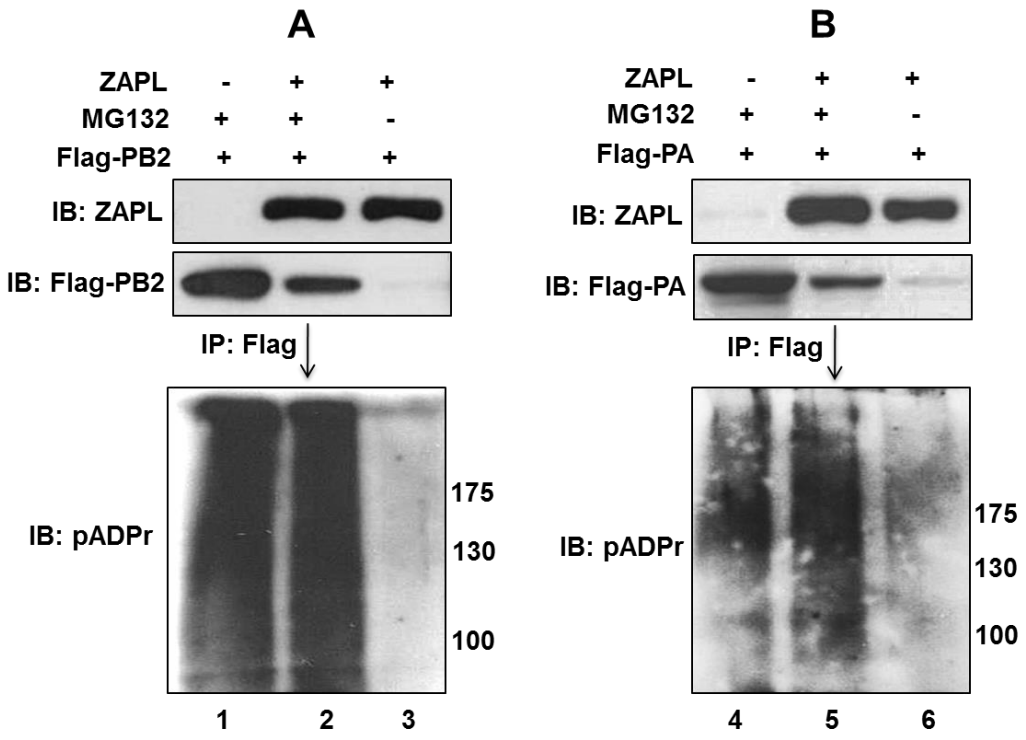

Figure 3.13 PA and PB2 protein are ploy-ADP-ribosylated under MG132 treatment. (A-B) 293T cells were transfected with Flag-PB2 or Flag-PA and with or without ZAPL plasmid 40 hours. Where indicated, the cells were treated with MG132 or DMSO. An aliquot of the cell extracts was immunoblotted with the indicated Abs as input for immunoprecipitation. Cell extracts were immunoprecipitated with Flag-antibody-conjugated beads (Sigma) and the immunoprecipitates were analyzed by immunoblots probed with an Ab against pADPr (LP96-10, BD-Pharmingen).

poly(ADP-ribosylation) of PA and PB2, the ZAP fragment was overexpressed in cells to sequester PB2 and PA from endogenous ZAPL. Cells were transfected with V5-Z1 ZAP fragment or control plasmid, followed by infection with a retrovirus expressing PB2 with 1xFlag tag and then MG132 treatment. Cell extracts were immunoprecipitated with Flag-PB2 and Flag-PA to detect presence of poly(ADP-ribosylation) (Figure 3.14A). Interestingly, overexpression of Z1 ZAP fragment did not reduce the poly(ADP-ribosylation) of PB2 in the absence of plasmid-expressed ZAPL, indicating that endogenous ZAPL itself is not responsible for catalyzing this poly(ADP-ribosylation). This result is as expected because ZAPL lacks the catalytic activity for poly(ADP-ribosylation) (Kleine et al., 2008).

The experiment in Figure 3.8 suggested that the poly(ADP-ribosylated) PB2 and PA protein accumulate in the Z2 region of ZAPL. To verify this conclusion, we determined whether PB2 bound on Z2 fragment is poly(ADP-ribosylated). Cells were transfected with PB2 and with or without Z2-1xFlag plasmid, followed by MG132 treatment. Cell extracts were immunoprecipitated with Flag-M2-beads to detected the presence of poly(ADP-ribosyalted) PB2. Figure 3.14B shows that poly(ADP-ribsyalted) PB2 was detected bound on the Z2 fragment of ZAPL, verifying poly(ADP-ribosylated) PB2 and PA are associated with the Z2 region of ZAPL.

We next determined whether the poly(ADP-ribosylation) of PA and PB2 is involved in ZAPL-mediated proteasomal degradation. It was known that poly(ADP-ribosylation) on certain cytoplasmic proteins was increased by siRNA knockdown of cytoplasmic PARG proteins (Poly(ADP-ribosylation)

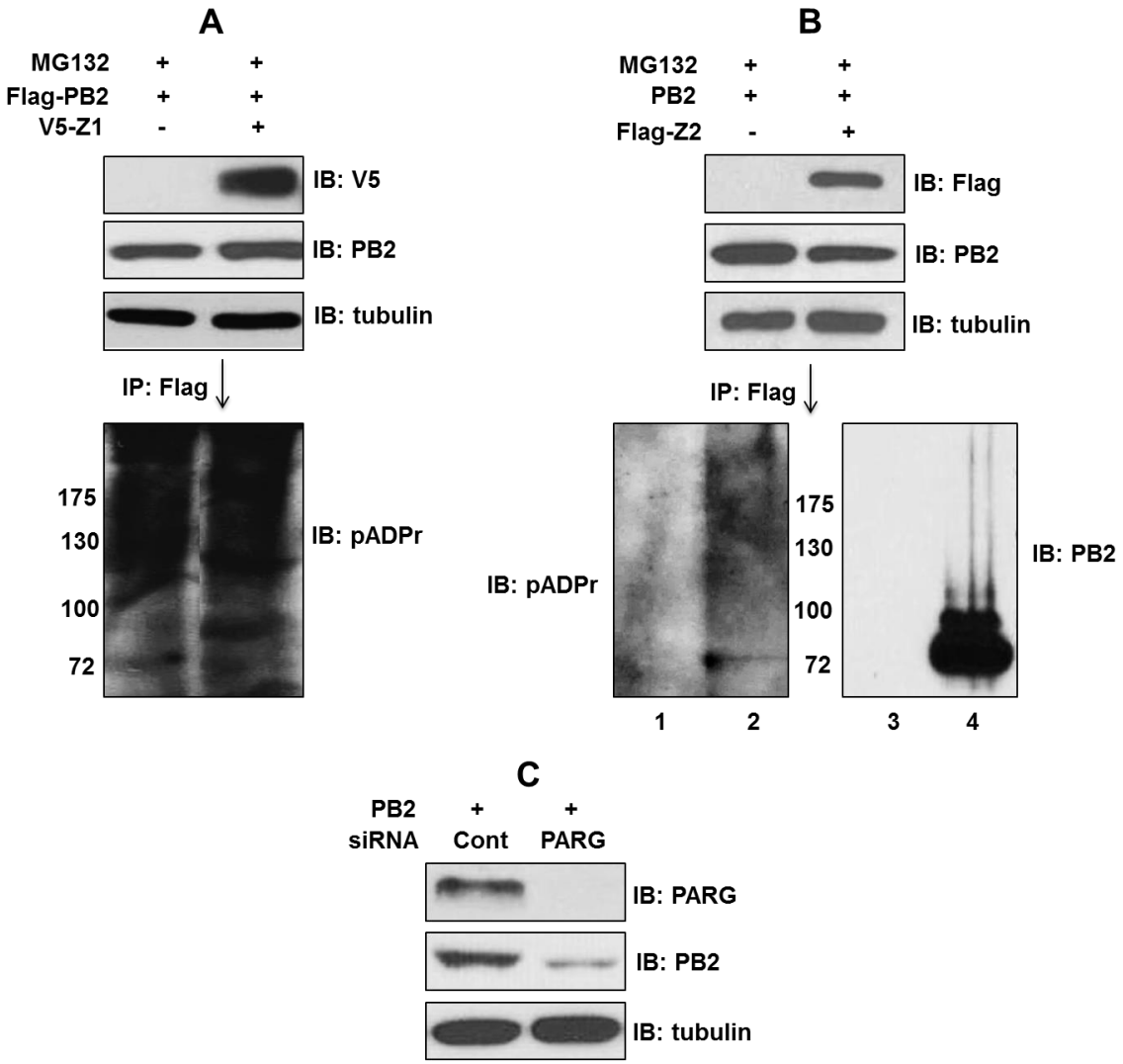

Figure 3.14 Poly(ADP-ribosylation) of PB2 is not catalyzed by ZAPL, but is involved for ZAPL-mediated degradation. (A) 293T cells were transfected with V5-Z1 ZAP fragment or control plasmid, followed by infection with a retrovirus expressing PB2 with 1xFlag tag and then MG132 treatment. An aliquot of the cell extracts was immunoblotted with the indicated Abs as input. Cell extracts were immunoprecipitated with Flag-antibody-conjugated beads and the immunoprecipitates were analyzed by immunoblots probed with an Ab against pADPr. **(B)** 293T cells were transfected with PB2 and with or without 1xFlag tagged Z2 plasmid, followed by MG132 treatment. Aliquots of the cell extracts were immunoblotted with the indicated Abs as input. After immunoprecipitation with Flag-M2-beads, the immunoprecipitates were immunoblotted with the indicated Abs. **(C)** 293T cells were transfected with

control siRNA or PARG-specific siRNA for 48 hours, followed by infection with a retrovirus expressing PB2 for 24 hours. Cell extracts were immunoblotted with the indicated Abs.

glycohydrolases) which is an enzyme to remove poly(ADP-ribose) modifications (Erdelyi et al., 2009; Leung et al., 2011). Cells were transfected with control siRNA or PARG-specific siRNA, followed by infection with a retrovirus expressing PB2. As shown in Figure 3.14C, knockdown of PARG significantly increased PB2 degradation, indicating that poly(ADP-ribosylation) of PB2 is involved in its degradation. Taken together, these results show that PB2 and PA are poly(ADP-ribosylated) and their poly(ADP-ribose) chains are likely associated with the ZAPL WWE domain, leading to the proteasomal degradation of PB2 and PA.

3.3.7 PB1 binding to ZAPL leads to the dissociation of PA and PB2 from ZAPL, thereby protecting PA and PB2 from degradation

We have shown that PB1 binds to a region on ZAPL that is relatively close to the PB2 and PA binding site (Figure 3.8), and PB1 is not degraded by ZAPL, therefore we postulated that the interaction of PB1 with ZAPL might lead to the dissociation of PB2 and PA from ZAPL. To test this possibility, a protein-protein competition assay was performed. Cells were transfected with ZAPL and the indicated amounts of the PA or PB2, and PB1 plasmids, and then treated with MG132, a condition under which PB2 and PA are stabilized and remain bound to ZAPL. Cell extracts were immunoprecipitated with ZAPL, and detected the interaction with PA, PB2 or PB1 (Figure 3.15). In addition, we first determined the levels of PA and PB2 that saturated the amount of ZAPL produced, so that PB1 would be expected to bind predominantly to the same ZAPL molecules that bind PA and PB2. Under this conditions, the MG132-stablized PA and PB2 that was bound to ZAPL was found to

dissociate from ZAPL by the presence of increasing amount of PB1, concomitant with PB1 binding to ZAPL (Lane 3-5 in Figure 3.15A, B). Furthermore, the dissociation of PA and PB2 would be expected to protect them from ZAPL-mediated degradation. To test this prediction, we determined whether co-expression of PB1 can protect PA and PB2 from ZAPL-mediated degradation in the absence of MG132 treatment (Figure 3.16A). We found that the degradation of PA and PB2 in cells transfected with ZAPL was largely reversed by co-transfection with PB1. These results show that PB1 binding to ZAPL dissociates PA and PB2 from ZAPL, thereby protecting PA and PB2 from degradation.

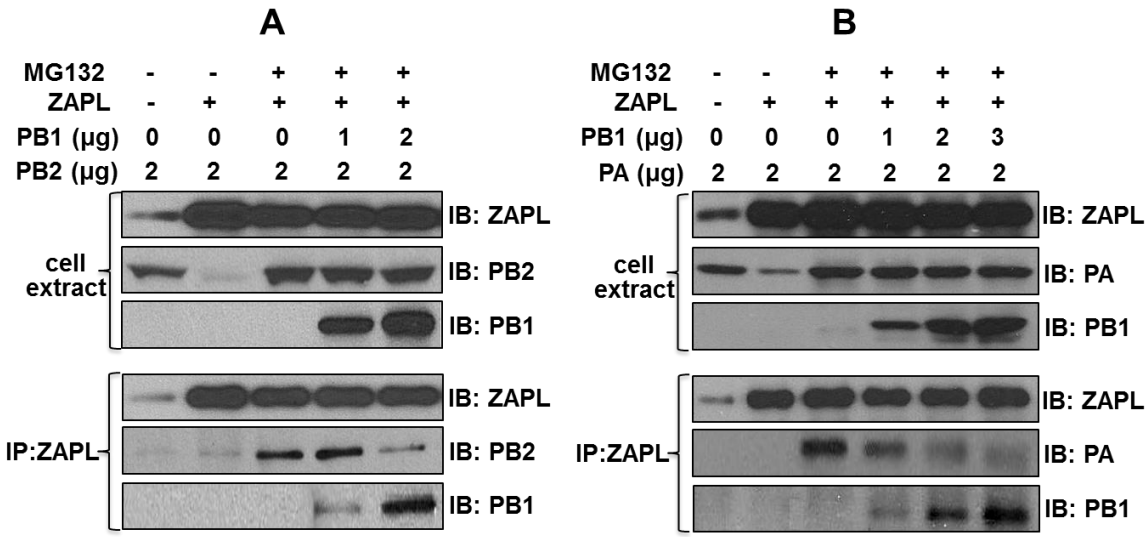

Figure 3.15 PB1 binding to ZAPL dissociates PA and PB2 from ZAPL. (A-B) 293T cells were treated with MG132 or DMSO after transfection with ZAPL and the indicated amounts of the PA (B), PB2 (A), and PB1 plasmids. Cell extracts were immunoprecipitated with ZAPL Ab, and the immunoprecipitates and the cell extracts were immunoblotted with ZAPL Ab, and PA, PB2, or PB1 Ab, as indicated.

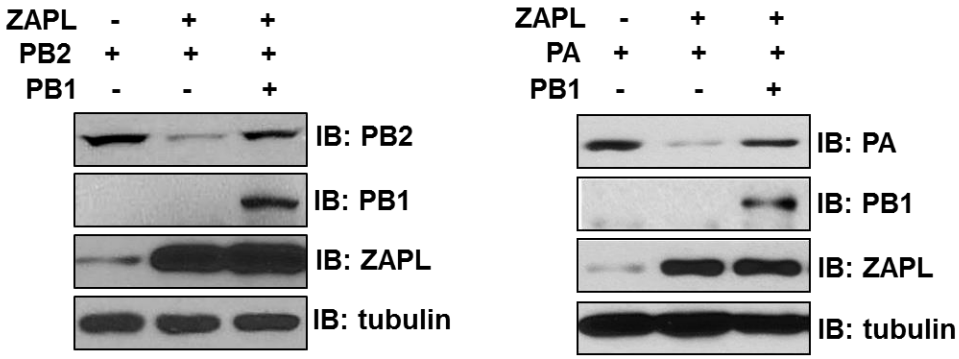

Figure 3.16 PB1 protects PA and PB2 from ZAPL-mediated degradation. 293T cells were transfected with ZAPL, PB2, PA, PB1 plasmids where indicated, and cell extracts were immunoblotted with the indicated Abs.

3.4 Discussion

In the present study we identified a new antiviral activity of ZAPL and showed that this activity is directed against influenza A virus. The previously identified ZAPL antiviral activity is mediated by its N-terminal fingers which bind to the mRNAs of several viruses and promote the degradation of these mRNAs (Bick et al., 2003; Gao et al., 2002; Guo et al., 2004; Guo et al., 2007a; Kerns et al., 2008; Muller et al., 2007; Zhu et al., 2011). In contrast, the newly identified ZAPL antiviral activity involves its C-terminal PARP domain, which binds the influenza A virus PB2 and PA polymerase proteins on separate ZAPL molecules. These two viral proteins are poly(ADP-ribosylated), presumably by PARP(s) other than ZAPL (Leung et al., 2011) which lacks this activity (Kleine et al., 2008). The ZAPL-associated, poly(ADP-ribosylated) PA and PB2 proteins are then ubiquitinated, followed by proteasomal degradation. This ZAPL mechanism explains why endogenous ZAPL inhibits influenza A virus replication, as we established by a siRNA knockdown experiment.

The PB1 protein counteracts the newly identified ZAPL antiviral activity by binding to the WWE region adjacent to the PARP domain, causing PB2 and PA to dissociate from ZAPL and therefore escape degradation. This function of the PB1 protein explains why influenza A virus infection is only moderately inhibited (20-30-fold) by endogenous ZAPL, indicating that influenza A virus has partially won the battle against this newly identified ZAPL antiviral activity. ZAPL, which is located in the cytoplasm (Charron et al., 2013; Leung et al., 2011), likely interacts with the PA, PB2 and PB1 proteins in the cytoplasm before they interact with each other and enter the nucleus to form tripartite

polymerase complex. Consistent with this cellular site of interaction, immunofluorescence of cells co-expressed with ZAPL and PA, PB2, or PB1 plasmid verified that ZAPL interacts with PA, PB2 and PB1 in the cytoplasm. The situation in virus-infected cells is more complicated. For example, in infected cells cytoplasmic PB1 could potentially interact not only with ZAPL, but also with PA and DDX21 (Chen et al., 2014; Fodor and Smith, 2004), indicating that only some, but not all the PB1 in the cytoplasm would be available to counteract ZAPL. Because the binding of PB1 to ZAPL suppresses ZAPL antiviral activity, eliminating this PB1 binding would be expected to substantially increase the inhibition of virus replication, so that the PB1 interface with ZAPL is a potential target for antiviral development. Furthermore, since PB1 structure was solved recently (Pflug et al., 2014; Reich et al., 2014), further study is needed to determine whether it is feasible to generate a PB1 mutant virus whose primary defect is in ZAPL binding. Because PB1 was shown to tightly interact with PA and PB2 proteins, it may not be feasible to determine such PB1 mutant that does not interfere with interaction with PA and PB2.

By purification of CPSF30-NS1A complexes from virus infected cells, we have identified not only DDX21 (Chen et al., 2014), but also ZAPL as restriction factors against influenza virus replication. We further determined the mechanism how influenza virus counteracts these antiviral activities. ZAPL likely through binding to PB1 (and NP) associates with CPSF30-NS1A complexes, which is presumably the end result of the battle between influenza A virus and the newly identified ZAPL antiviral activity. However, we do not know the consequence of such association of ZAPL in the CPSF30-NS1A

complexes to the virus replication.

ZAPL (PARP 13.1) also has an important cellular function as a PARP protein. It interacts with Argonaute proteins (as well as several other cellular RNA-binding proteins), and both the Argonaute protein and ZAPL itself are poly(ADP-ribosylated) presumably by other cytoplasmic PARP proteins (Leung et al., 2011). Poly(ADP-ribosylation) of Argonaute increases during stress, leading to the relief of microRNA-mediated silencing of translation and hence to uninhibited translation of cellular mRNAs that are regulated by microRNAs. It is not known whether this cellular function is compromised by the utilization of ZAPL for antiviral activity in influenza A virus-infected cells. In other studies, it was shown that poly(ADP-ribosylated) proteins associated with a different PARP-containing protein, tankyrase, are ubiquitinated by an E3 ligase (i.e. RNF146) which recognizes poly(ADP-ribose) chains via its WWE domain and also binds to specific domains in tankyrase itself (DaRosa et al., 2014; Guettler et al., 2011). Hence, tankyrase is an essential scaffold for the E3 ligase that ubiquitinates the poly(ADP-ribosylated) protein bound to tankyrase.

These previous studies, coupled with the results we report here, provide a working model for the ZAPL-dependent degradation of PB2 and PA (Figure 3.17). We showed that PB2 and PA are targeted by ZAPL PARP domain, and that after these two viral proteins are poly(ADP-ribosylated) they accumulate in the region containing WWE and PARP domain, most likely because the WWE domain specifically binds poly(ADP-ribose) chains (DaRosa et al., 2014; Wang et al., 2012). It is likely that this accumulation would be blocked by the

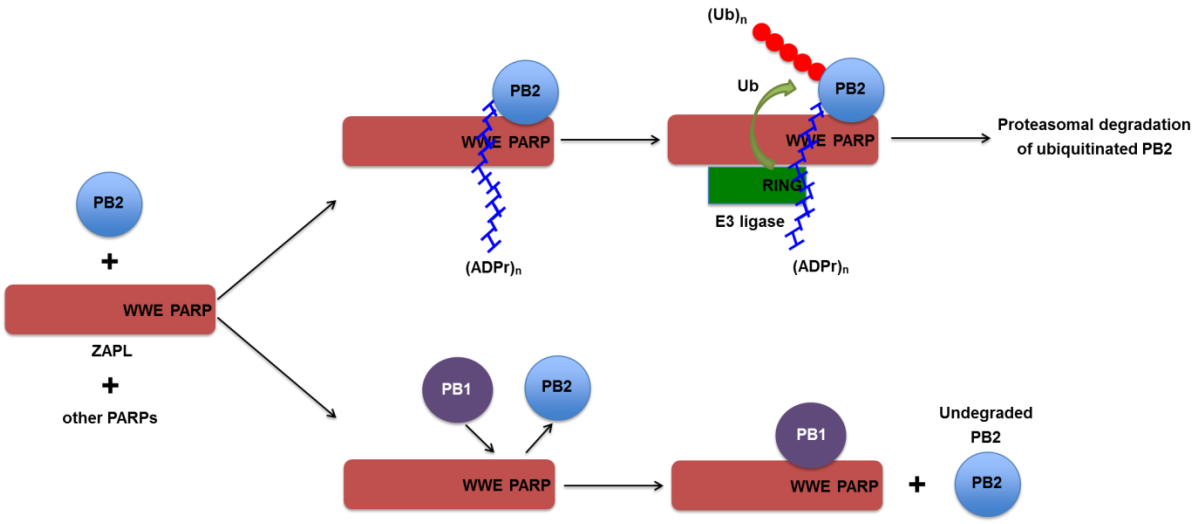

Figure 3.17 Working model for the ZAPL-dependent degradation of PB2 and PA. The model for PA degradation is the same as that shown here for PB2. The mechanism by which PB1 counters ZAPL-dependent degradation of PB2 is also shown. The model is described in the Discussion.

binding of the PB1 protein to the WWE region. Based on the tankyrase model, we proposed that poly(ADP-ribosylated) PA and PB2 are ubiquitinated by an E3 ligase that recognizes not only the poly(ADP-ribose) chains on PA and PB2 but also the ZAPL scaffold, specifically regions of ZAPL that are N-terminal to the WWE domain. It should be noted that in this mechanism ZAPL rather than the E3 ligase provides the WWE domain that binds poly(ADP-ribose) chains, whereas in the tankyrase model the E3 ligase provides the WWE domain (DaRosa et al., 2014). Basically ZAPL via its PARP domain is responsible for selecting the substrate (PB2 or PA) and then serves as a platform for the modification of the substrate that is catalyzed by other molecules, namely, ubiquitination of poly(ADP-ribosylated) substrate by an E3 ligase.

3.5 Future directions

In the present study we proposed a working model for the new ZAPL antiviral activity against influenza A virus that we identified. To further support our proposed model, several experiments are proposed.

First, to show the PA and PB2 proteins are targeted for proteasomal degradation by endogenous ZAPL in influenza A virus-infected cells, A549 cells with or without siRNA knockdown of ZAPL will be infected with Ud virus at low MOI and a pulse-chase labeling experiment will be performed. Viral proteins will be radiolabeled for one hour with S^{35}-cysteine and methionine, followed by incubation in tissue culture medium containing high levels of unlabeled cysteine and methionine for various time periods. We will measure the amount of radiolabeled PB2, PA, and PB1 as a control. Based on our

results, knockdown of endogenous ZAPL is expected to increase the PA and PB2 protein stability in virus infected cells, leading to enhanced virus replication.

Second, I will identify the PARP proteins and E3 ligase that are responsible for poly(ADP-ribosylation) and ubiquitination of PB2 and PA, respectively. It was reported that ZAPL binds to PARP12 and PARP15 to perform poly(ADP-ribosylation) of cellular proteins that are bound to ZAPL (Leung et al., 2011). To determine whether PARP12 and PARP15 poly(ADP-ribosylate) PA and PB2, PARP12 and PARP15 will be knocked down with siRNAs to determine the effect on PA and PB2 poly(ADP-ribosylation). For the identification of the E3 ligase, cells will be co-transfected with GST-ZAPL and Flag-PB2 and treated with MG132 to inhibit proteasomal degradation, and then ZAPL-PB2 protein complex will be purified by sequential GST and Flag selection, and sent to mass spectrometry analysis to identify the associated proteins including one or more E3 ligases that will be candidates for the E3 ligase that ubiquitinates PB2 and PA. Mass spectrometry may also identify the PARP proteins that catalyze PB2 poly(ADP-ribosylation. It is likely that a stable complex containing ZAPL, PB2 and E3 ligase exists because in the RNF146-tankyrase model it was reported that the RNF146 E3 ligase forms a stable complex with tankarase, a PARP-containing protein, to ubiquitinate the poly(ADP-ribosylated) target protein (DaRosa et al., 2014).

It is possible that ZAPL might inhibit the interaction of NS1 with CPSF30, leading to the inhibition of virus replication. The effect of ZAPL association with NS1-CPSF30 complexes will be determined. As the first approach, ZAPL

will be knocked down with a siRNA and the interaction of NS1 with CPSF30 will be determined.

Second, ZAPL was shown to destabilize TRAILR4 transcripts to regulate TRAIL-mediated apoptosis in the absence of viral infection (Todorova et al., 2014). The effect that knockdown of ZAPL leads to increased influenza A virus replication might be a result of reduced TRAIL-mediated apoptosis, which may favors virus replication. To test this possibility, cells will be transfected with siRNA to knockdown ZAPL and then infected with Ud virus, and then whether cells with or without knockdown of ZAPL are in different apoptotic status will be determined by measuring caspase-3 activity.

ZAPL was reported to block microRNA function during stress, specifically the relief of microRNA-mediated silencing of translation and hence to uninhibited translation of cellular mRNAs that are regulated by microRNAs. This cellular function is probably compromised in influenza A virus-infected cells by the diversion of ZAPL molecules to carry out its antiviral function. (Leung et al., 2011). As a consequence microRNAs that repress the translation of the mRNAs encoded by interferon-stimulated genes (ISGs) would continue to repress the translation of these mRNAs, a function which would favor virus replication (Seo et al., 2013). We intend to test this possibility.

References

Akarsu, H., Burmeister, W.P., Petosa, C., Petit, I., Muller, C.W., Ruigrok, R.W., and Baudin, F. (2003). Crystal structure of the M1 protein-binding domain of the influenza A virus nuclear export protein (NEP/NS2). EMBO J *22*, 4646-4655.

Bick, M.J., Carroll, J.W., Gao, G., Goff, S.P., Rice, C.M., and MacDonald, M.R. (2003). Expression of the zinc-finger antiviral protein inhibits alphavirus replication. J Virol *77*, 11555-11562.

Blaas, D., Patzelt, E., and Kuechler, E. (1982). Cap-recognizing protein of influenza virus. Virology *116*, 339-348.

Bradel-Tretheway, B.G., Mattiacio, J.L., Krasnoselsky, A., Stevenson, C., Purdy, D., Dewhurst, S., and Katze, M.G. (2011). Comprehensive proteomic analysis of influenza virus polymerase complex reveals a novel association with mitochondrial proteins and RNA polymerase accessory factors. J Virol *85*, 8569-8581.

Calo, E., Flynn, R.A., Martin, L., Spitale, R.C., Chang, H.Y., and Wysocka, J. (2014). RNA helicase DDX21 coordinates transcription and ribosomal RNA processing. Nature *518*, 249-253.

Charron, G., Li, M.M., MacDonald, M.R., and Hang, H.C. (2013). Prenylome profiling reveals S-farnesylation is crucial for membrane targeting and antiviral activity of ZAP long-isoform. Proc Natl Acad Sci U S A *110*, 11085-11090.

Chen, B.J., Leser, G.P., Morita, E., and Lamb, R.A. (2007). Influenza virus hemagglutinin and neuraminidase, but not the matrix protein, are required for assembly and budding of plasmid-derived virus-like particles. J Virol *81*, 7111-7123.

Chen, G., Guo, X., Lv, F., Xu, Y., and Gao, G. (2008). p72 DEAD box RNA helicase is required for optimal function of the zinc-finger antiviral protein. Proc Natl Acad Sci U S A *105*, 4352-4357.

Chen, G., Liu, C.H., Zhou, L., and Krug, R.M. (2014). Cellular DDX21 RNA helicase inhibits influenza A virus replication but is counteracted by the viral NS1 protein. Cell Host Microbe *15*, 484-493.

Chen, W., Calvo, P.A., Malide, D., Gibbs, J., Schubert, U., Bacik, I., Basta, S., O'Neill, R., Schickli, J., Palese, P.*, et al.* (2001). A novel influenza A virus mitochondrial protein that induces cell death. Nat Med *7*, 1306-1312.

Chen, Z., and Krug, R.M. (2000). Selective nuclear export of viral mRNAs in influenza-virus-infected cells. Trends Microbiol *8*, 376-383.

Chen, Z., Li, Y., and Krug, R.M. (1999). Influenza A virus NS1 protein targets poly(A)-binding protein II of the cellular 3'-end processing machinery. EMBO J *18*, 2273-2283.

Cheng, A., Wong, S.M., and Yuan, Y.A. (2009). Structural basis for dsRNA recognition by NS1 protein of influenza A virus. Cell Res *19*, 187-195.

Chien, C.Y., Tejero, R., Huang, Y., Zimmerman, D.E., Rios, C.B., Krug, R.M., and Montelione, G.T. (1997). A novel RNA-binding motif in influenza A virus non-structural protein 1. Nat Struct Biol *4*, 891-895.

Chien, C.Y., Xu, Y., Xiao, R., Aramini, J.M., Sahasrabudhe, P.V., Krug, R.M., and Montelione, G.T. (2004). Biophysical characterization of the complex between double-stranded RNA and the N-terminal domain of the NS1 protein from influenza A virus: evidence for a novel RNA-binding mode. Biochemistry *43*, 1950-1962.

Colgan, D.F., and Manley, J.L. (1997). Mechanism and regulation of mRNA polyadenylation. Genes Dev *11*, 2755-2766.

DaRosa, P.A., Wang, Z., Jiang, X., Pruneda, J.N., Cong, F., Klevit, R.E., and Xu, W. (2014). Allosteric activation of the RNF146 ubiquitin ligase by a poly(ADP-ribosyl)ation signal. Nature *517*, 223-226.

Das, K., Aramini, J.M., Ma, L.C., Krug, R.M., and Arnold, E. (2010). Structures of influenza A proteins and insights into antiviral drug targets. Nat Struct Mol Biol *17*, 530-538.

Deng, T., Sharps, J., Fodor, E., and Brownlee, G.G. (2005). In vitro assembly of PB2 with a PB1-PA dimer supports a new model of assembly of influenza A virus polymerase subunits into a functional trimeric complex. J Virol *79*, 8669-8674.

Dias, A., Bouvier, D., Crepin, T., McCarthy, A.A., Hart, D.J., Baudin, F., Cusack, S., and Ruigrok, R.W. (2009). The cap-snatching endonuclease of influenza virus polymerase resides in the PA subunit. Nature *458*, 914-918.

Donelan, N.R., Basler, C.F., and Garcia-Sastre, A. (2003). A recombinant influenza A virus expressing an RNA-binding-defective NS1 protein induces high levels of beta interferon and is attenuated in mice. J Virol *77*, 13257-13266.

Ehrhardt, C., Wolff, T., Pleschka, S., Planz, O., Beermann, W., Bode, J.G., Schmolke, M., and Ludwig, S. (2007). Influenza A virus NS1 protein activates the PI3K/Akt pathway to mediate antiapoptotic signaling responses. J Virol *81*, 3058-3067.

Erdelyi, K., Bai, P., Kovacs, I., Szabo, E., Mocsar, G., Kakuk, A., Szabo, C., Gergely, P., and Virag, L. (2009). Dual role of poly(ADP-ribose) glycohydrolase in the regulation of cell death in oxidatively stressed A549 cells. FASEB J *23*, 3553-3563.

Fodor, E., Mingay, L.J., Crow, M., Deng, T., and Brownlee, G.G. (2003). A single amino acid mutation in the PA subunit of the influenza virus RNA polymerase promotes the generation of defective interfering RNAs. J Virol *77*, 5017-5020.

Fodor, E., Pritlove, D.C., and Brownlee, G.G. (1994). The influenza virus panhandle is involved in the initiation of transcription. J Virol *68*, 4092-4096.

Fodor, E., and Smith, M. (2004). The PA subunit is required for efficient nuclear accumulation of the PB1 subunit of the influenza A virus RNA polymerase complex. J Virol *78*, 9144-9153.

Gack, M.U., Albrecht, R.A., Urano, T., Inn, K.S., Huang, I.C., Carnero, E., Farzan, M., Inoue, S., Jung, J.U., and Garcia-Sastre, A. (2009). Influenza A virus NS1 targets the ubiquitin ligase TRIM25 to evade recognition by the host viral RNA sensor RIG-I. Cell Host Microbe *5*, 439-449.

Gao, G., Guo, X., and Goff, S.P. (2002). Inhibition of retroviral RNA production by ZAP, a CCCH-type zinc finger protein. Science *297*, 1703-1706.

Glasker, S., Toller, M., and Kummerer, B.M. (2014). The alternate triad motif of the poly(ADP-ribose) polymerase-like domain of the human zinc finger antiviral protein is essential for its antiviral activity. J Gen Virol *95*, 816-822.

Guettler, S., LaRose, J., Petsalaki, E., Gish, G., Scotter, A., Pawson, T., Rottapel, R., and Sicheri, F. (2011). Structural basis and sequence rules for substrate recognition by Tankyrase explain the basis for cherubism disease. Cell *147*, 1340-1354.

Guilligay, D., Tarendeau, F., Resa-Infante, P., Coloma, R., Crepin, T., Sehr, P., Lewis, J., Ruigrok, R.W., Ortin, J., Hart, D.J.*, et al.* (2008). The structural basis for cap binding by influenza virus polymerase subunit PB2. Nat Struct Mol Biol *15*, 500-506.

Guo, X., Carroll, J.W., Macdonald, M.R., Goff, S.P., and Gao, G. (2004). The zinc finger antiviral protein directly binds to specific viral mRNAs through the CCCH zinc finger motifs. J Virol *78*, 12781-12787.

Guo, X., Ma, J., Sun, J., and Gao, G. (2007a). The zinc-finger antiviral protein recruits the RNA processing exosome to degrade the target mRNA. Proc Natl Acad Sci U S A *104*, 151-156.

Guo, Z., Chen, L.M., Zeng, H., Gomez, J.A., Plowden, J., Fujita, T., Katz, J.M., Donis, R.O., and Sambhara, S. (2007b). NS1 protein of influenza A virus inhibits the function of intracytoplasmic pathogen sensor, RIG-I. Am J Respir Cell Mol Biol *36*, 263-269.

Guu, T.S., Dong, L., Wittung-Stafshede, P., and Tao, Y.J. (2008). Mapping the domain structure of the influenza A virus polymerase acidic protein (PA) and its interaction with the basic protein 1 (PB1) subunit. Virology *379*, 135-142.

Hale, B.G., Jackson, D., Chen, Y.H., Lamb, R.A., and Randall, R.E. (2006). Influenza A virus NS1 protein binds p85beta and activates phosphatidylinositol-3-kinase signaling. Proc Natl Acad Sci U S A *103*, 14194-14199.

Hara, K., Schmidt, F.I., Crow, M., and Brownlee, G.G. (2006). Amino acid residues in the N-terminal region of the PA subunit of influenza A virus RNA polymerase play a critical role in protein stability, endonuclease activity, cap binding, and virion RNA promoter binding. J Virol *80*, 7789-7798.

Haussecker, D., Cao, D., Huang, Y., Parameswaran, P., Fire, A.Z., and Kay, M.A. (2008). Capped small RNAs and MOV10 in human hepatitis delta virus replication. Nat Struct Mol Biol *15*, 714-721.

He, Q.S., Tang, H., Zhang, J., Truong, K., Wong-Staal, F., and Zhou, D. (2008a). Comparisons of RNAi approaches for validation of human RNA helicase A as an essential factor in hepatitis C virus replication. J Virol Methods *154*, 216-219.

He, X., Zhou, J., Bartlam, M., Zhang, R., Ma, J., Lou, Z., Li, X., Li, J., Joachimiak, A., Zeng, Z.*, et al.* (2008b). Crystal structure of the polymerase PA(C)-PB1(N) complex from an avian influenza H5N1 virus. Nature *454*, 1123-1126.

Heikkinen, L.S., Kazlauskas, A., Melen, K., Wagner, R., Ziegler, T., Julkunen, I., and Saksela, K. (2008). Avian and 1918 Spanish influenza a virus NS1 proteins bind to Crk/CrkL Src homology 3 domains to activate host cell signaling. J Biol Chem *283*, 5719-5727.

Holmes, E.C., Ghedin, E., Miller, N., Taylor, J., Bao, Y., St George, K., Grenfell, B.T., Salzberg, S.L., Fraser, C.M., Lipman, D.J.*, et al.* (2005). Whole-genome analysis of human influenza A virus reveals multiple persistent lineages and reassortment among recent H3N2 viruses. PLoS Biol *3*, e300.

Jackson, D., Hossain, M.J., Hickman, D., Perez, D.R., and Lamb, R.A. (2008). A new influenza virus virulence determinant: the NS1 protein four C-terminal residues modulate pathogenicity. Proc Natl Acad Sci U S A *105*, 4381-4386.

Jagger, B.W., Wise, H.M., Kash, J.C., Walters, K.A., Wills, N.M., Xiao, Y.L., Dunfee, R.L., Schwartzman, L.M., Ozinsky, A., Bell, G.L.*, et al.* (2012). An overlapping protein-coding region in influenza A virus segment 3 modulates the host response. Science *337*, 199-204.

Kerns, J.A., Emerman, M., and Malik, H.S. (2008). Positive selection and increased antiviral activity associated with the PARP-containing isoform of human zinc-finger antiviral protein. PLoS Genet *4*, e21.

Kleine, H., Poreba, E., Lesniewicz, K., Hassa, P.O., Hottiger, M.O., Litchfield, D.W., Shilton, B.H., and Luscher, B. (2008). Substrate-assisted catalysis by PARP10 limits its activity to mono-ADP-ribosylation. Mol Cell *32*, 57-69.

Krishnakumar, R., and Kraus, W.L. (2010). PARP-1 regulates chromatin structure and transcription through a KDM5B-dependent pathway. Mol Cell *39*, 736-749.

Krug, R.M. (2014). Influenza: An RNA-synthesizing machine. Nature *516*, 338-339.

Krug, R.M. (2015). Functions of the influenza A virus NS1 protein in antiviral defense. Curr Opin Virol *12*, 1-6.

Krug, R.M., and Fodor, E. (2013). The virus genome and its replication. In: Textbook of Influenza, 2nd Edition.

Krug, R.M., and Garcia-Sastre, A. (2013). The NS1 protein: A master regulator of host and viral functions. In: Textbook of Influenza, 2nd edition.

Kuo, R.L., and Krug, R.M. (2009). Influenza a virus polymerase is an integral component of the CPSF30-NS1A protein complex in infected cells. J Virol *83*, 1611-1616.

Kuo, R.L., Zhao, C., Malur, M., and Krug, R.M. (2010). Influenza A virus strains that circulate in humans differ in the ability of their NS1 proteins to block the activation of IRF3 and interferon-beta transcription. Virology *408*, 146-158.

Lamb, R.A. (2013). Deadly H7N9 influenza virus: a pandemic in the making or a warning lesson? Am J Respir Crit Care Med *188*, 1-2.

Lamb, R.A., and Krug, R.M. (2001). Orthomyxoviridae: the viruses and their replication. In: Fields Virology.

Leung, A.K., Vyas, S., Rood, J.E., Bhutkar, A., Sharp, P.A., and Chang, P. (2011). Poly(ADP-ribose) regulates stress responses and microRNA activity in the cytoplasm. Mol Cell *42*, 489-499.

Li, K.S., Guan, Y., Wang, J., Smith, G.J., Xu, K.M., Duan, L., Rahardjo, A.P., Puthavathana, P., Buranathai, C., Nguyen, T.D.*, et al.* (2004). Genesis of a highly pathogenic and potentially pandemic H5N1 influenza virus in eastern Asia. Nature *430*, 209-213.

Li, M.Z., and Elledge, S.J. (2007). Harnessing homologous recombination in vitro to generate recombinant DNA via SLIC. Nat Methods *4*, 251-256.

Li, S., Min, J.Y., Krug, R.M., and Sen, G.C. (2006). Binding of the influenza A virus NS1 protein to PKR mediates the inhibition of its activation by either PACT or double-stranded RNA. Virology *349*, 13-21.

Li, Y., Chen, Z.Y., Wang, W., Baker, C.C., and Krug, R.M. (2001). The 3'-end-processing factor CPSF is required for the splicing of single-intron pre-mRNAs in vivo. RNA *7*, 920-931.

Liu, J., Lynch, P.A., Chien, C.Y., Montelione, G.T., Krug, R.M., and Berman, H.M. (1997). Crystal structure of the unique RNA-binding domain of the influenza virus NS1 protein. Nat Struct Biol *4*, 896-899.

Lu, Y., Wambach, M., Katze, M.G., and Krug, R.M. (1995). Binding of the influenza virus NS1 protein to double-stranded RNA inhibits the activation of the protein kinase that phosphorylates the eIF-2 translation initiation factor. Virology *214*, 222-228.

Mao, R., Nie, H., Cai, D., Zhang, J., Liu, H., Yan, R., Cuconati, A., Block, T.M., Guo, J.T., and Guo, H. (2013). Inhibition of hepatitis B virus replication by the host zinc finger antiviral protein. PLoS Pathog *9*, e1003494.

Marazzi, I., Ho, J.S., Kim, J., Manicassamy, B., Dewell, S., Albrecht, R.A., Seibert, C.W., Schaefer, U., Jeffrey, K.L., Prinjha, R.K.*, et al.* (2012). Suppression of the antiviral response by an influenza histone mimic. Nature *483*, 428-433.

Martin, K., and Helenius, A. (1991). Nuclear transport of influenza virus ribonucleoproteins: the viral matrix protein (M1) promotes export and inhibits import. Cell *67*, 117-130.

Massin, P., van der Werf, S., and Naffakh, N. (2001). Residue 627 of PB2 is a determinant of cold sensitivity in RNA replication of avian influenza viruses. J Virol *75*, 5398-5404.

Melen, K., Kinnunen, L., Fagerlund, R., Ikonen, N., Twu, K.Y., Krug, R.M., and Julkunen, I. (2007). Nuclear and nucleolar targeting of influenza A virus NS1 protein: striking differences between different virus subtypes. J Virol *81*, 5995-6006.

Mibayashi, M., Martinez-Sobrido, L., Loo, Y.M., Cardenas, W.B., Gale, M., Jr., and Garcia-Sastre, A. (2007). Inhibition of retinoic acid-inducible gene I-

mediated induction of beta interferon by the NS1 protein of influenza A virus. J Virol *81*, 514-524.

Min, J.Y., and Krug, R.M. (2006). The primary function of RNA binding by the influenza A virus NS1 protein in infected cells: Inhibiting the 2'-5' oligo (A) synthetase/RNase L pathway. Proc Natl Acad Sci U S A *103*, 7100-7105.

Min, J.Y., Li, S., Sen, G.C., and Krug, R.M. (2007). A site on the influenza A virus NS1 protein mediates both inhibition of PKR activation and temporal regulation of viral RNA synthesis. Virology *363*, 236-243.

Muller, S., Moller, P., Bick, M.J., Wurr, S., Becker, S., Gunther, S., and Kummerer, B.M. (2007). Inhibition of filovirus replication by the zinc finger antiviral protein. J Virol *81*, 2391-2400.

Nagata, K., Kawaguchi, A., and Naito, T. (2008). Host factors for replication and transcription of the influenza virus genome. Rev Med Virol *18*, 247-260.

Naldini, L., Blomer, U., Gallay, P., Ory, D., Mulligan, R., Gage, F.H., Verma, I.M., and Trono, D. (1996). In vivo gene delivery and stable transduction of nondividing cells by a lentiviral vector. Science *272*, 263-267.

Nemeroff, M.E., Barabino, S.M., Li, Y., Keller, W., and Krug, R.M. (1998). Influenza virus NS1 protein interacts with the cellular 30 kDa subunit of CPSF and inhibits 3'end formation of cellular pre-mRNAs. Mol Cell *1*, 991-1000.

Nemeroff, M.E., Qian, X.Y., and Krug, R.M. (1995). The influenza virus NS1 protein forms multimers in vitro and in vivo. Virology *212*, 422-428.

Neumann, G., and Kawaoka, Y. (2001). Reverse genetics of influenza virus. Virology *287*, 243-250.

Noah, D.L., and Krug, R.M. (2005). Influenza virus virulence and its molecular determinants. Adv Virus Res *65*, 121-145.

Noah, D.L., Twu, K.Y., and Krug, R.M. (2003). Cellular antiviral responses against influenza A virus are countered at the posttranscriptional level by the viral NS1A protein via its binding to a cellular protein required for the 3' end processing of cellular pre-mRNAS. Virology *307*, 386-395.

Obayashi, E., Yoshida, H., Kawai, F., Shibayama, N., Kawaguchi, A., Nagata, K., Tame, J.R., and Park, S.Y. (2008). The structural basis for an essential subunit interaction in influenza virus RNA polymerase. Nature *454*, 1127-1131.

Obenauer, J.C., Denson, J., Mehta, P.K., Su, X., Mukatira, S., Finkelstein, D.B., Xu, X., Wang, J., Ma, J., Fan, Y*., et al.* (2006). Large-scale sequence analysis of avian influenza isolates. Science *311*, 1576-1580.

Ochoa, M., Barcena, J., de la Luna, S., Melero, J.A., Douglas, A.R., Nieto, A., Ortin, J., Skehel, J.J., and Portela, A. (1995). Epitope mapping of cross-reactive monoclonal antibodies specific for the influenza A virus PA and PB2 polypeptides. Virus Res *37*, 305-315.

Opitz, B., Rejaibi, A., Dauber, B., Eckhard, J., Vinzing, M., Schmeck, B., Hippenstiel, S., Suttorp, N., and Wolff, T. (2007). IFNbeta induction by influenza A virus is mediated by RIG-I which is regulated by the viral NS1 protein. Cell Microbiol *9*, 930-938.

Pflug, A., Guilligay, D., Reich, S., and Cusack, S. (2014). Structure of influenza A polymerase bound to the viral RNA promoter. Nature *516*, 355-360.

Pichlmair, A., Schulz, O., Tan, C.P., Naslund, T.I., Liljestrom, P., Weber, F., and Reis e Sousa, C. (2006). RIG-I-mediated antiviral responses to single-stranded RNA bearing 5'-phosphates. Science *314*, 997-1001.

Plotch, S.J., Bouloy, M., Ulmanen, I., and Krug, R.M. (1981). A unique cap(m7GpppXm)-dependent influenza virion endonuclease cleaves capped RNAs to generate the primers that initiate viral RNA transcription. Cell *23*, 847-858.

Poon, L.L., Pritlove, D.C., Fodor, E., and Brownlee, G.G. (1999). Direct evidence that the poly(A) tail of influenza A virus mRNA is synthesized by reiterative copying of a U track in the virion RNA template. J Virol *73*, 3473-3476.

Randall, R.E., and Goodbourn, S. (2008). Interferons and viruses: an interplay between induction, signalling, antiviral responses and virus countermeasures. J Gen Virol *89*, 1-47.

Reich, S., Guilligay, D., Pflug, A., Malet, H., Berger, I., Crepin, T., Hart, D., Lunardi, T., Nanao, M., Ruigrok, R.W.*, et al.* (2014). Structural insight into cap-snatching and RNA synthesis by influenza polymerase. Nature *516*, 361-366.

Resa-Infante, P., Jorba, N., Coloma, R., and Ortin, J. (2011). The influenza virus RNA synthesis machine: advances in its structure and function. RNA Biol *8*, 207-215.

Robb, N.C., Chase, G., Bier, K., Vreede, F.T., Shaw, P.C., Naffakh, N., Schwemmle, M., and Fodor, E. (2011). The influenza A virus NS1 protein interacts with the nucleoprotein of viral ribonucleoprotein complexes. J Virol *85*, 5228-5231.

Sadler, A.J., and Williams, B.R. (2008). Interferon-inducible antiviral effectors. Nat Rev Immunol *8*, 559-568.

Seo, G.J., Kincaid, R.P., Phanaksri, T., Burke, J.M., Pare, J.M., Cox, J.E., Hsiang, T.Y., Krug, R.M., and Sullivan, C.S. (2013). Reciprocal inhibition between intracellular antiviral signaling and the RNAi machinery in mammalian cells. Cell Host Microbe *14*, 435-445.

Shapiro, G.I., and Krug, R.M. (1988). Influenza virus RNA replication in vitro: synthesis of viral template RNAs and virion RNAs in the absence of an added primer. J Virol *62*, 2285-2290.

Shin, Y.K., Liu, Q., Tikoo, S.K., Babiuk, L.A., and Zhou, Y. (2007). Influenza A virus NS1 protein activates the phosphatidylinositol 3-kinase (PI3K)/Akt pathway by direct interaction with the p85 subunit of PI3K. J Gen Virol *88*, 13-18.

Subbarao, E.K., London, W., and Murphy, B.R. (1993). A single amino acid in the PB2 gene of influenza A virus is a determinant of host range. J Virol *67*, 1761-1764.

Takeda, M., Pekosz, A., Shuck, K., Pinto, L.H., and Lamb, R.A. (2002). Influenza a virus M2 ion channel activity is essential for efficient replication in tissue culture. J Virol *76*, 1391-1399.

Takeuchi, O., and Akira, S. (2009). Innate immunity to virus infection. Immunol Rev *227*, 75-86.

Tian, B., and Mathews, M.B. (2001). Functional characterization of and cooperation between the double-stranded RNA-binding motifs of the protein kinase PKR. J Biol Chem *276*, 9936-9944.

Todorova, T., Bock, F.J., and Chang, P. (2014). PARP13 regulates cellular mRNA post-transcriptionally and functions as a pro-apoptotic factor by destabilizing TRAILR4 transcript. Nat Commun *5*, 5362.

Twu, K.Y., Kuo, R.L., Marklund, J., and Krug, R.M. (2007). The H5N1 influenza virus NS genes selected after 1998 enhance virus replication in mammalian cells. J Virol *81*, 8112-8121.

Twu, K.Y., Noah, D.L., Rao, P., Kuo, R.L., and Krug, R.M. (2006). The CPSF30 binding site on the NS1A protein of influenza A virus is a potential antiviral target. J Virol *80*, 3957-3965.

Ulmanen, I., Broni, B.A., and Krug, R.M. (1981). Role of two of the influenza virus core P proteins in recognizing cap 1 structures (m7GpppNm) on RNAs and in initiating viral RNA transcription. Proc Natl Acad Sci U S A *78*, 7355-7359.

Wang, Z., Michaud, G.A., Cheng, Z., Zhang, Y., Hinds, T.R., Fan, E., Cong, F., and Xu, W. (2012). Recognition of the iso-ADP-ribose moiety in poly(ADP-ribose) by WWE domains suggests a general mechanism for poly(ADP-ribosyl)ation-dependent ubiquitination. Genes Dev *26*, 235-240.

Watanabe, T., Watanabe, S., and Kawaoka, Y. (2010). Cellular networks involved in the influenza virus life cycle. Cell Host Microbe *7*, 427-439.

Watanabe, Y., Ohtaki, N., Hayashi, Y., Ikuta, K., and Tomonaga, K. (2009). Autogenous translational regulation of the Borna disease virus negative control factor X from polycistronic mRNA using host RNA helicases. PLoS Pathog *5*, e1000654.

World Health Organization (2014).

Xing, L., Liang, C., and Kleiman, L. (2010). Coordinate roles of Gag and RNA helicase A in promoting the annealing of formula to HIV-1 RNA. J Virol *85*, 1847-1860.

Yin, C., Khan, J.A., Swapna, G.V., Ertekin, A., Krug, R.M., Tong, L., and Montelione, G.T. (2007). Conserved surface features form the double-stranded RNA binding site of non-structural protein 1 (NS1) from influenza A and B viruses. J Biol Chem *282*, 20584-20592.

Zambon, M.C. (2001). The pathogenesis of influenza in humans. Rev Med Virol *11*, 227-241.

Zhang, Y., Liu, S., Mickanin, C., Feng, Y., Charlat, O., Michaud, G.A., Schirle, M., Shi, X., Hild, M., Bauer, A.*, et al.* (2011a). RNF146 is a poly(ADP-ribose)-directed E3 ligase that regulates axin degradation and Wnt signalling. Nat Cell Biol *13*, 623-629.

Zhang, Z., Kim, T., Bao, M., Facchinetti, V., Jung, S.Y., Ghaffari, A.A., Qin, J., Cheng, G., and Liu, Y.J. (2011b). DDX1, DDX21, and DHX36 helicases form a complex with the adaptor molecule TRIF to sense dsRNA in dendritic cells. Immunity *34*, 866-878.

Zhao, C., Hsiang, T.Y., Kuo, R.L., and Krug, R.M. (2010a). ISG15 conjugation system targets the viral NS1 protein in influenza A virus-infected cells. Proc Natl Acad Sci U S A *107*, 2253-2258.

Zhao, C., Kuo, R.L., and Krug, R.M. (2010b). The NS1 Protein of Influenza A Virus. In: Influenza: Molecular Virology.

Zhou, Y., Ma, J., Bushan Roy, B., Wu, J.Y., Pan, Q., Rong, L., and Liang, C. (2008). The packaging of human immunodeficiency virus type 1 RNA is restricted by overexpression of an RNA helicase DHX30. Virology *372*, 97-106.

Zhu, Y., Chen, G., Lv, F., Wang, X., Ji, X., Xu, Y., Sun, J., Wu, L., Zheng, Y.T., and Gao, G. (2011). Zinc-finger antiviral protein inhibits HIV-1 infection by selectively targeting multiply spliced viral mRNAs for degradation. Proc Natl Acad Sci U S A *108*, 15834-15839.

Vita

Chien-Hung Liu was born in Taipei, Taiwan (R.O.C.). He got B.S. degree from Department of Nuclear Science, College of Nuclear Science, National Tsing Hua University in 1999 with major in biology, nuclear medicine, chemistry. Then he joined Dr. Hai-Mei Huang's Lab in Institute of Biotechnology, College of Life Science, National Tsing Hua University with research project focusing on functional studies of the chromosome segregation proteins Spo0J (Hp1138) and Soj (Hp1139) from *Helicobacter pylori*. He earned M.S. degree in 2005. He went to mandatory military service in Army General Headquarters as a second lieutenant platoon leader, and retired in 2007. Then he worked as a research assistant in Dr. Yee-Chun Chen's Lab in the Division of Infectious Diseases, Department of Internal Medicine, National Taiwan University Hospital with research project focusing on characterization of pathogenic role of secreted aspartyl proteinase in *Candida* species. Then he entered the Graduate Program in Microbiology, Department of Molecular Biosciences, University of Texas at Austin, USA, in 2008. He joined Dr. Robert Krug's Lab, and worked in the project of replication of influenza Virus. His graduate works focused on the battle between influenza A virus and a newly identified ZAPL antiviral activity to date.

Permanent address (or email): chrisliu@utexas.edu

This dissertation was typed by Chien-Hung Liu.